

Reversible Small Molecule pan-Ras Inhibitors Display Tunable Affinity for the Active and Inactive forms of Ras.

Charles W. Parry^{a*}, Francesca Pellicano^a, Alexander W. Schüttelkopf^a, Kim Beyer^b, Justin Bower^{a#}, Amy Bryson^{a\$}, Kenneth S. Cameron^a, Nichole Cerutti^{a€}, Jonathan P. Clark^a, Stuart C. Davidson^a, Keneth Davies^a, Martin J. Drysdale^{a†}, Jeffrey Engelman^{c¥}, Anna Estevan-Barber^a, Andrea Gohlke^{aΔ}, Christopher H. Gray^a, Daniel A. Guthy^b, Min Hong^d, Alana Hopkins^a, Luke D. Hutchinson^a, Jennifer Konczal^a, Michel Maira^b, Duncan McArthur^{a†}, Mokdad Mezna^{aΦ}, Heather McKinnon^{a§}, Ridvan Nepravishta^a, Nils Ostermann^b, Camila C. Pasquali^a, Katie Pollock^a, Angelo Pugliese^{a†}, Nicholas Rooney^a, Niko Schmiedeberg^b, Paul Shaw^a, Camilo Velez-Vega^c, Christopher West^a, Ryan West^a, Frederic Zecri^c, John B. Taylor^{a*}.

^aCancer Research Horizons, CRUK Scotland Institute, Gartnavel Estate, Switchback Road, Glasgow, G61 1BD, UK

^bNovartis Institute for Biomedical Research, Fabrikstrasse 2, Novartis Campus, CH-4056, Basel, Switzerland

^cNovartis Institute for Biomedical Research, Inc., 181 Massachusetts Avenue, Cambridge, Massachusetts 02139, USA

^dNCI RAS Initiative, Frederick National Laboratory for Cancer Research, PO Box B, Frederick, MD, 21702, USA

*Email: Charles.Parry@cancer.org.uk; John.Taylor@cancer.org.uk

Activating mutations of Ras are one of the most prevalent drivers of cancer and are often associated with poor clinical outcomes. Despite FDA approval for two irreversible inhibitors that target the inactive state of KRas^{G12C}, significant unmet clinical need still exists, and the susceptibility of non-G12C mutants to inactive-state inhibition remains unclear. Here we report the discovery of a novel series of reversible inhibitors that bind in an enlarged version of the switch I-II pocket with nanomolar affinities. Dependent on chemotype these can either preferentially bind to the inactive or active state or bind both with similar affinity. The active-state binders inhibit the Raf interaction for wild-type Ras, and a broad range of oncogenic KRas mutants with nanomolar potency. A sub-series of these molecules displays cellular inhibition of Ras-Raf binding, as well as decreased phosphorylation of the downstream protein ERK, demonstrating that potent pan-Ras inhibitors can be accessed from this novel pocket.

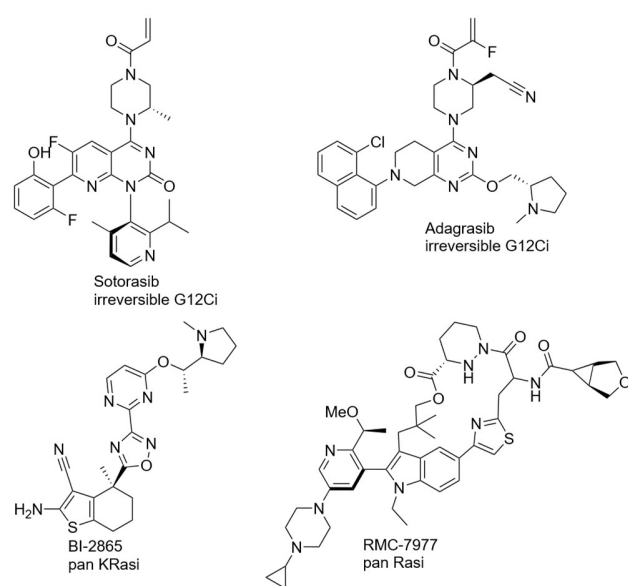
INTRODUCTION

Mutations of the *RAS* oncogenes are well established as major drivers of several forms of human cancer.^{1, 2} In humans, three *RAS* genes encode four different Ras isoforms, HRas, NRas and two KRas splice variants KRas4A and KRas4B. Ras proteins belong to a small family of GTPases that in normal cells act as molecular switches, cycling between an inactive GDP-bound state, and an active GTP-bound state. In the GTP-bound state, Ras signals from the plasma membrane through a functionally diverse set of downstream effector proteins including PI3K, Raf and RALGDS to pathways that control cellular growth, apoptosis, survival, and differentiation. Equilibrium between the two states is tightly regulated via a combination of exchange of GDP for GTP, regulated by GEFs, catalytic hydrolysis of GTP catalyzed by GAPs, and intrinsic GTP hydrolysis. However, activating mutations on Ras, predominantly at codons G12, G13 or Q61 can disrupt this process leading to higher levels of GTP-bound Ras, constitutive activation, persistent signaling and the potential for tumorigenesis.³ Although Ras

is a notoriously challenging drug target, progress has recently been made, notably with the FDA approval for two mutant-selective KRas^{G12C} irreversible inhibitors, AMG-510 (sotorasib) and MRTX849 (adagrasib) (Chart 1).⁴⁻⁷ Whilst encouraging, treatments with KRas^{G12C} mutant specific inhibitors are only applicable to cancers harboring a KRas^{G12C} mutation, and occurrence of both intrinsic and acquired mechanisms of resistance in the clinic and *in vitro* have been observed.⁸⁻¹⁴ Currently several other covalent G12C inhibitors are in pre-clinical development and studies are ongoing to understand and overcome mechanisms of resistance to G12C inhibitors, including combination therapies (for example combination with SHP2, EGFR or MEK inhibitors).¹⁵ Other approaches to drugging Ras are in development, including degrader and “molecular glue” approaches,¹⁶⁻¹⁹ and recently, a non-covalent pan-KRas inhibitor that binds in the switch-II pocket has been characterized (Chart 1).²⁰ The compound preferentially binds to the inactive state of multiple KRas mutants, whilst exhibiting significantly lower affinity for NRas and HRas, shows antiproliferative effect in

KRAS-mutant mouse models and no apparent toxicities. Recently, RMC-7977 (Chart 1) a reversible, tri-complex pan-Ras inhibitor, has shown activity with good tolerability against Ras-dependent cancers in several preclinical cancer models.²¹ These data suggest that pan-Ras inhibitors could be a promising option to treat a wide range of Ras-dependent cancers, whilst being less susceptible to many of the resistance mechanisms for mutant-selective approaches. Current clinical KRas^{G12C} irreversible inhibitors bind in an induced allosteric pocket beneath switch-II that is only present in the inactive GDP-bound state;^{22, 23} hence the strategy is reliant on active cycling between the two nucleotide binding states. Whilst G12C, and to a lesser extent G12D and G13D mutant KRas retain notable endogenous hydrolysis compared to other mutant forms,²⁴ it is expected that higher efficacy could be achieved by directly targeting the active form of Ras. Other attempts to target (K)Ras have identified a small polar pocket between the switch I and II regions (switch I-II pocket), in which several small molecules are known to bind.²⁵⁻²⁷ In this work we describe the identification of several fragments that bind in the same pocket and their optimization using structure-based design methods. Starting from these fragments we developed a series of novel inhibitors with nanomolar affinity for a range of GDP-bound Ras variants. These inhibitors also display *in vitro* and cellular inhibition of Ras-Raf effector binding, and moderate inhibition of downstream pERK signaling in a mutant KRas cell line. Attempts to improve ADME properties of these molecules and engage KRas mutation hotspots (G12, G13, Q61) unexpectedly led to the identification of a previously undisclosed pocket, proximal to the switch I-II pocket. Taking advantage of this expanded canvas we were able to design active-state inhibitors that show nanomolar potency for both the wild-type K/H/NRas proteins as well as a panel of oncogenic-relevant KRas mutants, demonstrating the susceptibility of Ras to pan and active-state inhibition. The present work provides useful insights and tools to enable further investigation of the clinical relevance and safety profile of pan-Ras inhibition.

Chart 1. Chemical structures of some recent Ras Inhibitors



RESULTS AND DISCUSSION

Identification and Characterization of Fragment Hits.

An in-house fragment collection of 656 compounds was screened against KRas^{G12D}-GTPγS using Surface Plasmon Resonance (SPR). Following SPR concentration-response and NMR (STD, WaterLOGSY, and ¹H-¹⁵N HSQC) cross validation we identified five (≈ 1.0% hit rate) confirmed hits, Chart S1. Validated fragment hits were subsequently tested in an isotopically labelled ¹H-¹⁵N HSQC NMR assay. The chemical shift perturbation (CSP)²⁸ of the N-H signals for the fragments had significant overlap with those of literature compounds^{26, 27} indicating, in the absence of structural data, that the fragments bound in a similar site (Figure 1 A, B).

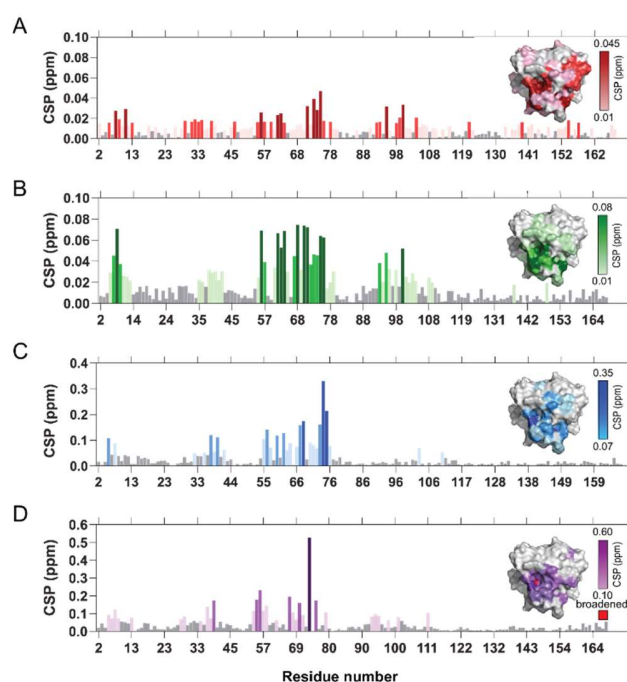
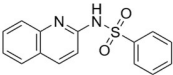
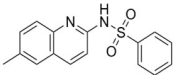
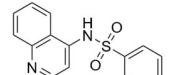
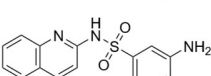


Figure 1. (A) ¹H-¹⁵N chemical shift perturbation (CSP) of KRas^{G12D}-GDP (44 μM) on addition of **5** (1 mM). (B) ¹H-¹⁵N CSP of KRas^{G12D}-GDP (111 μM) on addition of 2-(4,6-dichloro-2-methyl-1*H*-indol-3-yl)ethanamine²⁶ (1 mM). (C) ¹H-¹⁵N CSP of KRas^{G12D}-GDP (130 μM) on addition of **1** (800 μM). (D) ¹H-¹⁵N CSP of KRas^{G12D}-GDP (101 μM) on addition of (2*S*)-*N*-[2-(1*H*-indol-3-ylmethyl)-3*H*-benzimidazol-5-yl]pyrrolidine-2-carboxamide²⁷ (1 mM). Note that G75 is missing due to dynamic broadening.

We also tested close structural analogues of literature hits²⁹ using both commercial sources and chemical synthesis. This resulted in the identification of quinoline sulfonamide **1** that showed significantly greater CSP than the fragments and comparable shifts in ¹H-¹⁵N HSQC NMR experiments to contemporary literature compounds^{26, 27} (Figures 1C, D and S1). Having identified compound **1**, several single point changes were investigated (Table 1). Whilst aniline **4** had marginally improved NMR binding affinity, most changes resulted in inactive compounds (data only shown for compounds where an NMR *K*_D could be generated). Furthermore, due to their inherent fluorescence, the quinoline

compounds proved problematic³⁰ in a SOS1 nucleotide exchange assay (NEA) that we had introduced as a higher-throughput assay to complement the protein-observed NMR assay.

Table 1. NMR binding data for quinolines 1–4

Compd	Structure	KRas ^{G12D} .GDP <i>K_D</i> (μM) ^a
1		630
2		570
3		700
4		370

^a*K_D* values were determined as described in the Experimental Section.

However, hybridization of **1** with fragment hit **5** (Chart S1, Figure 2) provided compound **6**. Although **6** showed only minimal effects in the NEA assay (< 1% inhibition at 200 μM ligand concentration) it had similar affinity to the quinoline sulfonamide compounds in the NMR assay and none of the fluorescence issues. **6** also maintained ligand efficiency (LE)³¹ comparable with **1**, had good permeability in a Caco-2 assay, moderate kinetic solubility and was stable in mouse liver microsomes (Table S1).

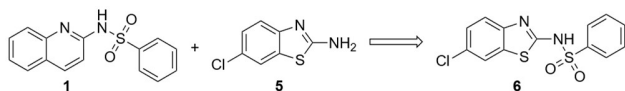


Figure 2. Hybridization of compounds **1** and **5**.

Because of these favourable properties, and absence of any assay interference, compound **6** underwent further investigation. Initial SAR investigation explored the substitution pattern of the 6-chlorobenzothiazole heteroaromatic in conjunction with the introduction of a hydrogen bond donor to either the 2, 3 or 4 position of the phenyl moiety (Table 2). Binding affinity for KRas^{G12D}.GDP, determined using HSQC NMR, showed that whilst 7-chloro analogue **7** had marginally improved binding affinity compared to **6**, introduction of a hydroxyl hydrogen bond donor, compounds **8** and **9**, gave a significant improvement. We also obtained several co-crystal structures with KRas^{C118S}.GDP 1-169 that

confirmed our compounds were binding in the switch I/II pocket. The crystal structure of **8** (Figure 3A), revealed that the 7-chloro benzothiazole heteroaromatic bound in the hydrophobic pocket formed by residues Lys5, Leu6, Val7, Ile55, Leu56, and Tyr74, forming a halogen bond between the 7-chloro substituent and the backbone carbonyl of Tyr71, and a hydrogen bond between the 3-hydroxy substituent and the carboxylate side chain of Glu37. On the other hand, the crystal structure for **9** (Figure 3B) revealed a switched binding mode where the 7-chloro benzothiazole was located outside the hydrophobic pocket and the 2-hydroxy phenyl moiety bound in the hydrophobic pocket group donating a hydrogen bond to Asp54. Aiming to maximize these interactions with Asp54, Tyr71 and Glu37, we synthesized compounds **10** and **11**. The binding mode of **11** (Figure 3C) revealed that the substitution pattern and the geometry of the sulfonamide allowed interactions with all three of these residues and a weaker interaction with the side chain of Gln70, and this resulted in a 40-fold improvement in binding affinity for the GDP-bound state (Table 2). These improvements also led to measurable affinity for KRas^{G12D}.GMPPNP in the NMR assay and moderate inhibition of SOS1-catalyzed nucleotide exchange. Subsequent incorporation of an amide linked basic amine to target the side chain of Asp38 and rigidification by alkylation of the benzothiazole aromatic nitrogen yielded compounds **12** and **13** respectively. Both compounds showed increased binding affinity for the inactive state (<3 μM) and in the case of **13** single-digit micromolar inhibition of SOS1-mediated nucleotide exchange (Tables 2, S6). As the latter compounds were reaching the lower limit for accurate *K_D* determination using the NMR assay²⁸, we introduced surface plasmon resonance (SPR) as our primary assay to measure direct binding of the compounds to KRas^{G12D}, loaded with either GDP or the non-hydrolysable GTP analogue GMPPNP. The binding characteristics of key compounds were also orthogonally verified using isothermal titration calorimetry (ITC) (Table S5). To complement the direct binding assays, we also utilized a homogeneous time-resolved fluorescence (HTRF) biochemical assay to characterise the Ras-Raf protein-protein interaction, and a modified NEA assay that incorporated a readout on Ras-Raf inhibition. The potencies measured in the HTRF assay aligned well with the GMPPNP SPR affinity measurements (Tables 3, 7), and together this suite of assays permitted robust profiling in terms of binding affinity to either the inactive GDP-bound or active GMPPNP-bound states, the ability to interfere with the Ras nucleotide loading/activation state and inhibition of the Ras-Raf effector binding interaction.

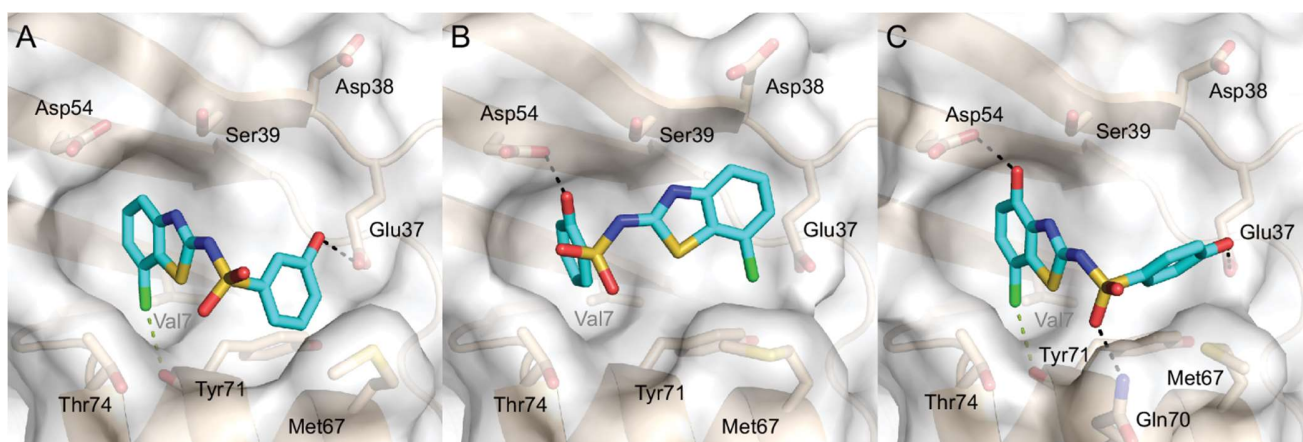
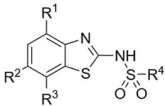
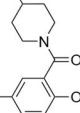
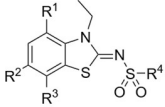
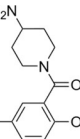
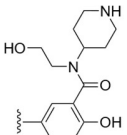


Figure 3. Comparison of the binding modes of **8** (A), **9** (B) and **11** (C). A cartoon representation of the protein is shown in beige with key residues highlighted as sticks and labelled. The ligand is shown in cyan, hydrogen bonding interactions between ligand and protein are indicated by black dashed lines and a likely halogen bond between the ligand chlorine and the backbone carbonyl of Tyr71 is shown as a green dashed line.

Table 2. Modifications to hybrid compound 6

Compd.	R ¹	R ²	R ³	R ⁴				
					NMR KRas ^{G12D} -GDP <i>K_D</i> (μM) ^a	NMR KRas ^{G12D} -GMPPNP <i>K_D</i> (μM) ^a	NEA IC ₅₀ (μM) ^b	NEA w HTRF readout IC ₅₀ (μM) ^b
6	H	Cl	H		870	n.d. ^d	n.d. ^d	n.d. ^d
7	H	H	Cl		620	n.d. ^d	>100 ^c	n.d. ^d
8	H	H	Cl		350	n.d. ^d	n.d. ^d	n.d. ^d
9	H	H	Cl		200	n.d. ^d	n.d. ^d	n.d. ^d
10	OH	H	Cl		41	290	116	39.1 ^c
11	OH	H	Cl		20	180	66.7	40.7 ^c
12	OH	H	Cl		<2 [*]	180	19.8	7.7 ^c
								
13	OH	H	Cl		<3 [*]	48	8.41	3.02

14	OH	H	Cl		n.d. ^d	n.d. ^d	63.1 ^c	n.d. ^d
-----------	----	---	----	-----------------------------------------------------------------------------------	-------------------	-------------------	-------------------	-------------------

^a K_D values were determined as described in the Experimental Section; ^{*} K_D is an estimate as most signals are in the NMR “slow exchange” regime. ^bUnless otherwise noted IC_{50} values are shown as the average of ($n \geq 2$) assay runs and were determined as described in the Experimental Section. ^cshown as $n = 1$ data. ^dNot determined.

Identification of the Benzothiazole Macrocycle Series.

As part of the work targeting Asp38, we synthesized alkylated analogue **14**. Inspection of the crystal structure showed the benzothiazole alkyl and amide ethanol groups were pointing towards each other (Figure 4A). Hypothesizing that macrocyclization could be exploited to gain further potency³² we introduced a five carbon linker between the secondary amide and the benzothiazole nitrogen, aiming to constrain **14** in its bioactive conformation. This strategy increased affinity significantly; compound **15** has a KRas^{G12D}·GDP SPR K_D of 70 nM and a corresponding value of 36.3 μ M in the GMPPNP-bound assay (Table 3, Figure 4B). The crystal structure shows that the binding mode is largely conserved post macrocyclization with the ligand making hydrogen bonds to Asp38, Glu37 and a halogen bond to the backbone carbonyl of Tyr71. The bridging alkyl of the macrocycle adopts a similar conformation to the less constrained alkyl substituents of the precursor suggesting that the macrocycle is in a reasonably unstrained conformation (Figure S2).

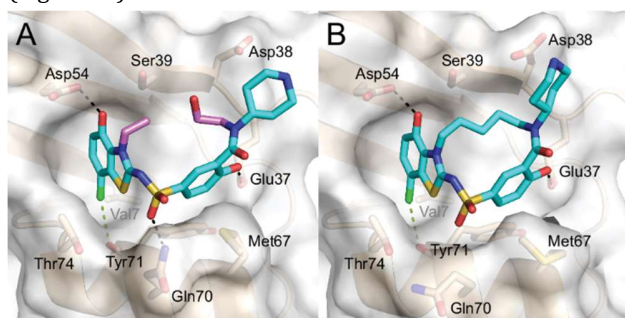


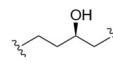
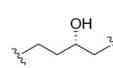
Figure 4. (A) The binding pose of **14** shows its two *N*-alkyl substituents (highlighted in violet) filling out the binding site and pointing towards each other, suggesting that linking them may be advantageous. (B) The resulting macrocycle **15** bound to KRas (see also Figure S2).

Inspection of the crystal structure showed that although the piperidine was oriented towards the side-chain of Asp38, the distance between the amine nitrogen and the

carboxylate was outside standard hydrogen bonding distance³³, at approximately 4.3 Å. With the potential to interact with Asp38 more productively, we therefore synthesized a series of primary, secondary and tertiary cyclic and bicyclic amine analogues, designed to target this residue (Table 3). This led to primary amine **16** that makes a bidentate interaction with Asp38 and the backbone carbonyl of Glu37 (Figure S3). However, the extra interaction afforded no significant improvement in affinity or inhibition of the Ras-Raf interaction, and we did not observe this binding mode for similar primary amine analogues (data not shown). Changing the length of the linker portion of the macrocycle to four carbons (**20**) showed only small differences in either binding affinity or inhibition of the Ras-Raf interaction. However, introduction of longer linkers, for example compound **17**, significantly decreased both binding affinity and inhibition of the Ras-Raf interaction (Table 3). Substitution on the linker was also investigated, inspired by the possibility of making a favorable interaction with the side chain of Ser39, shown in the crystal structure of **15** to be pointing into the binding site. This led to enantiomers **18** and **19**. The crystal structure for **19** shows the compound forms an additional hydrogen bond with Ser39 (Figure S4), however only marginal gains in affinity over unsubstituted compounds were made (Table 3), likely due to the suboptimal geometry and solvent-exposed nature of the introduced hydrogen bond. Unexpectedly the opposite (*R*) enantiomer **18** was significantly less potent than the unsubstituted parent, even though a crystal structure showed the ligand binding as expected, albeit with the linker hydroxyl pointing away from the protein (biochemical data not shown). Despite extensive SAR exploration, and achieving low nanomolar affinity for the inactive state, affinity for the active state in this pocket plateaued around 1 μ M, with the *cis*-azaspiro[4.5]decane **21** and the C-3 (*S*)-hydroxyl **19** compounds proving to be the most successful in terms of both GDP-bound and GMPPNP-bound affinity for KRas.

Table 3. Derivatization of the benzothiazole macrocycle scaffold

Compd.	R ^a		SPR	SPR	HTRF IC_{50} (μ M) ^b	NEA IC_{50} (μ M) ^b	NEA w HTRF readout IC_{50} (μ M) ^b	
			(KRas ^{G12D} ·GDP) K_D (μ M) ^b	(KRas ^{G12D} ·GMPPNP) K_D (μ M) ^b				
14	OH	H	Cl		n.d. ^d	n.d. ^d	63.1 ^c	n.d. ^d

15		-(CH ₂) ₅ -	0.070	36.3	1.72	1.52	0.182
16		-(CH ₂) ₅ -	0.112	5.75	1.43	0.414	0.068
17		-(CH ₂) ₆ -	0.350	9.97	6.46	1.65	0.287 ^c
18			1.88	38.1	15.3 ^c	n.d. ^d	1.47
19			0.041	1.04	1.10	n.d. ^d	0.119
20		-(CH ₂) ₄ -	0.044	1.45	1.31	2.76	0.163
21		-(CH ₂) ₅ -	0.011	1.25	1.39	0.463	0.140
22		-(CH ₂) ₅ -	0.044	2.61	2.01	0.791	0.211
23		-(CH ₂) ₅ -	0.067	2.94	3.09	1.14	0.070
24		-(CH ₂) ₅ -	0.558	12.2	10.6 ^c	n.d. ^d	0.353
25		-(CH ₂) ₅ -	0.582	22.1 ^c	7.36 ^c	n.d. ^d	0.283
26		-(CH ₂) ₅ -	0.866	23.1 ^c	9.47	3.11 ^c	1.85 [†]
27		-(CH ₂) ₅ -	0.064	3.53	2.87	1.21 ^c	0.070
28		-(CH ₂) ₅ -	0.087	1.94	2.69 ^c	1.57 ^c	0.061

^aCompounds containing a basic amine were synthesized and assayed as the HCl salt as described in the Experimental Section. ^bUnless otherwise noted IC₅₀ and K_D values are shown as the average of ($n \geq 2$) assay runs and were determined as described in the Experimental Section. ^cValue is shown as $n = 1$ data. ^dNot determined.

Preliminary *in vitro* ADME properties were measured for some macrocyclic compounds. In general, good kinetic solubilities were obtained, however low permeability (P_{app}

(A2B) in a Caco-2 assay) coupled with high efflux ratios, along with high intrinsic clearance in both mouse microsomes and hepatocytes suggested the compounds may

suffer from low peripheral exposure (Table 4.) To confirm this, a PK study in mice with **22** (single dose level of 1 mg/kg; dose volume 5 mL/kg) showed low exposure and high clearance (Tables S11, S12) consistent with the *in vitro* profile. A hepatocyte metabolite identification study on **22** and **23** indicated both phenols were subjected to glucuronidation combined with dealkylation at the tertiary amine

(Tables S8, S9). Calculated properties also indicated high tPSA and the potential for the macrocycles to exist in zwitterionic form at pH 7.4 (Table S7). However, strategies aiming to reduce the basicity of the cyclic amine, compounds **24** and **25** resulted in a significant drop-off in affinity, and deletion of the basic amine (**26**) was also detrimental.

Table 4. Solubility, Permeability, Microsomal and Hepatocyte clearance data for selected compounds.

	22	23	16
Kinetic Solubility ^a (μM)	>200	>200	>200
Caco-2 Permeability: P _{app} A2B (x 10 ⁻⁶ cm s ⁻¹) [Efflux Ratio]	0.05 [>50]	0.11 [>50]	0.0712 [10.4]
Microsomal stability Cl _{int} (μL/min/mg protein)	31.9	>200	15.9
Hepatocyte stability Cl _{int} (μL/min/10 ⁶ cells)	155	175	14.7

^a Solubilities were determined as described in the Experimental Section.

In order to measure inhibition of Ras-Raf binding in a cellular context a NanoLuc Binary Technology (NanoBit) engagement assay³⁴ was generated in HEK293A cells. In this assay the KRas^{G12C} inhibitor sotorasib and the EGFR inhibitor erlotinib were used to show mutant specific effect on the HEK293A cells expressing LgBiT-Ras variants (KRas^{G12C}, KRas^{G12D}, KRas^{WT}, NRas^{WT}, HRas^{WT}) (Figure 5A). As a negative control in the NanoBit assay, we generated HEK293A cells expressing KRas4B^{WT} bearing specific double point mutations (Y71N and T74W). Identified by *in silico* mutagenesis, these Ras mutants were chosen to disrupt compound binding whilst having minimal effect on effector binding (data not shown). Compounds **27** and **28** demonstrated moderate concentration-dependent inhibition of the WT/G12C/G12D KRas-Raf and H/NRas^{WT}-cRaf interaction (Table 5 and Figure 5A) after 3 h treatment and 25 min EGF stimulation, and as hypothesized significantly reduced binding affinity when assayed in KRas4B^{WT} cells bearing the double point mutations (Figure 5B). Some differences across the Ras variants were observed in the NanoBit assay where the strongest effects were observed against Ras^{WT} (all isoforms), followed by KRas^{G12C} and KRas^{G12D}, likely due to the selectivity of these compounds for the GDP-bound form and possibly differences in intrinsic GTPase activities between the wild-type and mutant cell lines. Inhibition of

Ras-Raf binding after treatment with a set of compounds active in the NanoBit assay was also confirmed by cellular pull-down assay. The GTP-bound forms of Ras were pulled down with GST fusion proteins corresponding to the Ras-binding domain of Raf in a Ras^{WT} PC3 cell line, and a dose-response inhibition was detected (IC₅₀ = 0.45–0.79 μM; Figure S7A). In addition, several tertiary amines such as **23**, **27** and **28** displayed inhibition of ERK phosphorylation in a MIA PaCa-2 KRas^{G12C} cell line (Table 5 and Figure 5C). It has been shown previously that cells grown in anchorage-independent settings are more dependent on KRas for growth than in more traditional 2D systems.³⁵ Therefore, having observed inhibition of Ras-Raf binding and of downstream pERK in KRas mutant cells, we investigated the impact of compound treatment on MIA PaCa-2 spheroid model survival (Figure S7B). Data analysis showed these compounds having a modest effect on cell survival, with **28** being the most active (IC₅₀ = 2.07 μM). To rule out any off-target effects on cell survival, lung cancer NCI-H1437 cells were used as a negative control. These are Ras wild-type cells but bear a Q56P activating mutation on the MEK protein, and therefore do not respond to Ras inhibition.³⁶ As expected, no significant effect on NCI-H1437 cells was observed (Figure S7B) suggesting that decreased cell survival was due to on-target inhibition.

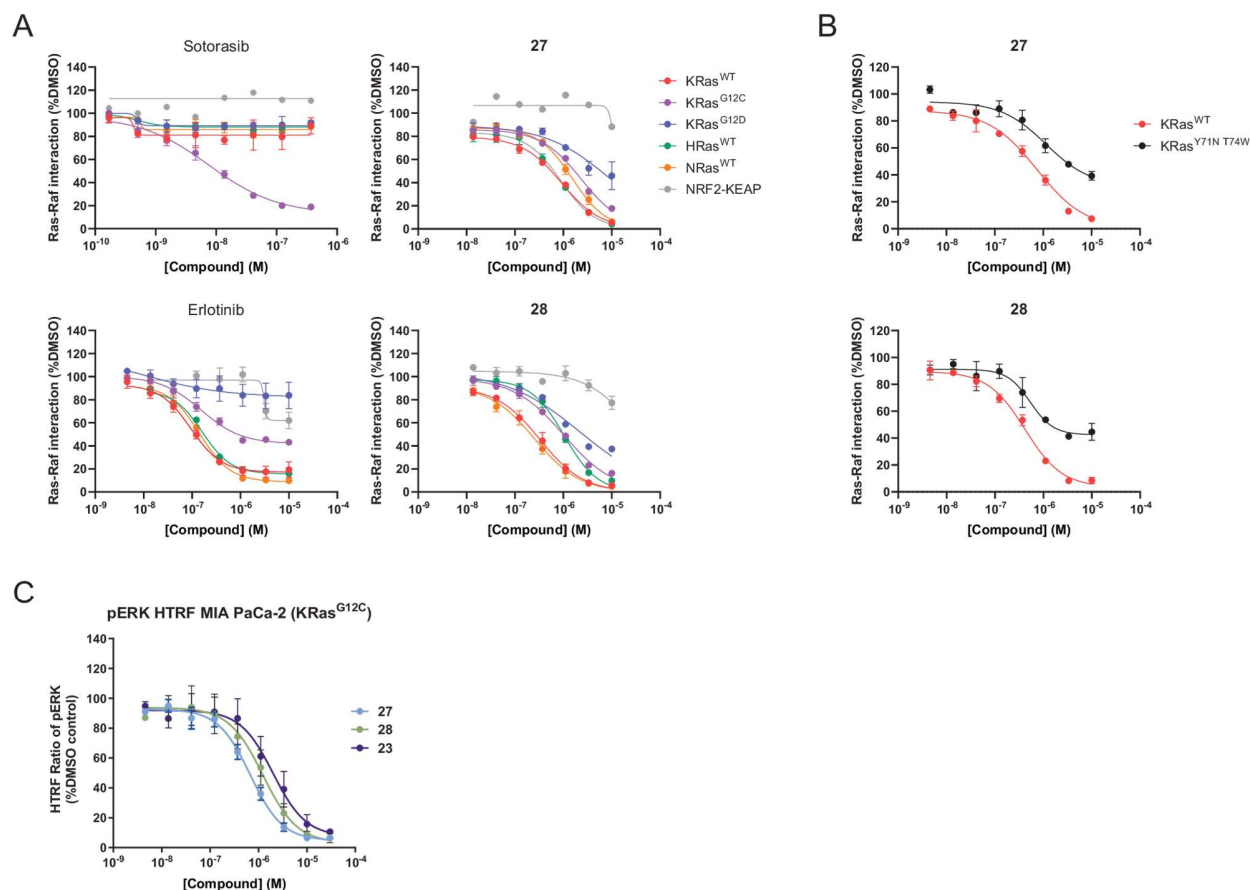


Figure 5. (A) Target engagement assay with NanoBiT performed on live HEK293A cells containing SmBiT-Raf and LgBiT-Ras (with KRas^{WT}, KRas^{G12C} and KRas^{G12D}, or NRas^{WT} or HRas^{WT}), after treatment with the mutant-specific inhibitors sotorasib (KRas^{G12C}) and erlotinib (Ras^{WT}) as well as selected in-house compounds. HEK293t containing SmBiT-NRF2 and LgBiT-KEAP1 were used as a negative control cell line. (B) NanoBiT assay performed in live cells expressing the binding-ablating KRas^{Y71N, T74W} mutant. For (a) and (b), the cells were treated for 3 h in 5% FBS media, followed by EGF stimulation for 25 min. Graphs represent the average of two independent experiments \pm the SEM (except for 27 and sotorasib in the NRF2-KEAP1 cell line, where only one experiment is represented). (C) Dose-dependent pERK modulation in HTRF assay using the KRas G12C-MIA PaCa-2 cell line for selected compounds. The cells were treated for 3 h in complete 10% FBS media. Graphs represent the average of two to five independent experiments \pm the SEM. Representative graphs for selected compounds are shown.

Table 5. NanoBiT and pERK Cell Data

Compd	NanoBiT IC ₅₀ (μ M) ^a					pERK HTRF IC ₅₀ (μ M) ^a	
	HEK293A-Raf-KRas ^{WT}	HEK293A-Raf-KRas ^{G12C}	HEK293A-Raf-KRas ^{G12D}	HEK293A-Raf-HRas ^{WT}	HEK293A-Raf-NRas ^{WT}	MIA PaCa-2 G12C	
22	>10	>10	>10	>10	3.45	5.69	
23	2.87	7.12	>10	5.79	2.73	1.99	
27	0.56	1.71	5.94	1.21	0.64	0.65	
28	0.27	0.99	2.53	1.00	0.21	1.17	

^aIC₅₀ values were determined as described in the Experimental Section.

Compounds based on **15** consistently showed a significant, and sometimes dramatic drop-off in affinity between the inactive and active forms of KRas. In part, this is likely to be due to the conformation of Glu37 in the two loading states. In the GDP state the conformation of switch-I enables Glu37 to position itself in a pocket formed by Leu56-Ala59 and Tyr71, to some extent folded away, but in a conformation allowing one of the carboxylate oxygens to hydrogen bond to the ligand. However, the switch conformation in GTP-bound KRas pushes Glu37 into the binding site

(Figure 6), making it unable to hydrogen-bond to Ala59 and partly blocking the site.

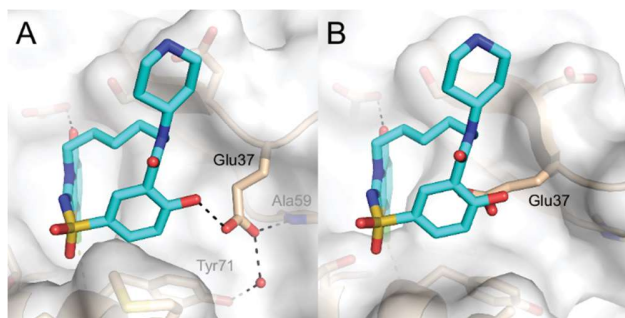


Figure 6. Comparison of the Glu37 conformation between KRas-GDP and KRas-GMPPNP. (A) The KRas-GDP·**15** complex shows the side chain of Glu37 (excluded from the molecular surface) clearly positioned by multiple hydrogen-bonding interactions with the rest of the protein and well-positioned to interact with the bound ligand. The same conformation is preformed in equivalent ligand-free structures (data not shown). (B) In a representative ligand-free KRas-GMPPNP structure (PDB ID 3GFT), the changes in switch conformations push a more exposed Glu37 into our ligand binding site, where it can be seen clashing with **15** superimposed from the model in panel A.

For these macrocycle compounds to bind to the GTP-bound conformation of KRas, they are required to push Glu37 aside, thereby incurring an energy penalty to binding. In addition, Asp38 exhibits extensive side chain flexibility, although two conformations are dominant. One of these conformations can interact with the ligand and is a conserved conformation across most of our ligand complexes. This is also the side-chain conformation observed in most GDP-bound apostructures. However, most GTP-bound apostructures show the conformation seen in Ras-effector complexes,³⁷ with the Asp38 carboxylate rotated away from the amine group. For these reasons and despite extensive SAR exploration, affinity of our ligands for the GMPPNP-bound state in this pocket plateaued at the one micromolar level.

Identification of the Aminopyridine “Interswitch” Macrocyces.

Literature and in-house molecular dynamic simulations (not shown) had indicated flexibility in the switch regions³⁸ that might allow growing of our ligands towards the Gly12 mutation site and the nucleotide binding site, utilizing the sulfonamide 2-hydroxy position as a growth vector (Figure 7A). This would potentially enable mutant selectivity, while also allowing us to investigate bioisosteric replacements for the phenolic moiety. Aiming to maintain similar interactions with Glu37 but potentially improve metabolic stability, we chose to incorporate an aminopyridine to replace the 2-hydroxy phenol moiety of the *cis*-azaspiro[4.5]decane compound **21**. Synthetic chemistry efforts towards this analogue employed a *para*-methoxy benzyl (PMB) protecting

group, and serendipitously the side-product **29** (Scheme 5) was submitted for testing. Although ITC binding affinity (Table S5), and potency in the biochemical HTRF assay was moderate (Table 6), we were successful in obtaining a GDP-bound KRas^{WT} crystal structure (Figure 7B). Surprisingly the compound had induced a novel pocket between switch-I and switch-II not seen in previous in-house or literature crystal structures. Further exploration of this hitherto unexplored “Interswitch” region of the protein was undertaken (Table 7). In contrast to the *bis*-phenol benzothiazole macrocycles (compounds **15–28**), where a significant drop-off in affinity between inactive and active loading states is invariably observed, pyrrolidine **31** has equipotent affinity for both nucleotide loading states. The crystal structure of the KRas^{WT}·GMPPNP·**31** complex (Figure 7C) shows both switch regions partly disordered and their structured parts adopting unusual conformations, which allows the ligand pyrrolidine to donate a hydrogen bond to Glu63. The major conformation of Glu37 shows its side chain pointing into the Interswitch region, suggesting it might be available for additional ligand interactions. These were realized by the piperazine analogue **32**, which regains a hydrogen-bond to a (shifted) Glu37 side chain (Figure 7D). Extending the compounds deeper into the Interswitch region gave the *cis*-cyclohexyl derivative **33**, which binds to KRas-GMPPNP with sub-micromolar affinity by SPR. Further exploration of the binding site with a series of basic amines yielded **34**, which has single-digit micromolar affinity for GDP-bound KRas and sub-micromolar affinity for GMPPNP-bound KRas, as well as **35**, which shows sub-micromolar affinities for both loading states of KRas. Both compounds also have sub-micromolar potency in the HTRF assay. The crystal structure of KRas-GMPPNP in complex with **34** reveals that, while the switch regions continue to be partially disordered, Glu37 and Asp38 are stabilised in a single (previously minor and unmodeled) conformation with the Asp38 side chain now pointing into the binding site, where it accepts a hydrogen bond from the ligand, while Glu37 now points outwards into solvent (Figure 7E). Rigidification of the pendant amine then led to **36**. This compound exhibits nanomolar affinity for GMPPNP-bound KRas in direct binding assays (SPR and ITC), and interestingly a high degree of selectivity for the GMPPNP-bound state (Table 7, Table S5). The crystal structure of **36** with KRas^{WT}·GMPPNP shows the C-terminal end of switch-I in the same Asp38-in conformation, with the Asp38 side chain making a bidentate interaction with two ligand amines (Figure 7F). In addition, the structure shows the compound making a water-mediated hydrogen bond to the γ -phosphate of the nucleotide (GMPPNP), which likely contributes to selectivity for the active state.

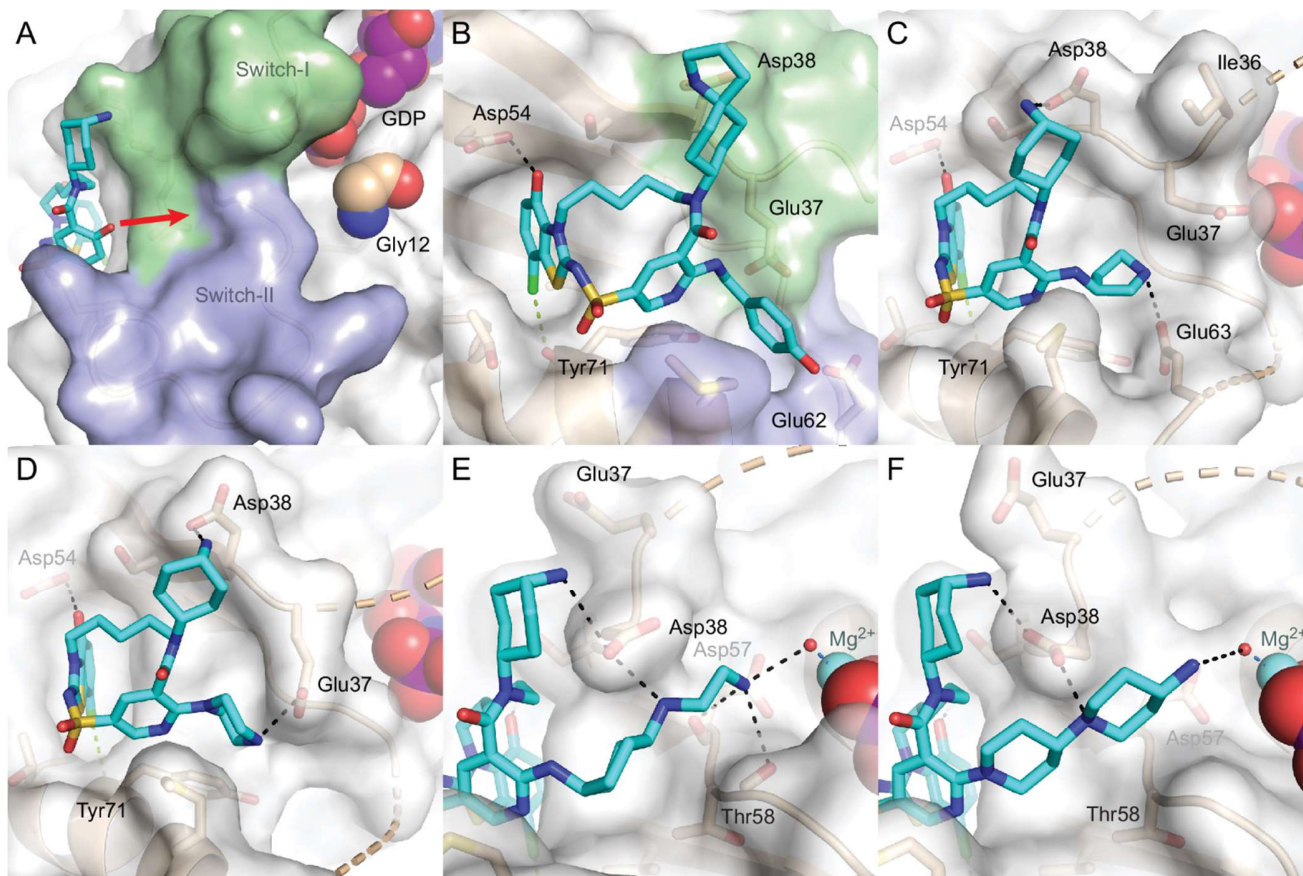


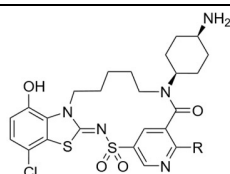
Figure 7. (A) The KRas-16 complex with the switch regions highlighted (switch-I in pale green, switch-II in pale blue). Gly12 is excluded from the molecular surface and shown as beige spheres, while the bound nucleotide is shown as purple spheres. The possible growth vector from the ligand is indicated by a red arrow. (B) The PHB of **29** opens up a new subpocket. (C) Binding of **31** displaces and partly disorders (dashed coil) switch-I. Glu37 still faces the ligand, but no longer hydrogen-bonds to it. Instead the pyrrolidine donates a hydrogen bond to Glu63 on switch-II (also partly disordered). (D) In the KRas-32 complex the switch regions are in similar conformations to those seen for KRas-31, but in this case Glu37 is positioned to accept a hydrogen bond from the ligand piperazine. (E) The crystal structure of **34** in complex with KRas shows switch-I further detached so that Asp38 is now facing the ligand. (F) **36** makes improved interactions with Asp38. Both **34** and **36** extend towards the nucleotide-binding site, hydrogen-bonding to one of the water molecules coordinating (blue dashed line) the Mg^{2+} (pale cyan).

Table 6. HTRF and NEA biochemical data for compound 29

Compound	R	SPR (KRas ^{G12D} ·GDP) K_D (μM) ^a	SPR (KRas ^{G12D} ·GMPPNP) K_D (μM) ^a	HTRF IC_{50} (μM) ^a	NEA IC_{50} (μM) ^a	NEA w HTRF readout (μM) ^a
29		n.d. ^b	n.d. ^b	6.84	3.63	6.19

^a IC_{50} values are shown as the average of ($n \geq 2$) assay runs and were determined as described in the Experimental Section. ^b Not determined.

Table 7. Exploration of the 2-position of the aminopyridine macrocycle



Compound	R ^a	SPR	SPR	HTRF IC ₅₀ (μM) ^b	NEA w HTRF readout (μM) ^b
		(KRas ^{G12D} ·GDP) K _D (μM) ^b	(KRas ^{G12D} ·GMPPNP) K _D (μM) ^b		
30	NH ₂	1.89	62.0	20.3 ^c	0.843
31		3.12	2.70	6.60	3.91
32		0.160	1.41	1.91 ^c	n.d. ^d
33		1.25	0.728	1.05 ^c	0.471
35		0.789	0.738	0.585	0.443
34		1.69	0.826	0.472	0.526
36		2.73	0.322	0.341	0.267

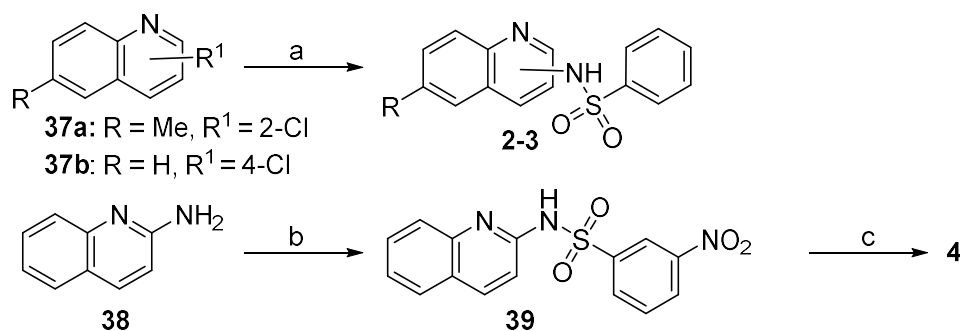
^aCompounds containing a basic amine were synthesized and assayed as their respective HCl salts as described in the Experimental Section. ^bUnless otherwise noted IC₅₀ and K_D values are shown as the average of ($n \geq 2$) assay runs and were determined as described in the Experimental Section. ^cValue is shown as $n = 1$ data. ^dNot determined.

To assess any mutant or isoform selectivity, selected compounds were profiled against a panel of biologically relevant KRas mutants (G12D/G13D/G12C/G12V/Q61K) and the wild-type K/H/NRas proteins using the biochemical HTRF assay (Table S3). The compounds tested demonstrated moderate selectivity for the KRas G12D, G13D and G12V mutants and, for most examples, wild-type HRas. In contrast, the Q61K mutant appeared slightly less susceptible in this assay, particularly with the aminopyridine macrocycle compounds. SPR binding affinities for both GMPPNP-loaded and GDP-loaded wild-type K/H/NRas were also determined for selected compounds (Table S4). Here only minor differences were observed between the isoforms. Despite some marginal differences between the variants as described above, the values obtained in the HTRF assay were within 5-fold ($Ras^{m/isoform} / KRas^{WT}$) (Figure S6), suggesting these compounds can target a broad range of KRas mutants and Ras isoforms *in vitro*.

Synthesis. The synthesis of compounds **2–4** and **6–14** is outlined in Schemes 1 and 2. Coupling of commercially available chloro-quinolines **37a** or **37b** with benzenesulfonamide using Buchwald-Hartwig conditions afforded quinoline sulfonamides **2** and **3**. Reaction of aminoquinoline **38** with 3-nitrobenzenesulfonyl chloride in anhydrous

pyridine afforded intermediate sulfonamide **39**. Compounds **6**, **7** and intermediates **41a–e** were obtained in a similar fashion starting from either **40a**, **40b** or **40c** and reacting with an appropriate commercially available sulfonyl chloride. Reduction of **39** in the presence of Palladium and ammonium formate afforded **4**, whilst compounds **8–11** were obtained from **41a–e** by conversion of the aryl methyl ether to the corresponding phenol using boron tribromide. Compound **12** was accessed starting from **41e**. Hydrolysis of the ester to the corresponding carboxylic acid **42**, followed by propylphosphonic anhydride mediated amide formation with *tert*-butyl *N*-(4-piperidyl)carbamate provided intermediate **43**, which was globally deprotected using boron tribromide to afford the desired final compound. To prepare compounds **13** and **14**, **42** was alkylated with bromoethane to afford a non-separable mixture of *N*-ethyl regioisomers (approximately 5:1 benzothiazole:sulfonamide nitrogen) as their corresponding ethyl esters. After hydrolysis of the ethyl ester, the resulting mixture of *N*-ethyl regioisomers were converted to amides **46a–46b** using the required secondary amine and propylphosphonic anhydride as coupling reagent. Subsequent methyl ether deprotection with boron tribromide yielded the desired final compounds.

Scheme 1. Synthetic Route for Quinoline Sulfonamides **2–4**^a



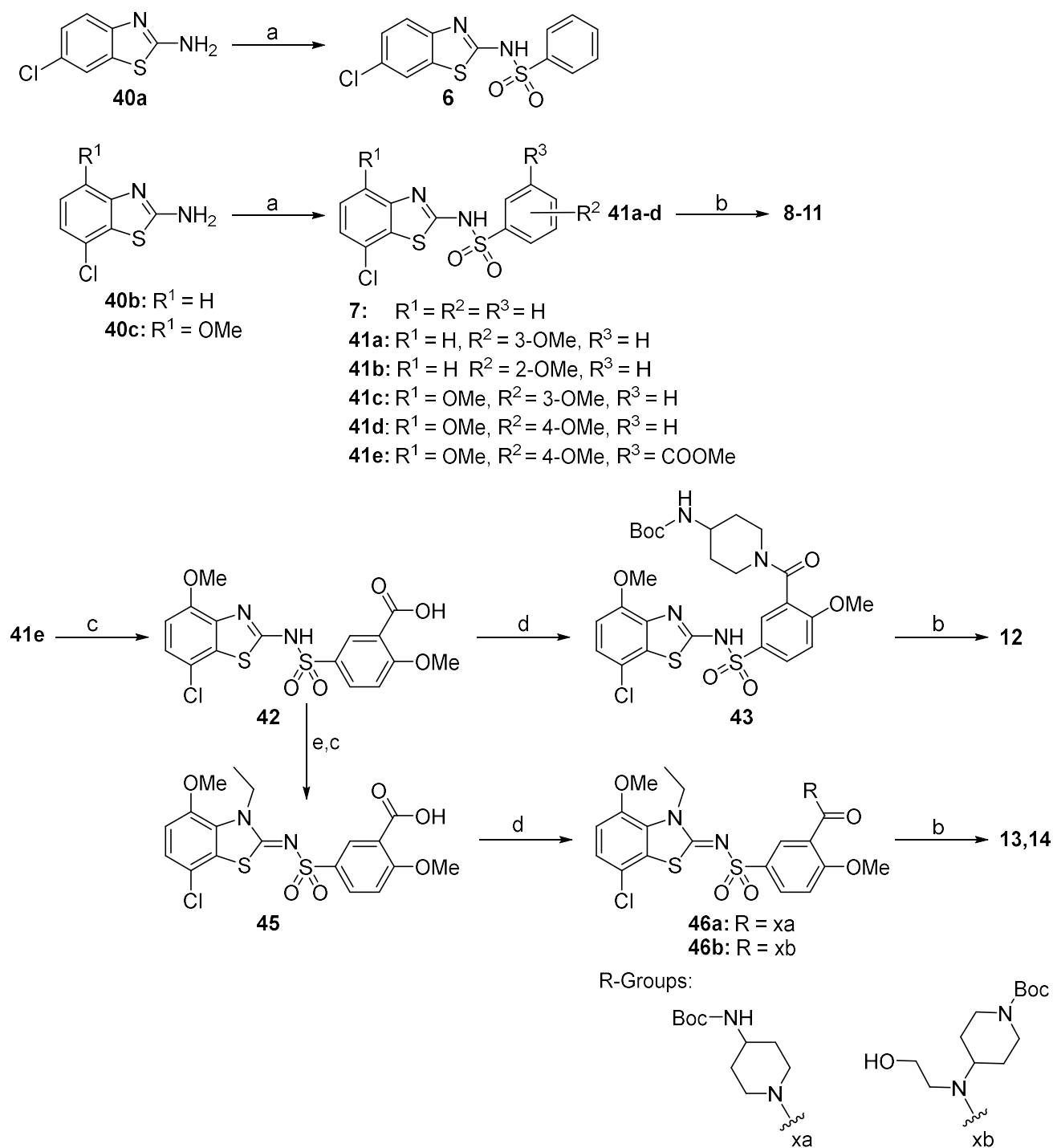
^aReagents and conditions: (a) [For **2-3**] **37a** (**2**) or **37b** (**3**), benzenesulfonamide, 1,1 *tris*(dibenzylideneacetone)dipalladium(0), 1,1-*bis*(diphenylphosphino)ferrocene, cesium carbonate, 1,4-dioxane, 140–180 °C, μ wave, 10 min; (b) 3-nitrobenzenesulfonyl chloride, anhyd pyridine, rt, 2 h; (c) Pd/C 10%, NH₄HCO₂, EtOH, 80 °C, 6 h, rt, 16 h.

Macrocycles **15–17**, **20**, **22** and **26** were synthesized as depicted in Scheme 3. Amidation of benzoic acid **42** with an appropriate primary amine afforded secondary amides **47a–c**. Alkylation of the aminobenzothiazole portion of the molecule with either 1,4-dibromobutane, 1,5-dibromopentane or 1,6-dibromopentane afforded a separable mixture of *N*-alkylated regioisomers (approximately 9:1 benzothiazole:sulfonamide nitrogen). Ring closure of the desired regioisomers **48a–e** via a sodium hydride mediated S_N2 reaction afforded macrolactams **49a–e** which underwent global deprotection using boron tribromide. Finally, compounds containing a basic amine were treated with a solution of HCl to afford compounds **15–17**, **20** and **26** as HCl salts. Alternatively as depicted in Scheme 4, alkylation of benzothiazole **50** with 2-(2-bromoethyl)oxirane afforded epoxide **51a**. In a similar fashion, bromide **51b** was obtained after alkylation of **50** with 1,5-dibromopentane. Ytterbium triflate catalyzed regioselective ring opening of epoxide **51a** with *cis-tert*-butyl *N*-(4-aminocyclohexyl)carbamate provided racemic β -amino alcohol **52**. Hydrolysis of the ester yielded key intermediate **53**, which when treated with 3-(diethoxyphosphoryloxy)-1,2,3-benzotriazin-4(3*H*)-one (DEPBT) afforded macrolactam **54**. To minimize any undesired heterocoupling reactions, this step was conducted at high dilution (0.005M concentration). Chiral separation provided enantiomeric pair **55a** and **55b**. Subsequently these were globally deprotected using boron tribromide followed by salting of the primary amine to afford compounds

18 and **19** as HCl salts. Similarly, reaction of **51b** with appropriate primary amines, followed by hydrolysis of the ester yielded key intermediates **57a–d**. Macrolactamization using either DEPBT or HATU afforded the macrocycles **49b** and **49h–j**. Boc group deprotection of **49b** and **49h** to afford the corresponding secondary amines **49f** and **49k**, followed by alkylation with an appropriate electrophile, furnished tertiary amines **49l–49o**. **49i**, **49j**, **49l–o**, were then treated with boron tribromide and the basic amines salted with a solution of HCl to give final compounds **21**, **23–25**, **27–28**. The initial route towards aminopyridine-containing compounds installed the aminopyridine substituent early in the synthesis (Scheme 5). Starting from PMB-substituted aminopyridine **58** (see Supporting Information), **29** was obtained in six steps in an analogous manner to compound **21**. Alternatively, variation of the substituted aminopyridine portion of the molecule was enabled from either late-stage intermediate **68a** or **68b** (Scheme 6). Thioethers **67a–b** were obtained using a similar strategy to compound **49b**. Oxidation of the thioether to the sulfone using *m*-CPBA followed by S_NAr reaction with the desired amine nucleophiles provided compounds **69a–g**. Global deprotection with either HCl (**32**) or boron tribromide (**30**, **31**, **33–36**) and salt formation provided final compounds **30**, **31–36**.

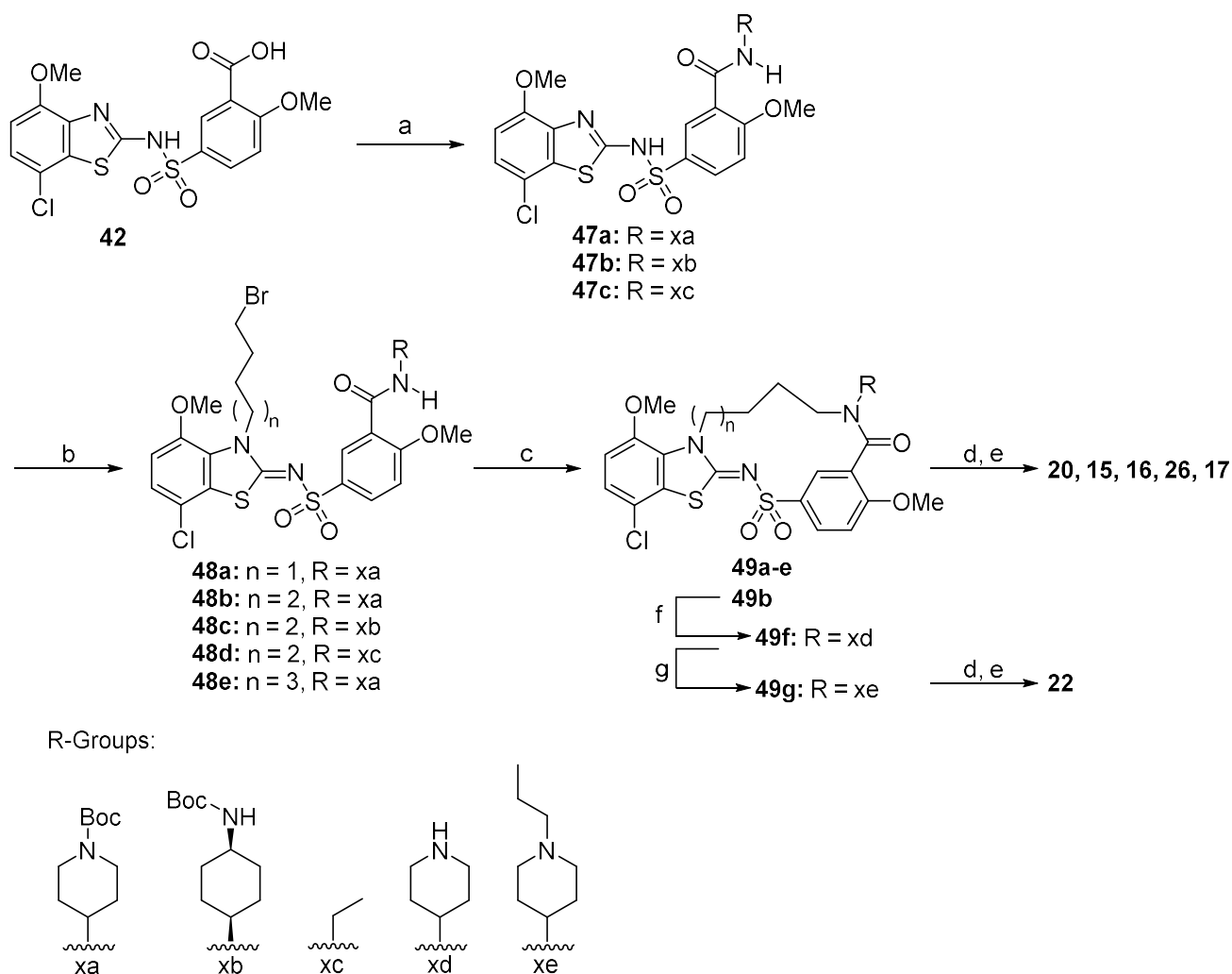
CONCLUSIONS

Scheme 2. Synthetic Route for Benzothiazole sulfonamides **6–14**^a



^aReagents and conditions: (a) [for **6**, **7**, **41a–41e**] benzenesulfonyl chloride (**6**, **7**) or 3-methoxybenzenesulfonyl chloride (**41a**, **41c**) or 2-methoxybenzenesulfonyl chloride (**41b**) or 4-methoxybenzenesulfonyl chloride (**41d**) or methyl 5-chlorosulfonyl-2-methoxybenzoate (**41e**), anhyd pyridine, rt, 6–16 h; (b) BBr₃, DCM, 0 °C – rt, 16 h; (c) 4 M LiOH (aq.), MeOH, rt, 1 h; (d) [for **43**, **46a**] *tert*-butyl *N*-(4-piperidyl)carbamate, propylphosphonic anhydride solution (50% w/v in ethyl acetate), DIPEA, DCM, rt, 16 h; [for **46b**] *tert*-butyl 4-(2-hydroxyethylamino)piperidine-1-carboxylate, HATU, DIPEA, DMF, rt, 5 h; (e) bromoethane, K₂CO₃, DMF, rt, 16 h.

Scheme 3. Synthetic Route for Benzothiazole Macrocycles **15–17**, **20** and **26**^a

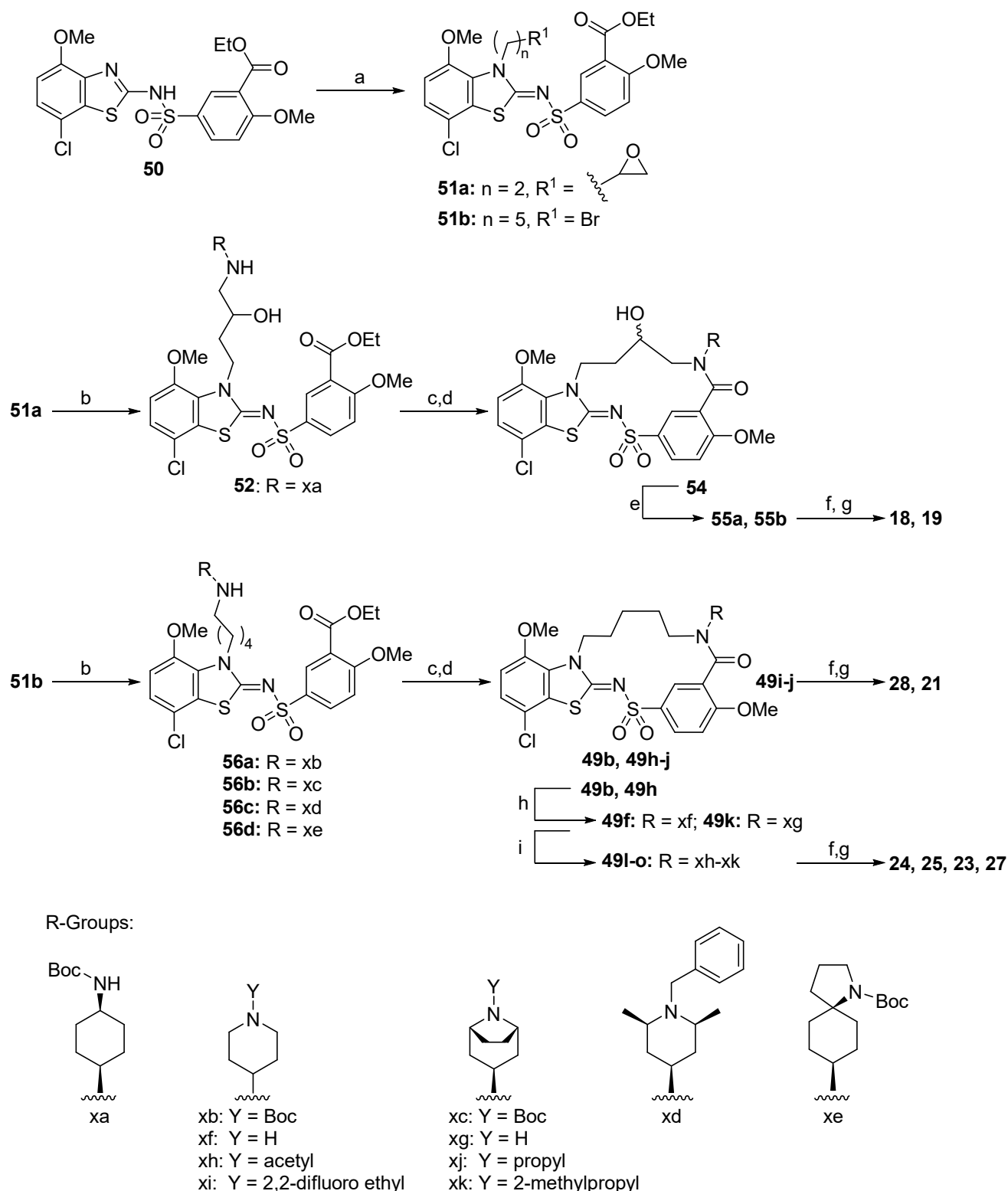


^aReagents and conditions: (a) [for **47a**, **47b**] *tert*-butyl 4-aminopiperidine-1-carboxylate (**47a**) or *cis-tert*-butyl *N*-(4-aminocyclohexyl)carbamate (**47b**), propylphosphonic anhydride solution in ethyl acetate (50% w/w), NEt₃, anhyd THF, rt, 16 h; [for **47c**] ethylamine 2.0 M in THF, propylphosphonic anhydride solution in ethyl acetate (50% w/w), DIPEA, anhyd DCM, rt, 16 h; (b) [for **48a-e**] 1,4-dibromobutane (**48a**) or 1,5-dibromopentane (**48b-d**) or 1,6-dibromohexane (**48e**), K₂CO₃, anhyd DMF, rt, 16–48 h; (c) sodium hydride, anhyd DMF, 0 °C to rt, 16 h; (d) BBr₃, anhyd DCM, 0 °C to rt; (e) 5–6 N HCl in 2-propanol or 4 N HCl in 1,4-dioxane; (f) TFA, DCM, rt, 24–60 h; (g) 1-bromopropane, sodium iodide [cat.], NEt₃, anhyd MeCN, 65 °C, 16 h.

In September of 2020, the first phase I clinical trial results for KRas^{G12C} inhibitor (sotorasib) treatment were published⁷ showing encouraging results for patients with NSCLC and CRC, reaching either a stable disease or an objective response after treatment. Whilst promising and FDA approved, only a limited portion of patients benefit from

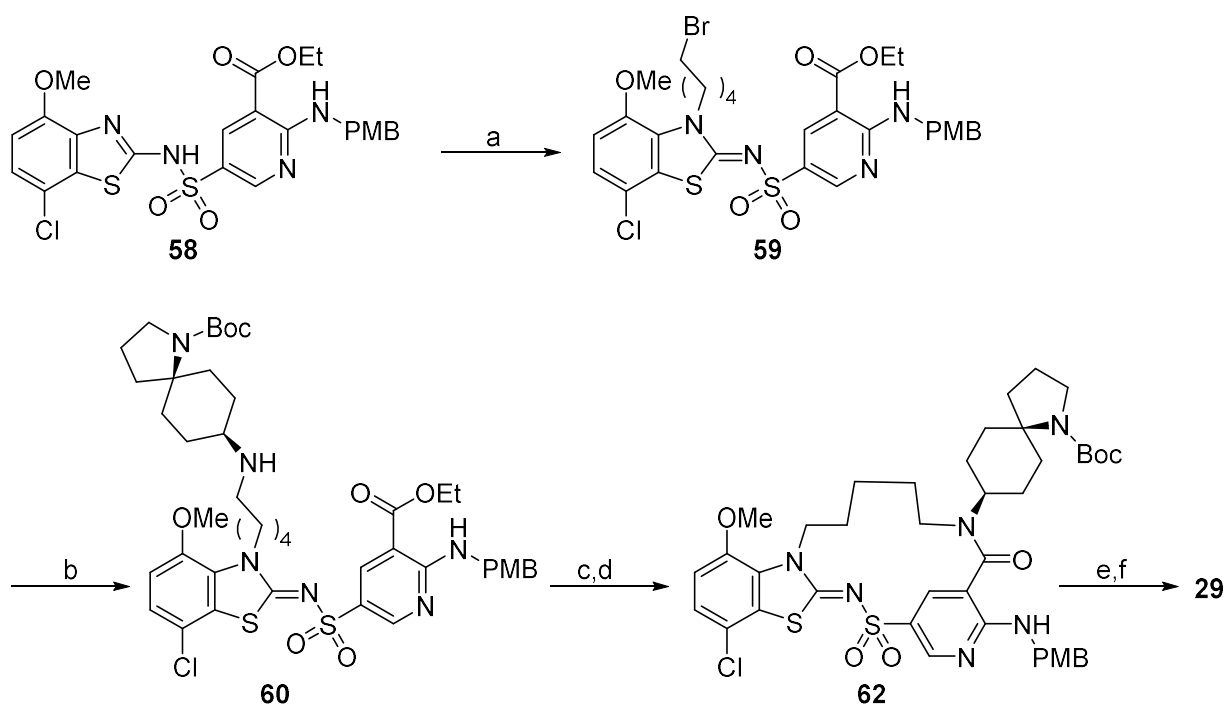
treatment with KRas^{G12C} specific inhibitors, and we now know that treatment with sotorasib and other KRas^{G12C} targeted therapies are often associated with resistance and that most patients eventually relapse.^{8-10, 12, 39, 40} Several studies are ongoing to

Scheme 4. Synthetic Route for Benzothiazole Macrocycles **18–19**, **21–25**, **27–28**^a



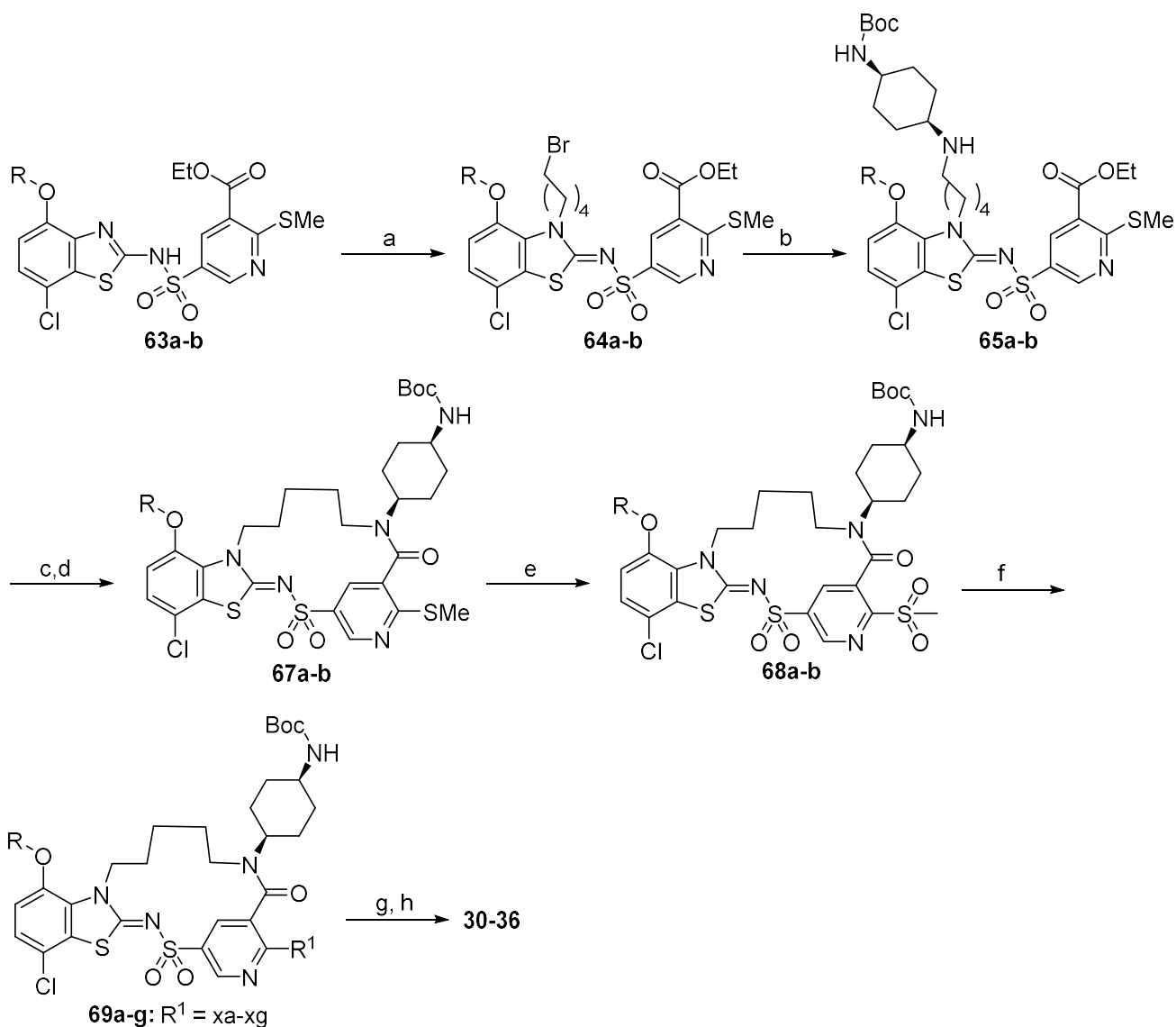
^aReagents and conditions: (a) [for **51a**] 2-[2-bromoethyl]oxirane, K_2CO_3 , 120°C , μwave , 5 min; [for **51b**] 1,5-dibromopentane, K_2CO_3 , anhyd DMF, rt, 2 d; (b) [for **52**] *cis-tert-butyl N*-(4-aminocyclohexyl)carbamate, ytterbium(III) trifluoromethanesulfonate, THF, 130°C , μwave , 60 min; [for **56a**] *tert-butyl 4-aminopiperidine-1-carboxylate*, K_2CO_3 , anhyd MeCN, 60°C , 3 d; [for **56b**, **56c**] *tert-butyl (1R,5S)-3-amino-8-azabicyclo[3.2.1]octane-8-carboxylate (56b)* or *(2R,4r,6S)-1-benzyl-2,6-dimethylpiperidin-4-amine (56c)*, K_2CO_3 , anhyd MeCN, 80°C , 24 h; [for **56d**] *tert-butyl cis-8-amino-1-azaspiro[4.5]decane-1-carboxylate (83)*, K_2CO_3 , anhyd MeCN, 55°C , 6 d; (c) 4 M LiOH (aq.), rt, 16 h; (d) [for **54**, **49i**, **49j**] 3-(diethoxyphosphoryloxy)-1,2,3-benzotriazin-4(3H)-one, NEt_3 , anhyd DMF, 16 h; [for **49b**, **49h**] HATU, NEt_3 , anhyd DMF, 16 h; (e) HPLC chiral separation; (f) BBr_3 , anhyd DCM, 0°C to rt, 16 h; (g) 5–6 N HCl in 2-propanol or 4 N HCl in 1,4-dioxane; (h) TFA, DCM, rt, 24–60 h; (i) [for **49l**] acetyl chloride, DMAP, NEt_3 , anhyd DCM, rt; [for **49m**] 2,2-difluoroethyl trifluoromethanesulfonate, anhyd MeCN, NEt_3 , reflux, 2 h; [for **49n**] 1-iodopropane, NEt_3 , anhyd MeCN, 80°C , 7 h; [for **49o**] 1-bromo-2-methyl-propane, sodium iodide (cat.), NEt_3 , anhyd MeCN, 80°C , 48 h.

Scheme 5. Synthetic Route for Aminopyridine Macrocycle **29**^a



^aReagents and conditions: (a) 1,5-dibromopentane, K₂CO₃, DMF, rt, 2 d; (b) *tert*-butyl *cis*-8-amino-1-azaspiro[4.5]decane-1-carboxylate (**83**), K₂CO₃, MeCN, 80 °C, 60 h; (c) 4 M NaOH (aq.), ethanol, rt, 16 h; (d) 3-(diethoxyphosphoryloxy)-1,2,3-benzotriazin-4(3*H*)-one, NEt₃, DMF/toluene, rt, 5 d; (e) BBr₃, DCM, 0 °C to rt; (f) 4 N HCl in 1,4-dioxane.

Scheme 6. Synthetic Route for Aminopyridine Macrocycles **30–36**^a

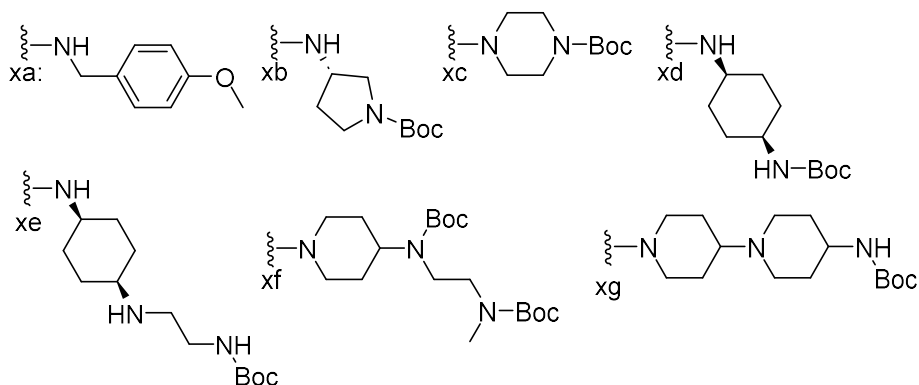


R Groups:

63a-68a, 69a-b, 69d-g: R = Me

63b-68b, 69c: R = CH₂OMe

R¹ Groups:



^aReagents and conditions: (a) 1,5-dibromopentane, K₂CO₃, DMF, rt, 16 h; (b) *cis-tert-butyl N*-(4-aminocyclohexyl)carbamate, K₂CO₃, KI, MeCN, 60 °C, 3 d; (c) 4 N LiOH (aq.), ethanol, rt, 16 h; (d) DEPBT, NEt₃, toluene / DMF, 16 h; (e) *m*-CPBA, DCM, 0 °C to rt, 16 h; (f) [for **69a**] 4-methoxyphenyl)methanamine, NEt₃, 70 °C, 16 h; [for **69b**] *tert*-butyl (3*S*)-3-aminopyrrolidine-1-carboxylate, NMP, 110 °C, 16 h; [for **69c, 69d**] *tert*-butyl piperazine-1-carboxylate (**69c**) or *tert*-butyl *N*-(*cis*-4-aminocyclohexyl)carbamate

(**69d**), DIPEA, DMF, 100 °C, μ wave, 6 h; [for **69e**, **69f**, **69g**] *tert*-butyl *N*-[2-[(*cis*-4-aminocyclohexyl)amino]ethyl]carbamate (**69e**) or *tert*-butyl *N*-[2-[*tert*-butoxycarbonyl(methyl)amino]ethyl]-*N*-(4-piperidyl)carbamate(**69f**) (**87**) or *tert*-butyl *N*-[1-(4-piperidyl)-4-piperidyl]carbamate (**69g**), DIPEA, DMSO, 100 °C, 6–16 h; (g) 4.0 M HCl in 1,4-dioxane, DCM, 0 °C (**32**) or BBr₃, DCM, 0 °C to rt; (h) 5–6 N HCl in 2-propanol or 4 N HCl in 1,4-dioxane.

overcome these mechanisms of relapse, including combination therapies or novel investigations on the use of inhibitors that target all Ras isozymes.¹⁵ Currently there are no approved pan-Ras targeted therapies; however, recently considerable progress has been made in this area by our organization and others.²⁰ As specificity for mutated proteins is traded for a broader Ras pathway inhibition, pan-Ras inhibition may be able to address the problem of resistance, overcome adaptive feedback observed with mutant selective inhibitors and increase the chances of successful treatment. Despite the fact that pan-Ras inhibition mediated toxicity has been suggested, many inhibitors of the Ras network (*e.g.* EGFR inhibitors that indirectly act as pan-Ras inhibitors) are FDA-approved and attest to good tolerability.^{41, 42} In this work, guided by multiple ligand-bound crystal structures encompassing wild-type and mutant protein, as well as GDP & GMPPNP loading states, we initially exploited an enlarged version of the switch I-II pocket on Ras to develop compounds that have low nanomolar affinities for the inactive form of a range of Ras proteins. These compounds block interactions with both the GEF SOS1 and the effector Raf and display cellular inhibition of Ras-Raf binding in a NanoBiT target engagement assay, as well as downstream phosphorylation of ERK. Subsequently, we identified a novel region of the protein that we were able to exploit to deliver molecules that also tightly bind to the active GMPPNP-bound form of Ras with up to 10-fold selectivity over the inactive form, and to the best of our knowledge these compounds are some of the most potent binders to the GMPPNP-loaded form of Ras. Furthermore, these compounds inhibit a range of biologically relevant KRas mutants and wild-type isoforms *in vitro*, demonstrating that potent pan-Ras inhibitors can be accessed from this expanded switch I-II pocket. Lead molecule **36** binds to GMPPNP-loaded Ras within 4 Å of the γ -phosphate, providing opportunities to directly interact with the nucleotide and possibly influence GTPase activity. Despite high affinity for Ras, sub-optimal ADME properties and resultant lack of efficacy in cells meant we were not able to progress these molecules. However, given the novel binding mode of these molecules we expect they could be used either as new inspiration to deliver potent pan-Ras inhibitors or as lead molecules to leverage a heterobifunctional strategy. Altogether, we believe this study offers exciting new starting points to explore both the biological relevance and safety profile of pan-Ras inhibition and the potential benefit of targeting the GTP-bound active state.

EXPERIMENTAL SECTION

Chemistry. All reagents were purchased from commercial sources and used as received without further purification unless otherwise stated. All solvents were of reagent grade unless otherwise stated, with Acros® anhydrous equivalents being sourced from Fisher Scientific. All reactions were performed under an inert atmosphere of nitrogen unless otherwise stated. Reaction monitoring and low-resolution mass spectrometry (LC-MS) was carried out using a Waters Acquity UPLC® Classic system with PDA and SQD detection using a BEH C18 1.7 μ m, 2.1 x 50 mm column (Method A or B). Final compound purity was carried out on

either a Waters Acquity UPLC® Classic system (Method A) or a Waters Acquity UPLC® H-Class SQD2 system incorporating ELSD and PDA detection using a BEH C18 1.7 μ m, 2.1 x 50 mm column (Method C). All tested compounds were determined to be >95% pure by HPLC/ELSD analysis unless otherwise stated. HRMS final compound mass spectrometry was carried out using a Waters Acquity UPLC® I-Class coupled to a Vion IMS QToF MS (Waters) using a BEH C18 1.7 μ m, 2.1 x 50 mm column. See the Supporting Information for details of HRMS and LC-MS methods. All final compounds were purified by preparative reverse phase HPLC using a Waters high performance liquid chromatography system, fitted with an XBridge Prep 19 x 100 mm C18 5 μ m OBD column, using appropriate gradients of acetonitrile and water, with either 0.1% formic acid or ammonium hydroxide + 10 mM ammonium bicarbonate as mobile phase modifiers. Chiral separations were performed on a Gilson Preparative LC system with a Waters Acquity UPC2® QDa Detector (ES/API) and a Waters Acquity UPC2® PDA Detector, using a Phenomenex Lux C4 (21.2mm x 250mm, 5 μ m) column. Chiral purity analysis was carried out by SFC on a Waters UPC2® using a Phenomenex Lux C4 (4.6mm x 250mm, 5 μ m) column; see Supporting Information for method details. NMR spectra were recorded using either a Varian 400 MHz or 600 MHz or a Bruker 400 MHz or 600 MHz spectrometer using the residual solvent as a reference; (CDCl₃: δ = 7.26 for ¹H NMR and δ = 77.16 for ¹³C NMR; DMSO-*d*₆: δ = 2.50 for ¹H NMR and δ = 39.52 for ¹³C NMR). Chemical shifts (δ) are given in parts per million (ppm) and abbreviations for signal multiplicities are as follows: s, singlet; bs, broad singlet; d, doublet; t, triplet; q, quartet; quint, quintet; m, multiplet; app, apparent.

General Procedures. *General Procedure for Methyl Ether Deprotection (GP1).* To a stirred solution of aryl methyl ether (1.0 equiv) in anhyd DCM (0.05 M), in a sealed tube equipped with a silicon cap, was added boron tribromide (3 equiv per protecting group) under nitrogen at 0 °C, and the resultant suspension was stirred for 18–24 h, warming to room temperature. Upon completion, (assessed by LC-MS analysis of a syringe extracted aliquot, diluted with acetonitrile), the reaction was cooled to <5 °C, opened to air and quenched by the dropwise addition of 2-propanol (approximately 100 volumes relative to the boron tribromide) with rapid stirring. The quenched reaction mixture was loaded onto an ion-exchange cartridge pre-equilibrated with 10% acetic acid in methanol. The cartridge was flushed with methanol (approximately 1 CV) then the product eluted with 2 N ammonia in MeOH. Solvent from the basic eluent was removed either by rotary evaporation, a stream of nitrogen at 40 °C, or centrifugal evaporation and the residue solubilised in an appropriate solvent and syringe filtered prior to further purification. Purification was carried out by reverse phase preparative HPLC using an appropriate gradient of acetonitrile and water with either a 0.1% formic acid or 0.1% ammonium hydroxide + 10 mM ammonium bicarbonate modifier. Final products were obtained after solvent removal and lyophilisation carried out by centrifugal evaporation.

General Procedure for HCl Salting of Final Compounds (GP2). Lyophilised product was salted by sonicating for 10 min in either 5–6 N HCl in 2-propanol or 4 N HCl in 1,4-dioxane ~1 mL per 50 mg). The solvent was removed either under a stream of nitrogen or by centrifugal evaporation. The residue was dissolved in 1:1 acetonitrile:water ~10 mg/mL and final product obtained by lyophilisation under reduced pressure.

N-(6-methyl-2-quinolyl)benzenesulfonamide (**2**). 1,1-bis(diphenylphosphino)ferrocene (9.4 mg, 0.017 mmol, 0.03 equiv), *tris*(dibenzylideneacetone)dipalladium (0) (5.2 mg, 0.006 mmol, 0.01 equiv) and cesium carbonate (220 mg, 0.68 mmol, 1.2 equiv) were weighed into a microwave vial which was sealed, evacuated and purged with nitrogen. A solution of benzenesulfonamide (106 mg, 0.68 mmol, 1.2 equiv) and 2-chloro-6-methylquinoline **37a** (100 mg, 0.56 mmol, 1.0 equiv) in degassed 1,4-dioxane (0.5 mL) was added and the mixture heated by microwave irradiation at 140 °C for 10 min. The cooled reaction was diluted with ethyl acetate, washed with water and the organics separated. The organics were dried (MgSO₄), filtered and the solvent removed under reduced pressure. Purified by flash column chromatography (SiO₂, gradient elution *i*-hexane/ethyl acetate = 100/0 to 50/50) to afford the title product (63 mg, 0.20 mmol, 36% yield) as a light-brown solid. ¹H NMR (600 MHz, DMSO-*d*₆) δ 13.20 (br s, 1H), 8.16 (d, *J* = 9.5 Hz, 1H), 7.89 (app. d, *J* = 7.3 Hz, 2H), 7.59 (s, 1H), 7.58 – 7.37 (m, 6H), 2.38 (s, 3H); ¹³C NMR (151 MHz, DMSO-*d*₆) δ 154.99, 143.68, 141.33, 135.59, 133.55, 131.58, 128.86 (2C), 127.34, 125.95, 120.90, 116.79, 115.51, 20.53; HRMS (ESI⁺) *m/z*: calcd for [C₁₆H₁₄N₂O₂S + H]⁺ 299.0849; found 299.0847.

N-(4-quinolyl)benzenesulfonamide (**3**). The title compound was synthesized according to the procedure for **2** using 4-chloroquinoline **37b** (81 mg, 0.50 mmol). The desired product was obtained as a white solid (41 mg, 0.14 mmol, 28% yield). ¹H NMR (600 MHz, DMSO-*d*₆) δ 13.10 (s, 1H), 8.39 (dd, *J* = 8.4, 1.5 Hz, 1H), 8.21 (d, *J* = 7.2 Hz, 1H), 7.91 – 7.86 (m, 2H), 7.80 (ddd, *J* = 8.4, 6.9, 1.5 Hz, 1H), 7.69 (d, *J* = 8.3 Hz, 1H), 7.57 – 7.48 (m, 4H), 7.13 (d, *J* = 7.1 Hz, 1H); ¹³C NMR (151 MHz, DMSO-*d*₆) δ 160.67, 143.82, 140.30, 138.26, 132.61, 131.28, 128.71, 125.97, 125.45, 125.05, 123.17, 118.86, 104.44; HRMS (ESI⁺) *m/z*: calcd for [C₁₅H₁₂N₂O₂S + H]⁺ 285.0692; found 285.0695.

3-nitro-*N*-(2-quinolyl)benzenesulfonamide (**39**). To a stirred solution of quinolin-2-amine **38** (5.00 g, 34.7 mmol, 1.0 equiv) in anhyd pyridine (100 mL) was added 3-nitrophenylsulfonyl chloride (9.99 g, 45.1 mmol, 1.3 equiv) portion-wise and the mixture stirred for 2 h at rt. The solvent was removed under reduced pressure and the residue suspended in methanol. The precipitated product was collected by filtration and dried in a vacuum desiccator (50 °C, 16 h) to afford the title product (8.60 g, 23.5 mmol, 68% yield). LC-MS (ESI⁺) *m/z*: 330.1 [M + H]⁺.

3-Amino-*N*-(2-quinolyl)benzenesulfonamide (**4**). Under an atmosphere of nitrogen a slurry of palladium metal on activated carbon (10%) (323 mg, 0.30 mmol, 0.05 equiv) in ethanol (0.5 mL) was added to a stirred mixture of 3-nitro-*N*-(2-quinolyl)benzenesulfonamide **39** (2.00 g, 6.07 mmol, 1.0 equiv) and ammonium formate (5.74 g, 9.11 mmol, 1.5 equiv) in ethanol (100 mL). The reaction was heated to 80 °C for 6 h then allowed to cool to rt and stirred overnight. The reaction mixture was filtered through a pad of celite and the filter was washed sequentially with ethanol,

methanol, ethyl acetate, DCM and water. The filtrate and washings were combined, and the organic solvents removed under reduced pressure to afford an aqueous residue that was extracted with DCM (2 x 20 mL). The organics were dried (MgSO₄), filtered and evaporated under reduced pressure. The residue was suspended in water and the resulting precipitate collected by filtration and dried in a vacuum desiccator (50 °C, 16 h) to afford the title product (1.50 g, 4.51 mmol, 74% yield) as a tan solid. ¹H NMR (600 MHz, DMSO-*d*₆) δ 13.12 (br s, 1H), 8.20 (d, *J* = 9.5 Hz, 1H), 7.80 (dd, *J* = 8.0, 1.4 Hz, 1H), 7.66 (ddd, *J* = 8.5, 7.0, 1.4 Hz, 1H), 7.56 (d, *J* = 8.4 Hz, 1H), 7.48 (d, *J* = 9.6 Hz, 1H), 7.40 – 7.31 (m, 1H), 7.12 (t, *J* = 7.8 Hz, 1H), 7.09 (s, 1H), 6.98 (d, *J* = 7.6 Hz, 1H), 6.70 – 6.65 (m, 1H), 5.47 (s, 2H); HRMS (ESI⁺) *m/z*: calcd for [C₁₅H₁₃N₃O₂S + H]⁺ 300.0801; found 300.0804.

N-(6-chloro-1,3-benzothiazol-2-yl)benzenesulfonamide (**6**). A mixture of 2-amino-6-chlorobenzothiazole **40a** (100 mg, 0.54 mmol, 1.0 equiv), benzenesulfonyl chloride (82.9 uL, 0.65 mmol, 1.2 equiv), pyridine (1 mL) and DCM (1 mL) was stirred for 60 h at rt. Water (3 mL) was added and the resulting precipitate collected by filtration and washed with DCM (5 mL) and water (5 mL). The solid was dried under vacuum to afford *N*-(6-chloro-1,3-benzothiazol-2-yl)benzenesulfonamide (127 mg, 0.37 mmol, 69% yield) as a white solid. ¹H NMR (600 MHz, DMSO-*d*₆) δ 13.32 (br s, 1H), 7.97 (d, *J* = 2.2 Hz, 1H), 7.89 – 7.82 (m, 2H), 7.66 – 7.60 (m, 1H), 7.60 – 7.54 (m, 2H), 7.42 (dd, *J* = 8.5, 2.2 Hz, 1H), 7.28 (d, *J* = 8.6 Hz, 1H); ¹³C NMR (151 MHz, DMSO-*d*₆) δ 167.06, 141.79, 135.24, 132.51, 129.16, 127.64, 127.33, 126.72, 125.76, 122.43, 114.07; HRMS (ESI⁺) *m/z*: calcd for [C₁₃H₉ClN₂O₂S₂ + H]⁺ 324.9867; found 324.9865.

N-(7-chloro-1,3-benzothiazol-2-yl)benzenesulfonamide (**7**). To a stirred solution of 7-chloro-1,3-benzothiazol-2-amine (100 mg, 0.54 mmol, 1.0 equiv) **40b** in anhyd pyridine (2 mL) cooled to 0 °C was added benzenesulfonyl chloride (83 uL, 0.65 mmol, 1.2 equiv) dropwise (reaction turned from pink to bright yellow). After addition was complete the mixture was stirred for 16 h at rt. A further 0.5 equiv ~40uL of benzenesulfonyl chloride was added and the mixture stirred for a further 16 h. The reaction was quenched with water (10 mL) and the resulting bright yellow precipitate collected by filtration and dried in a vacuum desiccator (45 °C, 16 h) to afford 145 mg of crude product. An aliquot (50 mg) was dissolved in DMSO-*d*₆ and purified by prep HPLC. Fractions containing pure product were lyophilised to afford the title product (39 mg, 0.11 mmol, 59% yield) as a white solid. ¹H NMR (600 MHz, DMSO-*d*₆) δ 13.49 (br s, 1H), 7.90 – 7.85 (m, 2H), 7.68 – 7.62 (m, 1H), 7.61 – 7.55 (m, 2H), 7.43 (t, *J* = 8.0 Hz, 1H), 7.37 (dd, *J* = 8.1, 0.9 Hz, 1H), 7.27 (dd, *J* = 8.0, 1.0 Hz, 1H); ¹³C NMR (151 MHz, DMSO-*d*₆) δ 165.66, 141.65, 137.66, 132.63, 129.23, 128.87, 126.05, 125.79, 124.10, 123.23, 111.82; HRMS (ESI⁺) *m/z*: calcd for [C₁₃H₉ClN₂O₂S₂ + H]⁺ 324.9867; found 324.9867.

N-(7-Chloro-1,3-benzothiazol-2-yl)-3-methoxybenzenesulfonamide (**41a**). 3-methoxybenzenesulfonyl chloride (0.23 mL, 1.62 mmol, 1.2 equiv) was dissolved in anhyd pyridine (5 mL). 7-chloro-1,3-benzothiazol-2-amine **40b** (250 mg, 1.35 mmol, 1.0 equiv) was added and the reaction mixture stirred at rt for 60 h. Water was added and the resulting precipitate collected by filtration and dried in a vacuum desiccator (50 °C, 16 h) to afford the title compound (480 mg, 1.08 mmol, 80% purity) which was used in the next step without further purification. ¹H NMR (400 MHz, DMSO-*d*₆)

δ 13.50 (br s, 1H), 7.54 – 7.25 (m, 6H), 7.21 (ddd, J = 8.0, 2.6, 1.3 Hz, 1H), 3.82 (s, 3H); LC-MS (ESI⁺) m/z : 355.1 [M + H]⁺.

N-(7-chloro-1,3-benzothiazol-2-yl)-2-methoxy-benzenesulfonamide (**41b**). The title compound was synthesized according to the procedure for **41a** using 2-methoxybenzenesulfonyl chloride. The desired product was isolated as a white solid (340 mg, 0.96 mmol, 71% yield). ¹H NMR (400 MHz, DMSO-*d*₆) δ 13.33 (br s, 1H), 7.86 (dt, J = 7.8, 1.4 Hz, 1H), 7.64 – 7.55 (m, 1H), 7.47 – 7.34 (m, 2H), 7.28 (dd, J = 7.8, 1.1 Hz, 1H), 7.19 (d, J = 8.8 Hz, 1H), 7.10 (td, J = 7.6, 1.0 Hz, 1H), 3.71 (s, 3H); LC-MS (ESI⁺) m/z : 355.1 [M + H]⁺.

N-(7-chloro-4-methoxy-1,3-benzothiazol-2-yl)-3-methoxy-benzenesulfonamide (**41c**). The title compound was synthesized according to the procedure for **41a** using 7-chloro-4-methoxy-1,3-benzothiazol-2-amine **40c**.⁴³ The desired product was isolated as a brown gum (60 mg, 0.14 mmol, 29% yield). ¹H NMR (400 MHz, DMSO-*d*₆) δ 13.59 (s, 1H), 7.53 – 7.39 (m, 2H), 7.36 – 7.28 (m, 2H), 7.20 (ddd, J = 8.1, 2.9, 1.1 Hz, 1H), 7.09 (d, J = 8.7 Hz, 1H), 3.88 (s, 3H), 3.81 (s, 3H); LC-MS (ESI⁺) m/z : 385.1 [M + H]⁺.

N-(7-chloro-4-methoxy-1,3-benzothiazol-2-yl)-4-methoxy-benzenesulfonamide (**41d**). The title compound was synthesized according to the procedure for **41a** using 7-chloro-4-methoxy-1,3-benzothiazol-2-amine **40c** and 4-methoxybenzenesulfonyl chloride. The desired product was isolated as a yellow solid (278 mg, 0.72 mmol, 67% yield). ¹H NMR (400 MHz, DMSO-*d*₆) δ 13.45 (s, 1H), 7.80 – 7.75 (m, 2H), 7.31 (d, J = 8.7 Hz, 1H), 7.11 – 7.05 (m, 3H), 3.87 (s, 3H), 3.80 (s, 3H); LC-MS (ESI⁺) m/z : 385.1 [M + H]⁺.

Methyl 5-[(7-chloro-4-methoxy-1,3-benzothiazol-2-yl)sulfamoyl]-2-methoxy-benzoate (**41e**). The title compound was synthesized according to the procedure for **41a** using 7-chloro-4-methoxy-1,3-benzothiazol-2-amine **40c** and methyl 5-chlorosulfonyl-2-methoxy-benzoate. The desired product was isolated as an off-white solid (13.1 g, 29.7 mmol, 63% yield). ¹H NMR (400 MHz, DMSO-*d*₆) δ 13.57 (br s, 1H), 8.10 (d, J = 2.5 Hz, 1H), 8.01 (dd, J = 8.9, 2.5 Hz, 1H), 7.36 – 7.29 (m, 2H), 7.09 (d, J = 8.8 Hz, 1H), 3.89 (s, 3H), 3.88 (s, 3H), 3.81 (s, 3H); LC-MS (ESI⁺) m/z : 443.1 [M + H]⁺.

N-(7-chloro-1,3-benzothiazol-2-yl)-3-hydroxy-benzenesulfonamide (**8**). The title compound was synthesized from **41a** (425 mg, 1.20 mmol, 1.0 equiv) according to general procedure GP1. The desired product was isolated as a white solid (340 mg, 0.95 mmol, 79% yield). ¹H NMR (600 MHz, DMSO-*d*₆) δ 13.48 (br s, 1H), 10.07 (s, 1H), 7.43 (t, J = 8.0 Hz, 1H), 7.40 – 7.32 (m, 2H), 7.31 – 7.25 (m, 2H), 7.28 – 7.21 (m, 1H), 6.99 (ddd, J = 8.1, 2.5, 1.1 Hz, 1H); ¹³C NMR (151 MHz, DMSO-*d*₆) δ 165.57, 157.66, 142.59, 137.49, 130.37, 128.91, 126.06, 123.99, 123.26, 119.65, 116.30, 112.19, 111.75; HRMS (ESI⁺) m/z : calcd for [C₁₃H₉ClN₂O₃S₂+H]⁺ 340.9816; found 340.9816.

N-(7-Chloro-1,3-benzothiazol-2-yl)-2-hydroxy-benzenesulfonamide (**9**). The title compound was synthesized from **41b** (320 mg, 0.90 mmol) according to general procedure GP1. The desired product was isolated as a white solid (230 mg, 0.64 mmol, 71% yield). ¹H NMR (600 MHz, DMSO-*d*₆) δ 13.25 (br s, 1H), 10.58 (s, 1H), 7.77 (dd, J = 7.9, 1.7 Hz, 1H), 7.45 – 7.38 (m, 2H), 7.36 (d, J = 8.0 Hz, 1H), 7.27 (d, J = 7.9 Hz, 1H), 6.93 (t, J = 7.6 Hz, 1H), 6.90 (d, J = 8.2 Hz, 1H) ¹³C NMR (151 MHz, DMSO-*d*₆) δ 166.24, 155.71, 134.02, 128.51, 128.21, 127.41, 125.87, 124.53, 122.92, 118.45, 117.01, 111.50, 111.45; HRMS (ESI⁺) m/z : calcd for [C₁₃H₉ClN₂O₃S₂+H]⁺ 340.9816; found 340.9812.

N-(7-Chloro-4-hydroxy-1,3-benzothiazol-2-yl)-3-hydroxy-benzenesulfonamide (**10**). The title compound was synthesized from **41c** (60 mg, 0.14 mmol) according to general procedure GP1. The desired product was isolated as a white solid (19 mg, 0.05 mmol, 36% yield). ¹H NMR (600 MHz, DMSO-*d*₆) δ 13.34 (br s, 1H), 10.53 (br s, 1H), 10.00 (s, 1H), 7.33 (t, J = 7.9 Hz, 1H), 7.26 (d, J = 8.0 Hz, 1H), 7.23 (t, J = 2.1 Hz, 1H), 7.12 (br s, 1H), 6.95 (d, J = 8.0 Hz, 1H), 6.81 (d, J = 8.6 Hz, 1H); δ 7.07 (t, J = 36.0 Hz, \approx 2.5wt.% ammonium impurity); HRMS (ESI⁺) m/z : calcd for [C₁₃H₉ClN₂O₄S₂+H]⁺ 356.9766; found 356.9762.

N-(7-Chloro-4-hydroxy-1,3-benzothiazol-2-yl)-4-hydroxy-benzenesulfonamide (**11**). The title compound was synthesized from **41d** (120 mg, 0.31 mmol) according to general procedure GP1. The desired product was isolated as a white solid (26 mg, 0.07 mmol, 23% yield). ¹H NMR (600 MHz, DMSO-*d*₆) δ 13.17 (br s, 1H), 10.58 (br s, 1H), 10.37 (s, 1H), 7.71 – 7.65 (m, 2H), 7.15 (d, J = 8.6 Hz, 1H), 6.91 – 6.86 (m, 2H), 6.84 (d, J = 8.6 Hz, 1H); ¹³C NMR (151 MHz, DMSO-*d*₆) δ 164.76, 161.07, 143.32, 131.95, 128.15, 124.85, 123.59, 115.47, 115.05, 114.16; one carbon is missing due to overlapping or broadening; HRMS (ESI⁺) m/z : calcd for [C₁₃H₉ClN₂O₄S₂+H]⁺ 356.9766; found 356.9755.

5-[(7-Chloro-4-methoxy-1,3-benzothiazol-2-yl)sulfamoyl]-2-methoxy-benzoic acid (**42**). To a suspension of **41e** (13.1 g, 29.7 mmol, 1.0 equiv) in methanol (75 mL) was added 4.0 M sodium hydroxide (aq.) (74.0 mL, 296 mmol, 10.0 equiv) portion-wise over a period of 20 min, keeping the reaction temperature below 30 °C (moderate exotherm was observed, and a brown solution was formed). The reaction mixture was stirred at rt for 1 h then the organics were removed under reduced pressure. Water (100ml) was added to re-dissolve the resultant precipitate and the solution acidified with 5 N HCl to pH 2. The resultant precipitate was collected by filtration, washed with water and air dried to afford a sticky solid. The solid was suspended in ethanol and concentrated under reduced pressure (\times 3) to afford the title compound (12.2 g, 28.5 mmol, 96% yield). ¹H NMR (400 MHz, DMSO-*d*₆) δ 12.92 (br s, 1H), 8.04 (d, J = 2.4 Hz, 1H), 7.92 (dd, J = 8.8, 2.4 Hz, 1H), 7.20 (d, J = 8.8 Hz, 1H), 7.07 (d, J = 8.6 Hz, 1H), 6.87 (d, J = 8.6 Hz, 1H), 3.84 (s, 3H), 3.83 (s, 3H); one proton is missing due to overlapping or broadening; LC-MS (ESI⁺) m/z : 429.1 [M + H]⁺.

tert-Butyl *N*-[1-[5-[(7-chloro-4-methoxy-1,3-benzothiazol-2-yl)sulfamoyl]-2-methoxy-benzoyl]-4-piperidyl]carbamate (**43**). To a solution of **42** (150 mg, 0.35 mmol, 1.0 equiv), *tert*-butyl *N*-(4-piperidyl)carbamate (140 mg, 0.70, 2.0 equiv) and DIPEA (0.14 mL, 1.05 mmol, 3.0 equiv) in DCM (3 mL) was added propylphosphonic anhydride solution (50% w/w in ethyl acetate) (0.42 mL, 0.70 mmol, 2.0 equiv) and the mixture stirred at rt for 16 h. The reaction was quenched with water and the mixture extracted with DCM. The organics were collected using a phase separator and concentrated under reduced pressure. The residue was purified by flash column chromatography (SiO₂, gradient elution DCM/MeOH = 100/0 to 95/5). The solvent was removed under reduced pressure to afford the title compound (155 mg, 0.25 mmol, 73% yield); LC-MS (ESI⁺) m/z : 555.1 [M – *t*Bu + H]⁺.

3-(4-Aminopiperidine-1-carbonyl)-*N*-(7-chloro-4-hydroxy-1,3-benzothiazol-2-yl)-4-hydroxy-benzenesulfonamide (**12**). The title compound was synthesized from **43**

(155 mg, 0.25 mmol) according to general procedure GP1. The desired product was isolated as a white solid (41 mg, 0.09 mmol, 36% yield); ¹H NMR (600 MHz, DMSO-*d*₆) δ 8.49 (br s, 4H), 7.63 (dd, *J* = 8.6, 2.4 Hz, 1H), 7.50 (d, *J* = 2.3 Hz, 1H), 6.88 (d, *J* = 8.6 Hz, 1H), 6.79 (d, *J* = 8.4 Hz, 1H), 6.54 (d, *J* = 8.4 Hz, 1H), 4.48 (s, 1H), 3.03 (s, 1H), 2.81 (s, 1H), 2.10 – 1.68 (m, 2H), 1.53 – 1.29 (m, 2H); two protons overlap with the residual water signal (confirmed by HSQC experiment) and one proton not observed due to broadening or overlap with the residual solvent signals; ¹³C NMR (151 MHz, DMSO-*d*₆) δ 166.14, 165.04, 154.96, 146.40, 140.76, 136.44, 131.62, 128.16, 126.23, 123.01, 119.94, 115.22, 114.00, 111.56, 47.53, 44.49, 30.48; HRMS (ESI⁺) *m/z*: calcd for [C₁₉H₁₉ClN₄O₅S₂+H]⁺ 483.0559; found 483.0558.

Ethyl 5-[(Z)-(7-chloro-3-ethyl-4-methoxy-1,3-benzothiazol-2-ylidene)amino]sulfonyl-2-methoxy-benzoate (**44**). To a stirred solution of **42** (2.50 g, 5.83 mmol, 1.0 equiv) and potassium carbonate, anhyd (2.42 g, 17.5 mmol, 3.0 equiv) in DMF (50 mL) at 0 °C under nitrogen was added bromoethane (0.96 mL, 12.8 mmol, 2.2 equiv) dropwise. The mixture was allowed to warm to rt and stirred for 16 h. Further bromoethane (0.44 mL, 5.83 mmol, 1.0 equiv) was added and the reaction stirred for a further 24 h. Water (100 mL) was added, and the resulting precipitate was collected *via* vacuum filtration to afford impure product as a mixture of *N*-ethyl regioisomers (2.07 g, 4.28 mmol) which was engaged in the next step without further purification.

5-[(Z)-(7-Chloro-3-ethyl-4-methoxy-1,3-benzothiazol-2-ylidene)amino]sulfonyl-2-methoxy-benzoic acid (**45**). To a stirred suspension of impure **44** (2.07 g, 4.28 mmol, 1.0 equiv) in methanol (25 mL) at 0 °C was added 4 N aqueous sodium hydroxide solution (10.7 mL, 42.8 mmol, 10.0 equiv) dropwise. The reaction mixture was stirred at rt for 24 h. The reaction mixture was concentrated under reduced pressure to remove most of the methanol. Water was then added (25 mL) and the solution was acidified to ~pH 2 with 5 N HCl. The resultant precipitate was collected by filtration, washed with water and dried (vacuum desiccator, 40 °C, 16 h) to afford the impure product (1.74 g, 3.81 mmol) as a mixture of *N*-ethyl regioisomers (≈85:15 alkylation on the benzothiazole nitrogen: alkylation on the sulfonamide nitrogen) which was engaged in the next step without further purification. ¹H NMR (major isomer) (400 MHz, DMSO-*d*₆) δ 7.95 (d, *J* = 2.5 Hz, 1H), 7.89 (dd, *J* = 8.8, 2.5 Hz, 1H), 7.40 (d, *J* = 8.8 Hz, 1H), 7.21 (d, *J* = 3.8 Hz, 1H), 7.19 (d, *J* = 3.9 Hz, 1H), 4.43 (q, *J* = 7.0 Hz, 2H), 3.93 (s, 3H), 3.84 (s, 3H), 1.19 (t, *J* = 7.0 Hz, 3H); LC-MS (ESI⁺) *m/z*: 457.0 [M + H]⁺.

tert-Butyl *N*-[1-[5-[(Z)-(7-chloro-3-ethyl-4-methoxy-1,3-benzothiazol-2-ylidene)amino]sulfonyl-2-methoxy-benzoyl]-4-piperidyl]carbamate (**46a**). The title compound was synthesized according to the procedure for **43** using **45** and *tert*-butyl *N*-(4-piperidyl)carbamate to afford the product (190 mg, 0.30 mmol, 91% yield) as a 85:15 mixture of *N*-alkylated regioisomers; LC-MS (ESI⁺) *m/z*: 583.1 [M-*t*Bu + H]⁺.

tert-Butyl 4-[[5-[(Z)-(7-chloro-3-ethyl-4-methoxy-1,3-benzothiazol-2-ylidene)amino]sulfonyl-2-methoxy-benzoyl]-(2-hydroxyethyl)amino]piperidine-1-carboxylate (**46b**). To a stirred solution of **45** (85.0 mg, 0.19 mmol, 1.0 equiv), DIPEA (0.07 mL, 0.56 mmol, 3.0 equiv) and *tert*-butyl 4-(2-hydroxyethylamino)piperidine-1-carboxylate (91.0 mg, 0.37 mmol, 2.0 equiv) in DMF (1.5 mL) was added HATU (141 mg, 0.37 mmol, 2.0 equiv) and the

mixture stirred for 5 h. The reaction was partitioned between water and DCM and the organics collected using a phase separator. Evaporation of volatiles afforded the crude product which was purified by flash column chromatography (SiO₂, gradient elution DCM/MeOH = 100/0 to 95/5) to afford the desired product (100 mg, 77% purity) as a 85:15 mixture of *N*-alkylated regioisomers; LC-MS (ESI⁺) *m/z*: 627.2 [M - *t*Bu + H]⁺.

(Z)-3-(4-aminopiperidine-1-carbonyl)-*N*-(7-chloro-3-ethyl-4-hydroxybenzo[d]thiazol-2(3*H*)-ylidene)-4-hydroxybenzenesulfonamide (**13**). The title compound was synthesized from **46a** (190 mg, 0.30 mmol) according to general procedure GP1. The desired product was isolated as a white solid (42 mg, 0.082 mmol, 27% yield). ¹H NMR (600 MHz, DMSO-*d*₆) δ 7.64 (dd, *J* = 8.7, 2.5 Hz, 1H), 7.50 (d, *J* = 2.5 Hz, 1H), 7.11 (d, *J* = 8.7 Hz, 1H), 6.87 (d, *J* = 8.7 Hz, 1H), 6.76 (d, *J* = 8.7 Hz, 1H), 4.56 (q, *J* = 6.9 Hz, 2H), 4.37 (br s, 1H), 3.01 – 2.93 (m, 2H), 2.84 (br s, 1H), 1.82 (br s, 1H), 1.68 (br s, 1H), 1.31 – 1.22 (m, 2H), 1.18 (t, *J* = 6.9 Hz, 3H); four protons are missing due to broadening and one proton overlaps with the residual water peak (confirmed by HSQC experiment); HRMS (ESI⁺) *m/z*: calcd for [C₂₁H₂₃ClN₄O₅S₂+H]⁺ 511.0872; found 511.0871.

5-[(Z)-(7-chloro-3-ethyl-4-hydroxy-1,3-benzothiazol-2-ylidene)amino]sulfonyl-2-hydroxy-*N*-(2-hydroxyethyl)-*N*-(4-piperidyl)benzamide (**14**). The title compound was synthesized from **46b** (100 mg, 0.15 mmol) according to general procedure GP1. The desired product was isolated as a white solid (3.0 mg, 0.005 mmol, 4% yield). ¹H NMR (400 MHz, DMSO-*d*₆) δ 7.72 (d, *J* = 9.0 Hz, 1H), 7.55 (s, 1H), 7.16 (d, *J* = 8.6 Hz, 1H), 6.98 (d, *J* = 8.6 Hz, 1H), 6.90 (d, *J* = 8.8 Hz, 1H), 4.54 (q, *J* = 7.0 Hz, 2H), 3.52 – 3.44 (m, 3H), 3.34 – 3.30 (m, 2H), 2.89 (d, *J* = 12.3 Hz, 2H), 2.31 – 2.11 (m, 2H), 1.73 – 1.43 (m, 4H), 1.23 (t, *J* = 7.0 Hz, 3H); four protons corresponding to the hydroxy, phenol and amine protons are missing due to broadening and/or overlapping with the residual solvent peak. HRMS (ESI⁺) *m/z*: calcd for [C₂₃H₂₇ClN₄O₆S₂+H]⁺ 555.1134; found 555.1136.

tert-Butyl 4-[[5-[(7-chloro-4-methoxy-1,3-benzothiazol-2-yl)sulfamoyl]-2-methoxy-benzoyl]amino]piperidine-1-carboxylate (**47a**). To a solution of **42** (5.0 g, 11.7 mmol, 1.0 equiv), *tert*-butyl 4-aminopiperidine-1-carboxylate (2.80 g, 14.0 mmol, 1.2 equiv) in anhyd THF (50 mL) was added triethylamine (6.5 mL, 46.6 mmol, 4.0 equiv). The solution was stirred for 5 min before (27.3 mL, 93.4 mmol, 8.0 equiv) was added and the cloudy solution stirred at rt for 18 h. The majority of the solvent was removed under reduced pressure and water (150 mL) added. The resulting precipitate was collected by filtration and washed with an aqueous solution of sodium hydroxide (1.0 M). The filtrate was acidified to pH = 8 with an aqueous solution of HCl (5.0 M) and the resulting precipitate collected by filtration and added to previously collected solids. Combined solids were further purified by flash column chromatography (SiO₂, gradient elution DCM/(MeOH + 0.1% NH₄OH aq.) = 100/0 to 80/20) to afford the title compound (6.2 g, 10.2 mmol, 87% yield) as a light-brown solid. ¹H NMR (400 MHz, DMSO-*d*₆) δ 13.55 (br s, 1H), 8.14 (d, *J* = 7.8 Hz, 1H), 8.03 (d, *J* = 2.5 Hz, 1H), 7.92 (dd, *J* = 8.8, 2.5 Hz, 1H), 7.32 (d, *J* = 8.8 Hz, 1H), 7.28 (d, *J* = 8.9 Hz, 1H), 7.09 (d, *J* = 8.8 Hz, 1H), 3.99 – 3.79 (m, 3H), 3.91 (s, 3H), 3.88 (s, 3H), 2.89 (br s, 2H), 1.87 – 1.70 (m, 2H), 1.46 – 1.32 (m, 2H), 1.40 (s, 9H); LC-MS (ESI⁺) *m/z*: 611.2 [M + H]⁺.

tert-Butyl *N*-[*cis*-4-[[5-[[7-chloro-4-methoxy-1,3-benzothiazol-2-yl]sulfonyl]-2-methoxy-benzoyl]amino]cyclohexyl]carbamate (**47b**). To a stirred suspension of **42** (1.20 g, 2.80 mmol, 1.0 equiv) and *cis-tert*-butyl *N*-(4-aminocyclohexyl)carbamate (720 mg, 3.36 mmol, 1.2 equiv) in anhyd THF (50 mL) was added triethylamine (1.6 mL, 11.2 mmol, 4.0 equiv). The solution was stirred for 10 min before propylphosphonic anhydride solution (50% w/v in ethyl acetate) (5.9 mL, 5.04 mmol, 1.8 equiv) was added and the solution stirred at rt for 20 h. After the reaction was complete water was added and the organics extracted with DCM. The organics were evaporated under reduced pressure and the residue purified by flash column chromatography (SiO₂, gradient elution DCM/(MeOH + 0.1% NH₄OH aq.) = 100/0 to 80/20) to afford the title compound as an off-white solid (1.13 g, 1.80 mmol, 64% yield). LC-MS (ESI⁺) *m/z*: 625.3 [M + H]⁺. ¹H NMR (400 MHz, DMSO-*d*₆) δ 13.56 (br s, 1H), 8.19 (d, *J* = 2.5 Hz, 1H), 8.08 (d, *J* = 7.5 Hz, 1H), 7.94 (dd, *J* = 8.7, 2.5 Hz, 1H), 7.41 – 7.22 (m, 2H), 7.04 (d, *J* = 8.8 Hz, 1H), 6.80 (d, *J* = 7.0 Hz, 1H), 4.00 (s, 3H), 3.94 (s, 1H), 3.87 (s, 3H), 3.42 – 3.28 (br s, 1H), 1.74 – 1.66 (m, 2H), 1.66 – 1.53 (m, 4H), 1.53 – 1.42 (m, 2H), 1.38 (s, 9H).

5-[[7-chloro-4-methoxy-1,3-benzothiazol-2-yl]sulfonyl]-*N*-ethyl-2-methoxy-benzamide (**47c**). The title compound was synthesized according to the procedure for **47b** but using ethylamine 2.0 M in THF and DIPEA. The desired product was obtained (330 mg, 0.72 mmol, 31% yield). LC-MS (ESI⁺) *m/z*: 456.2 [M + H]⁺.

tert-Butyl 4-[[5-[[*Z*]-[3-(4-bromobutyl)-7-chloro-4-methoxy-1,3-benzothiazol-2-ylidene]amino]sulfonyl]-2-methoxy-benzoyl]amino]piperidine-1-carboxylate (**48a**). To a solution **47a** (500 mg, 0.82 mmol, 1.0 equiv) and potassium carbonate, anhyd (1.36 g, 9.82 mmol, 12.0 equiv) in anhyd DMF (40 mL) under nitrogen at 0 °C was added 1,4-dibromobutane (0.98 mL, 8.18 mmol, 10.0 equiv). The reaction was then allowed to warm to rt and stirred overnight. The bulk of the DMF was removed under reduced pressure (~1 mL remaining) and then this solution was cooled to 0 °C and quenched by careful addition of water (~2 mL). Ethyl acetate (10 mL) was added, and the organics were washed with a solution of 5% aq. LiCl (3 x 5 mL). The organics were separated, dried (MgSO₄) and concentrated under reduced pressure to afford the crude as an amber gum. The material was purified by flash column chromatography (SiO₂, gradient elution DCM/MeOH = 100/0 to 95/5) to afford the title compound (390 mg, 0.50 mmol, 61% yield) as a clear gum. ¹H NMR (400 MHz, CDCl₃) δ 8.72 (d, *J* = 2.5 Hz, 1H), 8.10 (dd, *J* = 8.7, 2.5 Hz, 1H), 7.55 (d, *J* = 7.7 Hz, 1H), 7.16 (d, *J* = 8.8 Hz, 1H), 7.05 (d, *J* = 8.8 Hz, 1H), 6.85 (d, *J* = 8.8 Hz, 1H), 4.58 – 4.45 (m, 2H), 4.23 – 4.07 (m, 1H), 4.06 – 3.96 (m, 5H), 3.93 (s, 3H), 3.41 – 3.30 (m, 2H), 3.06 – 2.91 (m, 2H), 2.03 – 1.94 (m, 2H), 1.89 – 1.74 (m, 4H), 1.49 – 1.46 (m, 9H), 1.45 – 1.35 (m, 2H); LC-MS (ESI⁺) *m/z*: 747.4 [M + H]⁺.

tert-Butyl 4-[[5-[[*Z*]-[3-(5-bromopentyl)-7-chloro-4-methoxy-1,3-benzothiazol-2-ylidene]amino]sulfonyl]-2-methoxy-benzoyl]amino]piperidine-1-carboxylate (**48b**). The title compound was synthesized from **47a** according to the procedure for **48a** using 1,5-dibromopentane as alkylating reagent. The desired product was isolated as a clear gum (430 mg, 0.54 mmol, 55% yield). LC-MS (ESI⁺) *m/z*: 661.3 [M-Boc + H]⁺.

tert-Butyl *N*-[*cis*-4-[[5-[[*Z*]-[3-(5-bromopentyl)-7-chloro-4-methoxy-1,3-benzothiazol-2-

ylidene]amino]sulfonyl]-2-methoxy-benzoyl]amino]cyclohexyl]carbamate (**48c**). The title compound was synthesized from **47b** according to the procedure for **48a** using 1,5-dibromopentane as alkylating reagent. The desired product was isolated as a clear gum (310 mg, 0.38 mmol, 57% yield). ¹H NMR (400 MHz, CDCl₃) δ 8.72 (d, *J* = 2.5 Hz, 1H), 8.10 (dd, *J* = 8.7, 2.5 Hz, 1H), 7.72 (d, *J* = 7.5 Hz, 1H), 7.15 (d, *J* = 8.8 Hz, 1H), 7.06 (d, *J* = 8.8 Hz, 1H), 6.84 (d, *J* = 8.8 Hz, 1H), 4.54 (br s, 1H), 4.51 – 4.43 (m, 2H), 4.13 (br s, *J* = 6.2 Hz, 1H), 4.05 (s, 3H), 3.92 (s, 3H), 3.61 (br s, 1H), 3.30 (t, *J* = 6.8 Hz, 2H), 1.87 – 1.75 (m, 6H), 1.75 – 1.64 (m, 4H), 1.56 – 1.49 (m, 2H), 1.45 (s, 9H), 1.42 – 1.35 (m, 2H); LC-MS (ESI⁺) *m/z*: 675.3 [M-Boc + H]⁺.

5-[[*Z*]-[3-(5-bromopentyl)-7-chloro-4-methoxy-1,3-benzothiazol-2-ylidene]amino]sulfonyl-*N*-ethyl-2-methoxy-benzamide (**48d**). The title compound was synthesized from **47c** according to the procedure for **48a** using 1,5-dibromopentane as alkylating reagent. The desired product was isolated as an off-white solid. (93 mg, 0.15 mmol, 21% yield). LC-MS (ESI⁺) *m/z*: 606.3 [M + H]⁺.

tert-Butyl 4-[[5-[[*Z*]-[3-(6-bromohexyl)-7-chloro-4-methoxy-1,3-benzothiazol-2-ylidene]amino]sulfonyl]-2-methoxy-benzoyl]amino]piperidine-1-carboxylate (**48e**). The title compound was synthesized from **47a** according to the procedure for **48a** using 1,6-dibromohexane as alkylating reagent. The desired product was isolated as a clear gum (600 mg, 0.70 mmol, 53% yield). ¹H NMR (400 MHz, Chloroform-*d*) δ 8.73 (d, *J* = 2.5 Hz, 1H), 8.10 (dd, *J* = 8.7, 2.5 Hz, 1H), 7.56 (d, *J* = 7.7 Hz, 1H), 7.15 (d, *J* = 8.8 Hz, 1H), 7.05 (d, *J* = 8.8 Hz, 1H), 6.84 (d, *J* = 8.8 Hz, 1H), 4.52 – 4.43 (m, 2H), 4.20 – 4.08 (m, 1H), 4.01 (s, 3H), 3.98 (br s, 2H), 3.91 (s, 3H), 3.33 (t, *J* = 6.8 Hz, 2H), 3.03 – 2.92 (m, 2H), 2.04 – 1.96 (m, 2H), 1.80 – 1.61 (m, 4H), 1.46 (s, 9H), 1.45 – 1.32 (m, 4H), 1.31 – 1.21 (m, 2H); LC-MS (ESI⁺) *m/z*: 775.5 [M + H]⁺.

tert-Butyl 4-[[3*Z*]-7-chloro-10,20-dimethoxy-2,2,18-tri-oxo-2λ⁶,5-dithia-3,12,17-triazatetracyclo[17.3.1.0^{4,12}.0^{6,11}]tricoso-1(23),3,6,8,10,19,21-heptaen-17-yl]piperidine-1-carboxylate (**49a**). To a solution of **48a** (390 mg, 0.52 mmol, 1.0 equiv) in anhyd DMF (25 mL) at 0 °C was added sodium hydride (60% w/w, 62.7 mg, 1.57 mmol, 3 equiv). The reaction was stirred at 0 °C for 2 h. The reaction mixture was quenched at 0 °C by the addition of 2-propanol (1 mL). Ethyl acetate (~25 mL) was then added, and the organics were washed with aq. 5% LiCl (4 x 25 mL). The organics were separated, dried (MgSO₄) and concentrated under reduced pressure to yield the crude. The material was purified by flash column chromatography (SiO₂, gradient elution DCM/MeOH = 100/0 to 95/5) to afford the title compound (190 mg, 0.29 mmol, 55% yield) as a white waxy solid. ¹H NMR (400 MHz, CDCl₃) δ 7.91 (dd, *J* = 8.7, 2.3 Hz, 1H), 7.81 (br s, 1H), 7.16 (d, *J* = 8.7 Hz, 1H), 6.88 (d, *J* = 8.7 Hz, 1H), 6.83 (d, *J* = 8.8 Hz, 1H), 4.78 – 4.60 (m, 2H), 4.50 (br s, 1H), 4.22 (br s, 2H), 3.90 (s, 3H), 3.83 (s, 3H), 3.01 (br s, 1H), 2.83 (br s, 2H), 2.40 (br s, 1H), 1.88 – 1.65 (m, 3H), 1.55 – 1.37 (m, 13H), 0.40 (br s, 1H); LC-MS (ESI⁺) *m/z*: 565.3 [M-Boc + H]⁺.

tert-Butyl 4-[[3*Z*]-7-chloro-10,21-dimethoxy-2,2,19-tri-oxo-2λ⁶,5-dithia-3,12,18-triazatetracyclo[18.3.1.0^{4,12}.0^{6,11}]tetracoso-1(23),3,6,8,10,20(24),21-heptaen-18-yl]piperidine-1-carboxylate (**49b**). The title compound was synthesized from **48b** according to the procedure for **49a**. The desired product was isolated as an off-white solid (580 mg, 0.85 mmol, 47% yield). ¹H NMR (400

MHz, DMSO-*d*₆) δ 7.88 (dd, *J* = 8.7, 2.4 Hz, 1H), 7.60 (d, *J* = 2.4 Hz, 1H), 7.41 (d, *J* = 8.9 Hz, 1H), 7.16 (app t, *J* = 8.9 Hz, 2H), 4.63 – 4.49 (m, 1H), 4.47 – 4.34 (m, 1H), 4.12 – 3.97 (m, 2H), 3.89 (s, 3H), 3.82 (s, 3H), 3.08 (d, *J* = 15.2 Hz, 1H), 2.73 (br s, 2H), 2.63 – 2.52 (m, 2H), 1.91 – 1.47 (m, 6H), 1.46 – 1.35 (m, 10H), 1.34 – 1.25 (m, 1H), 1.01 (br s, 1H), 0.35 (s, 1H); LC-MS (ESI⁺) *m/z*: 579.3 [M-Boc + H]⁺.

tert-Butyl *N*-[*cis*-4-[(3*Z*)-7-chloro-10,21-dimethoxy-2,2,19-trioxo-2λ⁶,5-dithia-3,12,18-triazatetracyclo[18.3.1.0^{4,12}.0^{6,11}]tetracos-1(23),3,6,8,10,20(24),21-heptaen-18-yl]cyclohexyl]carbamate (**49c**). The title compound was synthesized from **48c** according to the procedure for **49a**. The desired product was isolated as an off-white solid (580 mg, 0.85 mmol, 47% yield). (95 mg, 0.1302 mmol, 32.511% yield). ¹H NMR (400 MHz, DMSO-*d*₆) δ 7.87 (dd, *J* = 8.7, 2.4 Hz, 1H), 7.58 (d, *J* = 2.4 Hz, 1H), 7.41 (d, *J* = 8.9 Hz, 1H), 7.18 (d, *J* = 9.0 Hz, 1H), 7.15 (d, *J* = 8.7 Hz, 1H), 6.96 (d, *J* = 7.3 Hz, 1H), 4.65 – 4.50 (m, 1H), 4.48 – 4.37 (m, 1H), 4.11 (t, *J* = 12.3 Hz, 1H), 3.89 (s, 3H), 3.82 (s, 3H), 3.65 (s, 1H), 3.28 – 3.15 (m, 1H), 1.98 – 1.76 (m, 2H), 1.75 – 1.64 (m, 2H), 1.63 – 1.45 (m, 5H), 1.45 – 1.30 (m, 12H), 1.19 (d, *J* = 35.6 Hz, 1H), 0.94 (s, 1H), 0.34 (br s, 1H); LC-MS (ESI⁺) *m/z*: 593.4 [M-Boc + H]⁺.

(3*Z*)-7-chloro-18-ethyl-10,21-dimethoxy-2,2-dioxo-2λ⁶,5-dithia-3,12,18-triazatetracyclo[18.3.1.0^{4,12}.0^{6,11}]tetracos-1(24),3,6(11),7,9,20,22-heptaen-19-one (**49d**). The title compound was synthesized from **48d** according to the procedure for **49a**. The desired product was isolated as a white solid (68 mg, 0.13 mmol, 84% yield). ¹H NMR (400 MHz, DMSO-*d*₆) δ 7.87 (dd, *J* = 8.6, 2.4 Hz, 1H), 7.56 (d, *J* = 2.4 Hz, 1H), 7.40 (d, *J* = 8.8 Hz, 1H), 7.22 – 7.11 (m, 2H), 4.63 – 4.36 (m, 2H), 3.90 (s, 3H), 3.83 (s, 3H), 3.62 – 3.49 (m, 1H), 3.24 – 3.11 (m, 1H), 3.11 – 2.98 (m, 1H), 2.77 – 2.59 (m, 1H), 1.66 – 1.40 (m, 2H), 1.33 – 1.18 (m, 2H), 1.16 – 1.00 (m, 4H), 0.34 (s, 1H); LC-MS (ESI⁺) *m/z*: 524.3 [M + H]⁺.

tert-Butyl 4-[(3*Z*)-7-chloro-10,22-dimethoxy-2,2,20-trioxo-2λ⁶,5-dithia-3,12,19-triazatetracyclo[19.3.1.0^{4,12}.0^{6,11}]pentacos-1(25),3,6,8,10,21,23-heptaen-19-yl]piperidine-1-carboxylate (**49e**). The title compound was synthesized from **48e** according to the procedure for **49a**. The desired product was isolated as a white solid (45 mg, 0.06 mmol, 8.0% yield). ¹H NMR (400 MHz, CDCl₃) δ 8.05 (dd, *J* = 8.8, 2.3 Hz, 1H), 7.80 (d, *J* = 2.3 Hz, 1H), 7.17 (d, *J* = 8.8 Hz, 1H), 6.97 (d, *J* = 8.8 Hz, 1H), 6.84 (d, *J* = 8.8 Hz, 1H), 4.74 – 4.59 (m, 1H), 4.54 – 4.34 (m, 2H), 4.22 (br s, 2H), 3.89 (s, 3H), 3.87 (s, 3H), 3.06 (br s, 1H), 2.94 – 2.68 (m, 3H), 1.92 – 1.71 (m, 2H), 1.70 – 1.45 (m, 4H), 1.47 (s, 9H), 1.37 (br s, 2H), 1.16 (br s, 2H), 0.97 – 0.66 (m, 2H); LC-MS (ESI⁺) *m/z*: 593.3 [M-Boc + H]⁺.

(3*Z*)-7-Chloro-10,21-dimethoxy-2,2-dioxo-18-(4-piperidyl)-2λ⁶,5-dithia-3,12,18-triazatetracyclo[18.3.1.0^{4,12}.0^{6,11}]tetracos-1(24),3,6(11),7,9,20,22-heptaen-19-one (**49f**). To a stirred solution of **49b** (4.00 g, 5.89 mmol, 1.0 equiv) in DCM (60 mL) was added TFA (5.00 mL, 65.3 mmol) and the mixture stirred at rt for 60 h. The solvent was removed under reduced pressure. The residue was loaded onto a pre-equilibrated ion-exchange cartridge and the cartridge washed with methanol (~2 CV). The product was eluted with 2N ammonia in methanol and fractions containing product were concentrated under reduced pressure to afford the title product (2.25 g, 3.69 mmol, 63% yield) as a pale-yellow solid. ¹H NMR (600 MHz, DMSO-*d*₆) δ 7.87 (d, *J* = 8.7 Hz, 1H), 7.58 (s, 1H), 7.39 (d, *J* = 8.8 Hz, 1H),

7.20 – 7.11 (m, 2H), 4.60 – 4.49 (m, 1H), 4.46 – 4.35 (m, 1H), 4.12 – 4.03 (m, 1H), 3.89 (s, 3H), 3.81 (s, 3H), 3.12 – 3.04 (m, 1H), 3.03 – 2.90 (m, 2H), 1.83 – 1.26 (m, 8H), 1.24 – 1.14 (m, 1H), 1.05 – 0.92 (m, 1H), 0.36 (br s, 1H); three protons are missing due to broadening and/or overlapping with the residual solvent signal; LC-MS (ESI⁺) *m/z*: 579.2 [M + H]⁺.

(3*Z*)-7-chloro-10,21-dimethoxy-2,2-dioxo-18-(1-propyl-4-piperidyl)-2λ⁶,5-dithia-3,12,18-triazatetracyclo[18.3.1.0^{4,12}.0^{6,11}]tetracos-1(23),3,6(11),7,9,20(24),21-heptaen-19-one (**49g**). To a stirred solution of **49f** (230 mg, 0.40 mmol, 1.0 equiv) in acetonitrile (30 mL) was added sodium iodide (6.0 mg, 0.04 mmol, 0.1 equiv) and triethylamine (55 μL, 0.40 mmol, 1.0 equiv), followed by 1-bromopropane (43 μL, 0.48 mmol, 1.2 equiv). The reaction was heated for 16 h at 65 °C. A further portion of 1-bromopropane and triethylamine were added and heating continued for a further 24 h. The reaction mixture was concentrated under reduced pressure and the residue partitioned between DCM and water. The phases were separated, the organics were filtered through a hydrophobic frit and concentrated under reduced pressure to afford the title product (200 mg, 0.29 mmol, 73% yield). LC-MS (ESI⁺) *m/z*: 621.4 [M + H]⁺.

(3*Z*)-7-Chloro-10,20-dihydroxy-2,2-dioxo-17-(4-piperidyl)-2λ⁶,5-dithia-3,12,17-triazatetracyclo[17.3.1.0^{4,12}.0^{6,11}]tricos-1(22),3,6(11),7,9,19(23),20-heptaen-18-one;hydrochloride (**20**). The title compound was synthesized from **49a** (50 mg, 0.08 mmol) according to general procedures GP1 and GP2. The desired product was isolated as a light-brown solid (24 mg, 0.038 mmol, 50% yield, 93% purity). ¹H NMR (400 MHz, DMSO-*d*₆) δ 11.04 (s, 1H), 10.78 (s, 1H), 8.76 – 8.60 (m, 1H), 8.59 – 8.41 (m, 1H), 7.66 (dd, *J* = 8.6, 2.4 Hz, 1H), 7.57 (d, *J* = 2.4 Hz, 1H), 7.25 (d, *J* = 8.7 Hz, 1H), 6.99 – 6.92 (m, 2H), 4.61 – 4.34 (m, 3H), 3.31 (2H)^{*}, 3.00 (q, *J* = 12.0 Hz, 2H), 2.72 (br s, 2H), 1.92 (q, *J* = 11.8 Hz, 2H), 1.85 – 1.72 (m, 2H), 1.56 – 1.41 (m, 2H), 0.87 (br s, 2H); ^{*}protons overlap with the residual water peak (confirmed by HSQC experiment). ¹³C NMR (151 MHz, DMSO-*d*₆) δ 167.27, 163.24, 156.59, 144.17, 132.82, 126.62, 126.14, 125.55, 125.18, 124.63, 124.29, 115.96, 115.67, 114.93, 48.80, 47.26, 43.91, 42.98, 29.25, 29.04, 26.01; HRMS (ESI⁺) *m/z*: calcd for [C₂₃H₂₅ClN₄O₅S₂+H]⁺ 537.1028; found 537.1041.

(3*Z*)-7-Chloro-10,21-dihydroxy-2,2-dioxo-18-(4-piperidyl)-2λ⁶,5-dithia-3,12,18-triazatetracyclo[18.3.1.0^{4,12}.0^{6,11}]tetracos-1(23),3,6,8,10,20(24),21-heptaen-19-one;hydrochloride (**15**). The title compound was synthesized from **49b** (90 mg, 0.13 mmol) according to general procedures GP1 and GP2. The desired product was isolated as a light-brown solid (5 mg, 0.008 mmol, 6% yield). ¹H NMR (400 MHz, DMSO-*d*₆) δ 10.91 (s, 1H), 10.84 (s, 1H), 8.67 (d, *J* = 10.9 Hz, 1H), 8.48 – 8.32 (m, 1H), 7.73 (dd, *J* = 8.5, 2.4 Hz, 1H), 7.55 (d, *J* = 2.4 Hz, 1H), 7.24 (d, *J* = 8.7 Hz, 1H), 6.94 (d, *J* = 8.7 Hz, 1H), 6.94 (d, *J* = 8.7 Hz, 1H), 4.50 (t, *J* = 6.0 Hz, 2H), 3.99 (t, *J* = 11.5 Hz, 1H), 3.03 – 2.89 (m, 4H), 2.36 – 2.19 (m, 2H), 1.87 (d, *J* = 13.1 Hz, 2H), 1.45 (br s, 2H), 1.34 (br s, 2H), 0.74 (br s, 2H); two protons are missing due to broadening or overlapping with the residual solvent signal; HRMS (ESI⁺) *m/z*: calcd for [C₂₄H₂₇ClN₄O₅S₂+H]⁺ 551.1185; found 551.1182.

(3*Z*)-18-(*cis*-4-Aminocyclohexyl)-7-chloro-10,21-dihydroxy-2,2-dioxo-2λ⁶,5-dithia-3,12,18-triazatetracyclo[18.3.1.0^{4,12}.0^{6,11}]tetracos-1(23),3,6(11),7,9,20(24),21-

heptaen-19-one;hydrochloride (**16**). The title compound was synthesized from **49c** (45 mg, 0.06 mmol) according to general procedures GP1 and GP2. The desired product was isolated as a light-brown solid (18 mg, 0.028 mmol, 47% yield). ¹H NMR (400 MHz, DMSO-*d*₆) δ 10.93 (s, 1H), 10.80 (s, 1H), 7.91 (d, *J* = 5.3 Hz, 3H), 7.71 (dd, *J* = 8.5, 2.3 Hz, 1H), 7.51 (d, *J* = 2.4 Hz, 1H), 7.23 (d, *J* = 8.7 Hz, 1H), 6.99 – 6.90 (m, 2H), 4.49 (t, *J* = 5.8 Hz, 2H), 3.99 – 3.83 (m, 1H), 3.01 (br s, *J* = 4.7 Hz, 1H), 2.88 (br s, 2H), 2.01 (d, *J* = 12.0 Hz, 2H), 1.87 – 1.70 (m, 4H), 1.58 – 1.37 (m, 4H), 1.36 – 1.25 (m, 2H), 0.68 (br s, 2H); ¹³C NMR (151 MHz, DMSO-*d*₆) δ 167.69, 163.58, 156.32, 144.15, 131.23, 127.92, 126.91, 126.53, 125.18, 124.65, 124.42, 116.10, 115.59, 114.34, 53.42, 48.44, 47.13, 45.54, 30.04, 29.71, 29.28, 27.17, 23.83; HRMS (ESI⁺) *m/z*: calcd for [C₂₅H₂₉ClN₄O₅S₂+H]⁺ 565.1341; found 565.1344.

(3Z)-7-Chloro-18-ethyl-10,21-dihydroxy-2,2-dioxo-2λ⁶,5-dithia-3,12,18-triazatetracyclo[18.3.1.0^{4,12}.0^{6,11}]tetracos-1(23),3,6,8,10,20(24),21-heptaen-19-one (**26**). The title compound was synthesized from **49d** (64 mg, 0.122 mmol) according to general procedure GP1. The desired product was isolated as a white solid. (17 mg, 0.033 mmol, 27% yield). ¹H NMR (400 MHz, DMSO-*d*₆) δ 7.68 (dd, *J* = 8.5, 2.4 Hz, 1H), 7.47 (d, *J* = 2.4 Hz, 1H), 7.19 (d, *J* = 8.7 Hz, 1H), 6.86 (t, *J* = 8.9 Hz, 2H), 4.52 (t, *J* = 5.8 Hz, 2H), 3.36 (q, *J* = 7.1 Hz, 2H), 2.94 – 2.86 (m, 2H), 1.46 – 1.33 (m, 2H), 1.26 (br s, 2H), 1.10 (t, *J* = 7.0 Hz, 3H), 0.75 (br s, 2H); the two ArOH protons are missing due to broadening; LC-MS (ESI⁺) *m/z*: calcd for [C₂₁H₂₂ClN₃O₅S₂+H]⁺ 496.1; found 496.2.

(3Z)-7-chloro-10,22-dihydroxy-2,2-dioxo-19-(4-piperidyl)-2λ⁶,5-dithia-3,12,19-triazatetracyclo[19.3.1.0^{4,12}.0^{6,11}]pentacos-1(24),3,6,8,10,21(25),22-heptaen-20-one;hydrochloride (**17**). The title compound was synthesized from **49e** (45 mg, 0.06 mmol) according to general procedures GP1 and GP2. The desired product was isolated as a light-brown solid (24 mg, 0.036 mmol, 55% yield). ¹H NMR (400 MHz, DMSO-*d*₆) δ 10.96 (s, 1H), 10.82 (s, 1H), 8.75 (d, *J* = 10.9 Hz, 1H), 8.56 – 8.49 (m, 1H), 7.78 (dd, *J* = 8.6, 2.3 Hz, 1H), 7.56 (d, *J* = 2.4 Hz, 1H), 7.24 (d, *J* = 8.6 Hz, 1H), 7.03 (d, *J* = 8.6 Hz, 1H), 6.97 (d, *J* = 8.7 Hz, 1H), 4.43 – 4.35 (m, 2H), 4.32 – 4.21 (m, 1H), 3.02 – 2.87 (m, 5H), 2.20 – 2.07 (m, 2H), 1.83 (d, *J* = 13.1 Hz, 2H), 1.43 – 1.33 (m, 5H), 1.01 – 0.94 (m, 2H), 0.93 – 0.88 (m, 2H); ¹³C NMR (151 MHz, DMSO-*d*₆) δ 167.05, 162.23, 157.02, 144.11, 131.61, 127.59, 126.13, 125.38, 125.23, 124.46, 124.14, 116.01, 115.61, 115.56, 50.09, 47.09, 44.70, 43.08, 29.33, 27.91, 25.80, 24.71, 24.52; HRMS (ESI⁺) *m/z*: calcd for [C₂₅H₂₉ClN₄O₅S₂+H]⁺ 565.1341; found 565.1337.

(3Z)-7-chloro-10,21-dihydroxy-2,2-dioxo-18-(1-propyl-4-piperidyl)-2λ⁶,5-dithia-3,12,18-triazatetracyclo[18.3.1.0^{4,12}.0^{6,11}]tetracos-1(23),3,6(11),7,9,20(24),21-heptaen-19-one;hydrochloride (**22**). The title compound was synthesized from **49g** (200 mg, 0.322 mmol) according to general procedures GP1 and GP2. The desired product was isolated as a white solid (43.8 mg, 0.07 mmol, 21% yield). ¹H NMR (400 MHz, DMSO-*d*₆) δ 10.91 (s, 1H), 10.84 (s, 1H), 9.61 (br s, 1H), 7.73 (dd, *J* = 8.5, 2.3 Hz, 1H), 7.56 (d, *J* = 2.4 Hz, 1H), 7.24 (d, *J* = 8.7 Hz, 1H), 6.94 (d, *J* = 8.8 Hz, 1H), 6.94 (d, *J* = 8.6 Hz, 1H), 4.55 – 4.47 (m, 2H), 4.11 – 3.99 (m, 1H), 3.58 – 3.45 (m, 2H), 3.11 – 2.84 (m, 6H), 2.44 – 2.29 (m, 2H), 1.97 – 1.89 (m, 2H), 1.73 – 1.62 (m, 2H), 1.46 (br s, 2H), 1.35 (br s, 2H), 0.91 (t, *J* = 7.4 Hz, 3H), 0.74 (br s, 2H);

HRMS (ESI⁺) *m/z*: calcd for [C₂₇H₃₃ClN₄O₅S₂+H]⁺ 593.1654; found 593.1661.

Ethyl 5-[(Z)-[7-chloro-4-methoxy-3-[2-(oxiran-2-yl)ethyl]-1,3-benzothiazol-2-ylidene]amino]sulfonyl-2-methoxy-benzoate (**51a**). 5 oven dried microwave vials were charged with **50** (2.5 g, 5.47 mmol, 1.0 equiv) (500 mg in each vial) and potassium carbonate, anhyd (2.27 g, 16.4 mmol, 3.0 equiv) (453mg per vial) and purged with nitrogen. DMF (25 mL) (5ml per vial) and 2-(2-bromoethyl)oxirane (2.48 g, 16.41 mmol, 3.0 equiv) (495 mg per vial) were added and the reactions heated to 120 °C (5 min hold time) by microwave irradiation. Cooled reactions were filtered to remove potassium carbonate, combined, dry loaded (50 °C water bath) and purified by flash column chromatography (SiO₂, gradient elution DCM/MeOH = 100/0 to 98/2) to afford the title compound (2.32 g, 4.40 mmol, 80% yield). ¹H NMR (400 MHz, CDCl₃) δ 8.39 (d, *J* = 2.4 Hz, 1H), 8.10 (dd, *J* = 8.8, 2.5 Hz, 1H), 7.17 (d, *J* = 8.8 Hz, 1H), 7.02 (d, *J* = 8.9 Hz, 1H), 6.84 (d, *J* = 8.8 Hz, 1H), 4.68 (hept, *J* = 6.7 Hz, 2H), 4.36 (q, *J* = 7.1 Hz, 2H), 3.95 (s, 3H), 3.91 (s, 3H), 2.91 – 2.82 (m, 1H), 2.55 (dd, *J* = 5.0, 4.0 Hz, 1H), 2.26 (dd, *J* = 5.0, 2.6 Hz, 1H), 2.03 – 1.91 (m, 1H), 1.91 – 1.76 (m, 1H), 1.38 (t, *J* = 7.1 Hz, 3H); LC-MS (ESI⁺) *m/z*: 527.2 [M + H]⁺.

Ethyl 5-[(Z)-[3-[4-[[*cis*-4-(*tert*-butoxycarbonylamino)cyclohexyl]amino]-3-hydroxy-butyl]-7-chloro-4-methoxy-1,3-benzothiazol-2-ylidene]amino]sulfonyl-2-methoxy-benzoate (**52**). A microwave vial was charged with **51a** (1.22 g, 2.31 mmol, 1.0 equiv), *tert*-butyl *N*-(*cis*-4-aminocyclohexyl)carbamate (992 mg, 4.63 mmol, 2.0 equiv) and ytterbium(III) trifluoromethanesulfonate (144 mg, 0.23 mmol, 0.1 equiv) and purged with nitrogen. THF (12 mL) was added and the reaction heated to 130 °C by microwave irradiation for 1 h. The reaction mixture was filtered through a PTFE frit, dry loaded and purified by flash column chromatography (SiO₂, gradient elution DCM / (MeOH w/10% NH₃) = 100/0 to 80/20). Third major peak was evaporated under reduced pressure to afford the title compound (681 mg, 0.92 mmol, 40% yield). ¹H NMR (400 MHz, CDCl₃) δ 8.39 (d, *J* = 2.4 Hz, 1H), 8.10 (dd, *J* = 8.8, 2.5 Hz, 1H), 7.17 (d, *J* = 8.8 Hz, 1H), 7.03 (d, *J* = 8.9 Hz, 1H), 6.85 (d, *J* = 8.8 Hz, 1H), 4.71 (br s, 1H), 4.68 – 4.53 (m, 2H), 4.36 (q, *J* = 7.2 Hz, 2H), 3.94 (s, 3H), 3.91 (s, 3H), 3.62 (br s, 1H), 3.53 (t, *J* = 7.6 Hz, 1H), 2.68 (dd, *J* = 11.8, 3.1 Hz, 1H), 2.62 – 2.53 (m, 1H), 2.44 (dd, *J* = 11.8, 8.7 Hz, 1H), 1.90 – 1.53 (m, 12H), 1.43 (s, 9H), 1.38 (t, *J* = 7.1 Hz, 3H); LC-MS (ESI⁺) *m/z*: 741.4 [M + H]⁺.

5-[(Z)-[3-[4-[[*cis*-4-(*tert*-butoxycarbonylamino)cyclohexyl]amino]-3-hydroxy-butyl]-7-chloro-4-methoxy-1,3-benzothiazol-2-ylidene]amino]sulfonyl-2-methoxy-benzoic acid (**53**). To a suspension of **52** (680 mg, 0.92 mmol, 1.0 equiv) in methanol (5 mL) was added 4 N lithium hydroxide (aq.) (2.29 mL, 9.17 mmol, 10 equiv) and the reaction stirred at rt for 16 h. The reaction was concentrated to remove excess methanol, diluted with water (25ml) and adjusted to pH 6 with 2N HCl (aq.). The resulting precipitate was collected by filtration, dried under vacuum to give the title compound (575 mg, 0.81 mmol, 88% yield). LC-MS (ESI⁺) *m/z*: 713.5 [M + H]⁺.

tert-Butyl *N*-[*cis*-4-[(3Z)-7-chloro-15-hydroxy-10,20-dimethoxy-2,2,18-trioxo-2λ⁶,5-dithia-3,12,17-triazatetracyclo[17.3.1.0^{4,12}.0^{6,11}]tricos-1(22),3,6(11),7,9,19(23),20-heptaen-17-yl]cyclohexyl]carbamate (**54**). To a flask

charged with **53** (570 mg, 0.80 mmol, 1.0 equiv) was added DMF (20 mL), triethylamine (0.45 mL, 3.2 mmol, 4.0 equiv) and DEPBT (956 mg, 3.2 mmol, 4.0 equiv) and the reaction stirred for 36 h at rt. Reaction was dry loaded and purified by purified by flash column chromatography (SiO₂, gradient elution DCM/MeOH = 100/0 to 98/2) to afford the title compound (189 mg, 0.27 mmol, 34% yield). ¹H NMR (400 MHz, CDCl₃) δ 7.88 (dd, *J* = 8.6, 2.3 Hz, 1H), 7.69 (s, 1H), 7.17 (d, *J* = 8.8 Hz, 1H), 6.86 (dd, *J* = 8.8, 6.8 Hz, 2H), 4.84 (d, *J* = 28.2 Hz, 2H), 4.57 (s, 1H), 4.27 (s, 1H), 3.92 (s, 3H), 3.92 – 3.75 (m, 2H), 3.83 (s, 3H), 3.08 (s, 1H), 2.72 (d, *J* = 16.2 Hz, 1H), 2.02 – 1.53 (m, 9H), 1.46 (s, 9H), 0.83 (s, 1H), 0.61 (s, 1H); LC-MS (ESI⁺) *m/z*: 595.3 [M-Boc + H]⁺.

tert-Butyl *N*-[*cis*-4-[(3Z,15R)-7-chloro-15-hydroxy-10,20-dimethoxy-2,2,18-trioxo-2λ⁶,5-dithia-3,12,17-triazatetracyclo[17.3.1.0^{4,12}.0^{6,11}]tricoso-1(22),3,6(11),7,9,19(23),20-heptaen-17-yl]cyclohexyl]carbamate (**55a**) and *tert*-Butyl *N*-[*cis*-4-[(3Z,15S)-7-chloro-15-hydroxy-10,20-dimethoxy-2,2,18-trioxo-2λ⁶,5-dithia-3,12,17-triazatetracyclo[17.3.1.0^{4,12}.0^{6,11}]tricoso-1(22),3,6(11),7,9,19(23),20-heptaen-17-yl]cyclohexyl]carbamate (**55b**). Racemate **54** (120 mg, 0.17 mmol) was dissolved to 17 mg / mL in methanol and purified by chiral HPLC. Relevant fractions of each isomer were then evaporated to near dryness using a rotary evaporator. The resultant solids were then transferred into final vessels with DCM which was removed on a Biotage V10 at 35 °C before being stored in a vacuum oven at 35 °C and 5 mbar until constant weight to afford **55a** (46 mg, 0.07 mmol, 39% yield, 99.8% ee); ¹H NMR (400 MHz, CDCl₃) δ 7.87 (dd, *J* = 8.6, 2.3 Hz, 1H), 7.72 (s, 1H), 7.17 (d, *J* = 8.8 Hz, 1H), 6.87 (d, *J* = 8.7 Hz, 1H), 6.85 (d, *J* = 8.9 Hz, 1H), 4.88 – 4.77 (m, 2H), 4.55 (br s, 1H), 4.28 (br s, 1H), 3.96 – 3.80 (m, 2H), 3.92 (s, 3H), 3.83 (s, 3H), 3.08 (d, *J* = 15.7 Hz, 1H), 2.85 (br s, 1H), 2.71 (d, *J* = 16.1 Hz, 1H), 1.98 – 1.57 (m, 9H), 1.45 (s, 9H), 0.58 (br s, 1H); LC-MS (ESI⁺) *m/z*: 595.7 [M-Boc + H]⁺ and **55b** (45 mg, 0.06 mmol, 37% yield, 100% ee); ¹H NMR (400 MHz, CDCl₃) δ 7.88 (dd, *J* = 8.6, 2.3 Hz, 1H), 7.70 (s, 1H), 7.17 (d, *J* = 8.8 Hz, 1H), 6.87 (d, *J* = 8.7 Hz, 1H), 6.86 (d, *J* = 8.9 Hz, 1H), 4.93 – 4.73 (m, 2H), 4.56 (br s, 1H), 4.28 (br s, 1H), 3.96 – 3.80 (m, 2H), 3.93 (s, 3H), 3.83 (s, 3H), 3.08 (d, *J* = 15.7 Hz, 1H), 2.86 – 2.56 (m, 2H), 2.02 – 1.63 (m, 9H), 1.46 (s, 9H), 0.60 (br s, 1H); LC-MS (ESI⁺) *m/z*: 595.8 [M-Boc + H]⁺.

(3E,15R)-17-(*cis*-4-aminocyclohexyl)-7-chloro-10,15,20-trihydroxy-2,2-dioxo-2λ⁶,5-dithia-3,12,17-triazatetracyclo[17.3.1.0^{4,12}.0^{6,11}]tricoso-1(22),3,6(11),7,9,19(23),20-heptaen-18-one;hydrochloride (**18**). The title compound was synthesized from **55a** (43 mg, 0.06 mmol) according to general procedures GP1 and GP2. The desired product was isolated as a white solid (19 mg, 0.03 mmol, 50% yield). ¹H NMR (400 MHz, DMSO-*d*₆) δ 11.01 (s, 1H), 10.74 (s, 1H), 8.01 (br s, 3H), 7.64 – 7.55 (m, 2H), 7.23 (d, *J* = 8.7 Hz, 1H), 6.95 (d, *J* = 8.7 Hz, 1H), 6.90 (d, *J* = 8.4 Hz, 1H), 5.08 (v br s, 1H), 4.88 – 4.73 (m, 1H), 4.37 – 4.18 (m, 2H), 3.26 (dd, *J* = 15.9, 6.3 Hz, 1H), 2.16 – 1.59 (m, 8H), 1.59 – 1.40 (m, 2H), 0.23 (br s, 1H); two protons are missing due to broadening or overlapping with the residual solvent signal; ¹³C NMR (151 MHz, DMSO-*d*₆) δ 167.93, 163.37, 156.39, 144.29, 132.54, 126.72, 126.50, 126.08, 125.22, 124.65, 124.30, 115.92, 115.61, 115.00, 52.22, 50.54, 46.32, 45.03, 40.43, 27.52, 27.41, 23.54, 23.04; one aliphatic carbon is missing due to overlapping or broadening; HRMS (ESI⁺) *m/z*: calcd for [C₂₄H₂₇ClN₄O₆S₂+H]⁺ 567.1134; found 567.1129.

(3E,15S)-17-(*cis*-4-aminocyclohexyl)-7-chloro-10,15,20-trihydroxy-2,2-dioxo-2λ⁶,5-dithia-3,12,17-triazatetracyclo[17.3.1.0^{4,12}.0^{6,11}]tricoso-1(22),3,6(11),7,9,19(23),20-heptaen-18-one;hydrochloride (**19**). The title compound was synthesized from **55b** (45 mg, 0.06 mmol) according to general procedures GP1 and GP2. The desired product was isolated as a white solid (18 mg, 0.03 mmol, 46% yield). ¹H NMR (400 MHz, DMSO-*d*₆) δ 11.01 (s, 1H), 10.75 (s, 1H), 8.01 (br s, 3H), 7.64 – 7.55 (m, 2H), 7.23 (d, *J* = 8.7 Hz, 1H), 6.95 (d, *J* = 8.7 Hz, 1H), 6.90 (d, *J* = 8.4 Hz, 1H), 5.03 (v br s, 1H), 4.88 – 4.73 (m, 1H), 4.41 – 4.16 (m, 2H), 3.25 (dd, *J* = 15.8, 6.3 Hz, 1H), 2.16 – 1.58 (m, 8H), 1.58 – 1.40 (m, 2H), 0.23 (br s, 1H); two protons are missing due to broadening or overlapping with the residual solvent signal; ¹³C NMR (151 MHz, DMSO-*d*₆) δ 167.92, 163.37, 156.40, 144.32, 132.53, 126.73, 126.50, 126.08, 125.22, 124.64, 124.28, 115.93, 115.59, 115.00, 52.12, 50.54, 46.32, 45.03, 40.43, 27.52, 27.41, 23.58, 23.05; one aliphatic carbon is missing due to overlapping or broadening; HRMS (ESI⁺) *m/z*: calcd for [C₂₄H₂₇ClN₄O₆S₂+H]⁺ 567.1134; found 567.1137.

Ethyl 5-[(Z)-[3-(5-bromopentyl)-7-chloro-4-methoxy-1,3-benzothiazol-2-ylidene]amino]sulfonyl-2-methoxybenzoate (**51b**). To a suspension of **50** (16.0 g, 35.0 mmol, 1.0 equiv) and potassium carbonate, anhyd (24.2 g, 175 mmol, 5.0 equiv) in anhyd DMF (300 mL) was added 1,5-dibromopentane (19.1 mL, 140 mmol, 4.0 equiv) and the suspension was stirred at rt for 48 h. Further 1,5-dibromopentane (4.75 mL, 35 mmol, 1.0 equiv) was added and stirring continued for 5 d. The suspension was filtered before the reaction solvent was removed under reduced pressure and the resultant oil left to stand overnight, forming a yellow solid. The solid was suspended in diethyl ether (200 mL) and filtered, washing with further diethyl ether, then air dried to yield the title compound (11.3 g, 18.6 mmol, 53% yield) as a light-brown solid. ¹H NMR (400 MHz, DMSO-*d*₆) δ 8.09 (d, *J* = 2.5 Hz, 1H), 8.03 (dd, *J* = 8.8, 2.5 Hz, 1H), 7.40 (d, *J* = 8.8 Hz, 1H), 7.32 (d, *J* = 8.9 Hz, 1H), 7.19 (d, *J* = 8.9 Hz, 1H), 4.39 (t, *J* = 7.3 Hz, 2H), 4.27 (q, *J* = 7.1 Hz, 2H), 3.92 (s, 3H), 3.88 (s, 3H), 3.40 (t, *J* = 6.7 Hz, 2H), 1.72 (p, *J* = 6.9 Hz, 2H), 1.60 (p, *J* = 7.5 Hz, 2H), 1.34 – 1.22 (m, 5H); LC-MS (ESI⁺) *m/z*: 607.1 [M + H]⁺.

tert-Butyl 8-[5-[(2Z)-7-chloro-2-(3-ethoxycarbonyl-4-methoxy-phenyl)sulfonylimino-4-methoxy-1,3-benzothiazol-3-yl]pentylamino]*cis*-1-azaspiro[4.5]decane-1-carboxylate (**56d**). To a solution of **51b** (1.23 g, 2.02 mmol, 1.2 equiv) in anhyd acetonitrile (20 mL) was added *tert*-butyl *cis*-8-amino-1-azaspiro[4.5]decane-1-carboxylate (476 mg, 1.68 mmol, 1.0 equiv) and potassium carbonate, anhyd (698 mg, 5.05 mmol, 3.0 equiv) under nitrogen. The reaction mixture was stirred at 55 °C for 6 d. The cooled reaction was filtered through a short pad of silica washing with methanol and ethyl acetate. Filtrate and washings were dry loaded and purified by flash column chromatography (SiO₂; gradient elution DCM/MeOH = 100/0 to 90/10) to afford the title compound (661 mg, 0.85 mmol, 50% yield) as a glassy, colourless solid. ¹H NMR (400 MHz, DMSO-*d*₆) δ 8.09 (d, *J* = 2.5 Hz, 1H), 8.07 – 7.96 (m, 2H), 7.43 (d, *J* = 8.9 Hz, 1H), 7.32 (d, *J* = 8.9 Hz, 1H), 7.22 (d, *J* = 9.0 Hz, 1H), 4.44 – 4.36 (m, 2H), 4.27 (q, *J* = 7.1 Hz, 2H), 3.93 (s, 3H), 3.92 – 3.86 (m, 4H), 3.36 – 3.27 (m, 2H), 2.84 (br s, 2H), 2.48 – 2.40 (m, 2H), 1.95 – 1.78 (m, 4H), 1.77 – 1.53 (m, 8H), 1.40 (s, 9H), 1.34 – 1.18 (m, 7H); LC-MS (ESI⁺) *m/z*: 779.6 [M + H]⁺.

tert-Butyl 4-[5-[(2*Z*)-7-chloro-2-(3-ethoxycarbonyl-4-methoxy-phenyl)sulfonylimino-4-methoxy-1,3-benzothiazol-3-yl]pentylamino]piperidine-1-carboxylate (**56a**). The title compound was synthesized according to the procedure for **56d** using *tert*-butyl 4-aminopiperidine-1-carboxylate as described in Scheme 4. The desired product was isolated as an off-white solid (4.71 g, 5.84 mmol, 71% yield). ¹H NMR (400 MHz, DMSO-*d*₆) δ 8.09 (d, *J* = 2.5 Hz, 1H), 8.03 (dd, *J* = 8.9, 2.5 Hz, 1H), 7.42 (d, *J* = 8.8 Hz, 1H), 7.32 (d, *J* = 9.0 Hz, 1H), 7.20 (d, *J* = 9.0 Hz, 1H), 4.40 (t, *J* = 7.2 Hz, 2H), 4.27 (q, *J* = 7.1 Hz, 2H), 3.92 (s, 3H), 3.89 (s, 3H), 3.76 (d, *J* = 13.6 Hz, 2H), 2.76 (br s, 2H), 2.38 – 2.28 (m, 2H), 1.75 – 1.61 (m, 2H), 1.57 (q, *J* = 7.6 Hz, 2H), 1.46 – 1.35 (m, 11H), 1.34 – 1.24 (m, 5H), 1.18 (q, *J* = 7.8 Hz, 2H), 1.11 – 0.93 (m, 2H); LC-MS (ESI⁺) *m/z*: 725.4 [M + H]⁺.

tert-Butyl (1*S*,5*R*)-3-[5-[(2*Z*)-7-chloro-2-(3-ethoxycarbonyl-4-methoxy-phenyl)sulfonylimino-4-methoxy-1,3-benzothiazol-3-yl]pentylamino]-8-azabicyclo[3.2.1]octane-8-carboxylate (**56b**). The title compound was synthesized according to the procedure for **56d** using *tert*-butyl (1*R*,5*S*)-3-amino-8-azabicyclo[3.2.1]octane-8-carboxylate as described in Scheme 4. The desired product was isolated as a solid (1.56 mg, 2.08 mmol, 50% yield). ¹H NMR (400 MHz, Chloroform-*d*) δ 8.39 (d, *J* = 2.5 Hz, 1H), 8.08 (dd, *J* = 8.8, 2.4 Hz, 1H), 7.15 (d, *J* = 8.8 Hz, 1H), 7.02 (d, *J* = 8.9 Hz, 1H), 6.84 (d, *J* = 8.8 Hz, 1H), 4.53 – 4.42 (m, 2H), 4.35 (q, *J* = 7.1 Hz, 2H), 4.23 – 4.01 (m, 2H), 3.94 (s, 3H), 3.90 (s, 3H), 2.85 (t, *J* = 6.1 Hz, 1H), 2.48 (t, *J* = 6.8 Hz, 2H), 2.15 – 1.91 (m, 4H), 1.90 – 1.77 (m, 2H), 1.74 – 1.58 (m, 2H), 1.45 (s, 9H), 1.50 – 1.23 (m, 10H); LC-MS (ESI⁺) *m/z*: 751.5 [M + H]⁺.

Ethyl 5-[(*Z*)-[3-[5-[(2*S*,6*R*)-1-benzyl-2,6-dimethyl-4-piperidyl]amino]pentyl]-7-chloro-4-methoxy-1,3-benzothiazol-2-ylidene]amino]sulfonyl-2-methoxy-benzoate (**56c**).

The title compound was synthesized according to the procedure for **56d** using (2*R*,4*r*,6*S*)-1-benzyl-2,6-dimethylpiperidin-4-amine as described in Scheme 4. The desired product was isolated as an off-white glassy solid (1.28 g, 1.46 mmol, 96% yield). ¹H NMR (400 MHz, DMSO-*d*₆) δ 8.10 (d, *J* = 2.5 Hz, 1H), 8.03 (ddd, *J* = 8.1, 5.5, 2.5 Hz, 1H), 7.41 (d, *J* = 8.8 Hz, 1H), 7.30 (dtd, *J* = 23.8, 7.4, 1.7 Hz, 5H), 7.22 – 7.09 (m, 2H), 4.39 (t, *J* = 7.3 Hz, 2H), 4.32 – 4.18 (m, 2H), 3.93 (s, 3H), 3.91 – 3.84 (m, 3H), 3.71 – 3.61 (m, 2H), 2.68 – 2.43 (m, 5H), 1.77 (dd, *J* = 12.6, 3.6 Hz, 2H), 1.61 (p, *J* = 7.5 Hz, 2H), 1.40 (q, *J* = 7.6 Hz, 2H), 1.33 – 1.20 (m, 5H), 1.15 – 1.03 (m, 2H), 1.00 – 0.94 (m, 6H). (N-H very broad); LC-MS (ESI⁺) *m/z*: 743.6 [M + H]⁺.

5-[(*Z*)-[3-[5-[(*cis*-1-*tert*-butoxycarbonyl-1-azaspiro[4.5]decan-8-yl]amino]pentyl]-7-chloro-4-methoxy-1,3-benzothiazol-2-ylidene]amino]sulfonyl-2-methoxy-benzoic acid (**57d**). To a stirred solution of **56d** (661 mg, 0.85 mmol, 1.0 equiv) in methanol (20 mL) was added 2 N aqueous sodium hydroxide solution (5.0 mL, 10 mmol, 11.8 equiv). The mixture was stirred for 2 h at rt. The reaction mixture was diluted with DCM and the phases separated. The aqueous layer was acidified to pH = 3 and extracted with DCM (2 × 10 mL). The combined organics were washed with brine, dried (MgSO₄), filtered and evaporated under reduced pressure to afford the title compound (97.0 mg, 0.13 mmol, 15% yield) as a clear glassy solid. LC-MS (ESI⁺) *m/z*: 751.5 [M + H]⁺.

5-[(*Z*)-[3-[5-[(1-*tert*-butoxycarbonyl-4-piperidyl]amino]pentyl]-7-chloro-4-methoxy-1,3-benzothiazol-2-ylidene]amino]sulfonyl-2-methoxy-benzoic acid

(**57a**). To a solution of **56a** (4.71 g, 6.49 mmol, 1.0 equiv) in ethanol (40 mL) at 0 °C was added an aqueous solution of 4N sodium hydroxide (10.0 mL, 40 mmol). After addition was complete the reaction was stirred for 16 h at rt. The organic solvent was removed under reduced pressure and the aqueous residue acidified to pH 6 by the dropwise addition of 5 N HCl (aq). The precipitated solid was collected by filtration, air dried and further dried under vacuum to afford the desired product (4.28 g, 5.52 mmol, 85% yield). LC-MS (ESI⁺) *m/z*: 697.4 [M + H]⁺.

5-[(*Z*)-[3-[5-[(1*S*,5*R*)-8-*tert*-butoxycarbonyl-8-azabicyclo[3.2.1]octan-3-yl]amino]pentyl]-7-chloro-4-methoxy-1,3-benzothiazol-2-ylidene]amino]sulfonyl-2-methoxy-benzoic acid (**57b**). To a suspension of **56b** (1.56 g, 2.08 mmol, 1.0 equiv) in methanol (25 mL) was added 2N aqueous sodium hydroxide solution (10.4 mL, 20.8 mmol, 10 equiv) and the reaction stirred at rt for 16 h. Analysis showed ~10% conversion to the desired product. The reaction was heated to reflux for 2 h (pale yellow solution formed). The organic solvent was removed under reduced pressure and the residue diluted with water (100ml) and pH adjusted to 5 using 2N HCl (aq.) (~12ml). The resulting sticky solid was collected by filtration, air dried and further dried under vacuum to afford the desired product as a white solid (978 mg, 1.35 mmol, 65% yield); ¹H NMR (400 MHz, DMSO-*d*₆) δ 7.83 – 7.77 (m, 2H), 7.36 (d, *J* = 8.8 Hz, 1H), 7.17 (d, *J* = 9.0 Hz, 1H), 7.11 (d, *J* = 8.5 Hz, 1H), 4.39 (t, *J* = 7.2 Hz, 2H), 4.03 (s, 2H), 3.91 (s, 3H), 3.80 (s, 3H), 2.93 – 2.77 (m, 1H), 2.53 (d, *J* = 7.4 Hz, 2H), 2.16 (dt, *J* = 13.5, 6.5 Hz, 2H), 1.92 – 1.73 (m, 4H), 1.65 – 1.50 (m, 4H), 1.46 – 1.32 (m, 2H), 1.39 (s, 9H), 1.20 – 1.05 (m, 2H). (N-H and COOH peaks are very broad); LC-MS (ESI⁺) *m/z*: 723.5 [M + H]⁺.

5-[(*Z*)-[3-[5-[(2*R*,6*S*)-1-benzyl-2,6-dimethyl-4-piperidyl]amino]pentyl]-7-chloro-4-methoxy-1,3-benzothiazol-2-ylidene]amino]sulfonyl-2-methoxy-benzoic acid (**57c**). The title compound was synthesized from **56c** according to the procedure for **57a** but using a 4 N aqueous lithium hydroxide solution. The desired product was isolated as a light-brown solid (834 mg, 0.99 mmol, 85% yield). ¹H NMR (400 MHz, DMSO-*d*₆) δ 7.79 – 7.61 (m, 2H), 7.43 – 6.99 (m, 8H), 4.49 – 4.24 (m, 2H), 3.91 (s, 3H), 3.84 – 3.73 (m, 5H), 3.66 (s, 2H), 2.93 – 2.77 (m, 1H), 2.72 – 2.58 (m, 2H), 2.00 – 1.70 (m, 2H), 1.65 – 1.05 (m, 9H), 1.03 – 0.86 (m, 6H); one proton is missing due to broadening or overlapping; LC-MS (ESI⁺) *m/z*: 715.5 [M + H]⁺.

tert-Butyl 8-[(3*Z*)-7-chloro-10,21-dimethoxy-2,2,19-trioxo-2λ⁶,5-dithia-3,12,18-triazatetracyclo[18.3.1.0^{4,12}.0^{6,11}]tetracosan-1(23),3,6(11),7,9,20(24),21-heptaen-18-yl]-*cis*-1-azaspiro[4.5]decan-1-carboxylate (**49j**). To a stirred solution of **57d** (97.0 mg, 0.13 mmol, 1.0 equiv) and triethylamine (0.07 mL, 0.52 mmol, 4.0 equiv) in anhyd DMF (15 mL) and anhyd toluene (15 mL) was added DEPBT (97.0 mg, 0.32 mmol, 2.5 equiv) and the reaction mixture was stirred under nitrogen at rt for 5 d. The majority of the solvent was removed under reduced pressure. The residue was re-solubilised in DCM and loaded onto a Teledyne C18 dry-load cartridge, evaporating the solvent under a stream of nitrogen. The crude material was purified by reverse phase flash column chromatography (SiO₂-C18, gradient elution water/ MeCN (pH = 9) = 95/5 to 5/95) to afford the title compound (62.0 mg, 0.09 mmol, 66% yield) as an off-white solid. ¹H NMR (400 MHz, DMSO-*d*₆) δ 7.87 (dd, *J* = 8.7, 2.3 Hz, 1H), 7.59 (d, *J* = 2.4 Hz, 1H),

7.40 (d, $J = 8.9$ Hz, 1H), 7.21 – 7.12 (m, 2H), 4.64 – 4.48 (m, 1H), 4.45 – 4.32 (m, 1H), 4.20 – 4.11 (m, 1H), 3.89 (s, 3H), 3.82 (s, 3H), 3.35 – 3.26 (m, 2H), 2.69 – 2.55 (m, 1H), 2.41 – 2.24 (m, 2H), 2.23 – 2.04 (m, 2H), 1.87 – 1.65 (m, 5H), 1.63 – 1.48 (m, 4H), 1.46 – 1.27 (m, 13H), 0.96 (br s, 1H), 0.38 (br s, 1H); ^{13}C NMR (101 MHz, DMSO- d_6) δ 166.96, 163.96, 157.51, 153.17, 146.08, 132.62, 128.16, 127.32, 126.98, 126.14, 124.50, 124.48, 117.55, 112.67, 110.43, 78.02, 61.40, 56.88, 56.19, 49.98, 47.71, 47.55, 39.91*, 31.79, 31.44, 29.95, 28.87, 28.23, 25.27, 23.84, 21.02; *observed in HSQC; LC-MS (ESI $^+$) m/z : 733.5 [M + H] $^+$.

(3Z)-18-[(2R,6S)-1-benzyl-2,6-dimethyl-4-piperidyl]-7-chloro-10,21-dimethoxy-2,2-dioxo-2 λ^6 ,5-dithia-3,12,18-triazatetracyclo[18.3.1.0 4,12 .0 6,11]tetracos-1(24),3,6(11),7,9,20,22-heptaen-19-one (**49i**). The title compound was synthesized from **57c** according to the procedure for **49j**. The desired product was isolated as a yellow solid (666 mg, 0.96 mmol, 82% yield). ^1H NMR (400 MHz, DMSO- d_6) δ 7.52 – 6.95 (m, 8H), 4.72 – 4.27 (m, 2H), 4.06 (t, $J = 12.0$ Hz, 1H), 3.99 – 3.59 (m, 8H), 3.22 – 2.94 (m, 1H), 2.60 (d, $J = 7.9$ Hz, 4H), 1.96 – 1.10 (m, 10H), 1.08 – 0.70 (m, 6H), 0.36 (s, 1H); Complex spectra due to nitrogen inversion; LC-MS (ESI $^+$) m/z : 697.5 [M + H] $^+$.

tert-Butyl 4-[(3Z)-7-chloro-10,21-dimethoxy-2,2,19-trioxo-2 λ^6 ,5-dithia-3,12,18-triazatetracyclo[18.3.1.0 4,12 .0 6,11]tetracos-1(23),3,6,8,10,20(24),21-heptaen-18-yl]piperidine-1-carboxylate (**49b**). To a solution of **57a** (2.14 g, 3.07 mmol, 1.0 equiv) in chloroform (500 mL) was added HATU (1.45 g, 6.14 mmol, 2.0 equiv) and triethylamine (0.86 mL, 6.14 mmol, 2.0 equiv). The reaction was stirred at rt for 5 d. A second reaction was carried out in parallel using identical conditions to the above. These reactions were combined, and the solvent volume reduced to ~30 mL and the organics washed with water (2 x 30 mL). The phases were separated, dried (MgSO $_4$), filtered and concentrated under reduced pressure to afford the crude. Purified by flash column chromatography (SiO $_2$, gradient elution DCM/MeOH = 100/0 to 90/10). Product fractions were combined and concentrated under reduced pressure to afford the title compound (4.00 g, 5.59 mmol, 91% yield). ^1H NMR (400 MHz, CDCl $_3$) δ 7.98 (dd, $J = 8.6, 2.3$ Hz, 1H), 7.85 (d, $J = 2.3$ Hz, 1H), 7.16 (d, $J = 8.7$ Hz, 1H), 6.88 (d, $J = 8.7$ Hz, 1H), 6.83 (d, $J = 8.8$ Hz, 1H), 4.72 (br s, 1H), 4.57 – 4.48 (m, 1H), 4.47 – 4.37 (m, 1H), 4.23 (d, $J = 13.3$ Hz, 2H), 3.89 (s, 3H), 3.84 (s, 3H), 3.01 (br s, 1H), 2.82 (br s, 2H), 2.69 (br s, 1H), 1.87 (br s, 1H), 1.75 (br s, 1H), 1.71–1.42 (m, 5H), 1.47 (s, 9H), 1.25 (br s, 1H), 0.99 (s, 1H), 0.59 (s, 1H); LC-MS (ESI $^+$) m/z : 579.3 [M-Boc + H] $^+$.

tert-Butyl (1S,5R)-3-[(3Z)-7-chloro-10,21-dimethoxy-2,2,19-trioxo-2 λ^6 ,5-dithia-3,12,18-triazatetracyclo[18.3.1.0 4,12 .0 6,11]tetracos-1(24),3,6(11),7,9,20,22-heptaen-18-yl]-8-azabicyclo[3.2.1]octane-8-carboxylate (**49h**). The title compound was synthesized from **57b** according to the procedure for **49b**. The desired product was isolated as a white solid (611 mg, 0.85 mmol, 63% yield). ^1H NMR (400 MHz, CDCl $_3$) δ 7.98 – 7.91 (m, 1H), 7.78 (s, 1H), 7.15 (dd, $J = 8.8, 2.4$ Hz, 1H), 6.84 (app t, $J = 8.9$ Hz, 2H), 4.72 – 4.67 (m, 1H), 4.51 – 4.43 (m, 1H), 4.33 (br s, 1H), 4.24 (br s, 1H), 3.89 (s, 3H), 3.83 (s, 3H), 3.22 (br s, 1H), 2.92 – 2.84 (m, 1H), 2.80 (d, $J = 2.4$ Hz, 1H), 2.45 – 2.09 (m, 4H), 2.01 – 1.84 (m, 4H), 1.54 (br s, 2H), 1.47 (s, 9H), 1.19 (s, 2H), 0.58 (s, 1H), 1.38 – 1.30 (m, 1H); LC-MS (ESI $^+$) m/z : 649.3 [M-*t*Bu + H] $^+$.

(3Z)-18-[(2S,6R)-1-Benzyl-2,6-dimethyl-4-piperidyl]-7-chloro-10,21-dihydroxy-2,2-dioxo-2 λ^6 ,5-dithia-3,12,18-triazatetracyclo[18.3.1.0 4,12 .0 6,11]tetracos-1(23),3,6,8,10,20(24),21-heptaen-19-one;hydrochloride; (**28**). The title compound was synthesized from **49i** according to general procedures GP1 and GP2. The desired product was isolated as a white solid (34 mg, 0.049 mmol, 14% yield). ^1H NMR (400 MHz, DMSO- d_6) δ 11.00 (app. d, 1H), 10.91 (app. d, 1H), (10.10 (app. t), 9.75 (br s), 1H), 7.78 – 7.67 (m, 1H), 7.65 – 7.37 (m, 6H), 7.27 – 7.22 (m, 1H), 7.05 – 6.93 (m, 2H), 4.61 – 4.36 (m, 4H), 4.01 – 3.86 (m, 1H), 3.66 – 3.54 (m, 1H), (3.06 – 2.79 (m, 2H), 1.99 (d, $J = 12.8$ Hz, 1H), 1.84 (d, $J = 13.5$ Hz, 1H), 1.62 – 1.25 (m, 10H), 0.73 (br s, 2H); two protons overlap with the residual solvent signal and one proton overlaps with the residual water signal (observed in HSQC experiment); Complex spectra due to nitrogen inversion at the tertiary amine; HRMS (ESI $^+$) m/z : calcd for [C $_{33}$ H $_{37}$ ClN $_4$ O $_5$ S $_2$ +H] $^+$ 669.1967; found 669.1963.

(3Z)-18-(*cis*-1-azaspiro[4.5]decan-8-yl)-7-chloro-10,21-dihydroxy-2,2-dioxo-2 λ^6 ,5-dithia-3,12,18-triazatetracyclo[18.3.1.0 4,12 .0 6,11]tetracos-1(23),3,6(11),7,9,20(24),21-heptaen-19-one;hydrochloride (**21**). The title compound was synthesized from **49j** according to general procedures GP1 and GP2. The desired product was isolated as a white solid (4.0 mg, 0.006 mmol, 8% yield). ^1H NMR (400 MHz, DMSO- d_6) δ 11.01 (s, 1H), 10.86 (s, 1H), 9.08 (t, $J = 5.7$ Hz, 2H), 7.71 (dd, $J = 8.5, 2.4$ Hz, 1H), 7.52 (d, $J = 2.4$ Hz, 1H), 7.22 (d, $J = 8.7$ Hz, 1H), 7.00 (d, $J = 8.7$ Hz, 1H), 6.96 (d, $J = 8.5$ Hz, 1H), 4.48 (t, $J = 5.6$ Hz, 2H), 4.17 (t, $J = 12.4$ Hz, 1H), 3.24 (p, $J = 6.4$ Hz, 2H), 2.94 (br s, 2H), 2.10 – 1.86 (m, 6H), 1.81 – 1.73 (m, 2H), 1.72 – 1.57 (m, 4H), 1.48 (p, $J = 6.7$ Hz, 2H), 1.36 (p, $J = 6.9$ Hz, 2H), 0.67 (br s, 2H); ^{13}C NMR (101 MHz, DMSO- d_6) δ 167.78, 163.56, 156.44, 144.24, 131.16, 127.84, 126.88, 126.52, 125.17, 124.62, 124.40, 116.14, 115.53, 114.37, 65.11, 52.65, 47.09, 44.86, 43.93, 37.60, 32.76, 30.42, 29.30, 25.48, 23.85, 21.68; HRMS (ESI $^+$) m/z : calcd for [C $_{28}$ H $_{33}$ ClN $_4$ O $_5$ S $_2$ +H] $^+$ 605.1654; found 605.1659.

(3Z)-7-Chloro-10,21-dimethoxy-2,2-dioxo-18-(4-piperidyl)-2 λ^6 ,5-dithia-3,12,18-triazatetracyclo[18.3.1.0 4,12 .0 6,11]tetracos-1(24),3,6(11),7,9,20,22-heptaen-19-one (**49f**). To a stirred solution of **49b** (4.00 g, 5.89 mmol, 1.0 equiv) in DCM (60 mL) was added TFA (5.00 mL, 65.3 mmol) and the mixture stirred at rt for 60 h. The solvent was removed under reduced pressure. The residue was loaded onto a pre-equilibrated ion-exchange cartridge and the cartridge washed with methanol (~2 CV). The product was eluted with 2N ammonia in methanol and fractions containing product were concentrated under reduced pressure to afford the title product (2.25 g, 3.69 mmol, 63% yield) as a pale-yellow solid. ^1H NMR (600 MHz, DMSO- d_6) δ 7.87 (d, $J = 8.7$ Hz, 1H), 7.58 (s, 1H), 7.39 (d, $J = 8.8$ Hz, 1H), 7.19 – 7.12 (m, 2H), 4.59 – 4.51 (m, 1H), 4.44 – 4.37 (m, 1H), 4.10 – 4.02 (m, 1H), 3.89 (s, 3H), 3.81 (s, 3H), 3.12 – 3.04 (m, 1H), 3.03 – 2.96 (m, 2H), 2.61 – 2.53 (m, 1H), 1.80 – 1.71 (m, 2H), 1.69 – 1.59 (m, 1H), 1.56 – 1.51 (m, 2H), 1.45 (s, 1H), 1.37 – 1.26 (m, 1H), 1.21 – 1.13 (m, 1H), 0.99 (s, 1H), 0.40 – 0.30 (m, 1H); two protons overlap with the residual water peak and the N-H resonance is not observed due to broadening; LC-MS (ESI $^+$) m/z : 579.2 [M + H] $^+$.

(3Z)-18-[(1S,5R)-8-azabicyclo[3.2.1]octan-3-yl]-7-chloro-10,21-dimethoxy-2,2-dioxo-2 λ^6 ,5-dithia-3,12,18-triazatetracyclo[18.3.1.0 4,12 .0 6,11]tetracos-1(24),3,6(11),7,9,20,22-heptaen-19-one (**49k**). To a

solution of **49h** (611 mg, 0.87 mmol, 1.0 equiv) in a mixture of DCM (6 mL) and methanol (6 mL) was added HCl in 1,4-dioxane (4 M) (2.17 mL, 8.66 mmol, 10.0 equiv) and the reaction stirred at rt for 17 h. The reaction mixture was loaded onto 20 g ion-exchange cartridge and the cartridge washed with methanol:DCM (1:1) (3CV) followed by 2 N ammonia in methanol:DCM (1:1). Basic eluent was evaporated under reduced pressure to afford the title product (472 mg, 0.780 mmol, 90% yield). ¹H NMR (400 MHz, DMSO-*d*₆) δ 7.86 (dd, *J* = 8.7, 2.4 Hz, 1H), 7.56 (d, *J* = 2.4 Hz, 1H), 7.40 (d, *J* = 8.9 Hz, 1H), 7.17 (d, *J* = 9.0 Hz, 1H), 7.14 (d, *J* = 8.8 Hz, 1H), 4.62 – 4.48 (m, 1H), 4.48 – 4.33 (m, 1H), 4.01 – 3.91 (m, 1H), 3.90 (s, 3H), 3.81 (s, 3H), 3.77 – 3.68 (m, 2H), 3.35 (br s, 1H), 2.96 (d, *J* = 14.9 Hz, 1H), 2.61 (t, *J* = 10.7 Hz, 1H), 2.40 – 2.22 (m, 1H), 2.22 – 2.10 (m, 1H), 1.94 (t, *J* = 11.9 Hz, 1H), 1.89 – 1.71 (m, 5H), 1.62 – 1.47 (m, 1H), 1.47 – 1.34 (m, 1H), 1.34 – 1.18 (m, 1H), 1.17 – 1.01 (m, 2H), 0.48 – 0.23 (m, 1H); LC-MS (ESI⁺) *m/z*: 605.4 [M + H]⁺.

(3Z)-18-(1-acetyl-4-piperidyl)-7-chloro-10,21-dimethoxy-2,2-dioxo-2λ⁶,5-dithia-3,12,18-triazatetracyclo[18.3.1.0^{4,12}.0^{6,11}]tetracos-1(23),3,6(11),7,9,20(24),21-heptaen-19-one (**49i**). **49f** (120 mg, 0.21 mmol, 1.0 equiv) was dissolved in DCM (2 mL). DMAP (2.50 mg, 0.02 mmol, 0.1 equiv), triethylamine (160 μL, 0.56 mmol, 2.7 equiv) and acetyl chloride (20 μL, 0.28 mmol, 1.4 equiv) were added sequentially and the resulting mixture stirred at rt for 30 min. The reaction was quenched by the addition of a saturated aqueous solution of sodium hydrogen carbonate (~1 mL) and the biphasic mixture filtered through a phase separator. The organic phase was concentrated under reduced pressure and the residue purified by flash column chromatography (SiO₂, gradient elution with heptane/EtOAc = 100/0 to 0/100) to afford the title compound afford the title product (95 mg, 0.15 mmol, 74% yield). ¹H NMR (400 MHz, CDCl₃) δ 7.95 (dd, *J* = 8.6, 2.3 Hz, 1H), 7.82 (d, *J* = 2.3 Hz, 1H), 7.14 (d, *J* = 8.7 Hz, 1H), 6.87 (d, *J* = 8.7 Hz, 1H), 6.82 (d, *J* = 8.8 Hz, 1H), 4.88 – 4.62 (m, 2H), 4.62 – 4.32 (m, 2H), 3.88 (s, 4H), 3.83 (s, 3H), 3.18 (t, *J* = 13.4 Hz, 1H), 2.99 (s, 1H), 2.65 (d, *J* = 28.2 Hz, 2H), 2.10 (s, 3H), 1.95 – 1.36 (m, 8H), 0.98 (s, 1H), 0.56 (s, 1H); LC-MS (ESI⁺) *m/z*: 621.5 [M + H]⁺.

(3Z)-7-chloro-18-[1-(2,2-difluoroethyl)-4-piperidyl]-10,21-dimethoxy-2,2-dioxo-2λ⁶,5-dithia-3,12,18-triazatetracyclo[18.3.1.0^{4,12}.0^{6,11}]tetracos-1(24),3,6(11),7,9,20,22-heptaen-19-one (**49m**). Intermediate **49f** (100 mg, 0.17 mmol, 1.0 equiv) was suspended in acetonitrile (3 mL). Triethylamine (0.10 mL, 0.69 mmol, 4.0 equiv) and 2,2-difluoroethyl trifluoromethanesulfonate (74 mg, 0.35 mmol, 2.0 equiv) were added and the reaction heated to reflux for 2 h. The reaction was cooled to rt and concentrated under reduced pressure. The residue was diluted with DCM:isopropanol (1:1) (2 mL), acidified by the addition of 4N HCl in 1,4-dioxane (1 drop) and loaded onto an ion exchange cartridge. The cartridge was washed with methanol and the product eluted with 2N ammonia in methanol. The basic eluent was concentrated to afford the title product as an overweight solid that was used in the next step without further purification. ¹H NMR (400 MHz, CDCl₃) δ 7.94 (dd, *J* = 8.6, 2.4 Hz, 1H), 7.82 (d, *J* = 2.3 Hz, 1H), 7.14 (d, *J* = 8.8 Hz, 1H), 6.86 (d, *J* = 8.7 Hz, 1H), 6.82 (d, *J* = 8.9 Hz, 1H), 5.85 (tt, *J* = 56.0, 4.3 Hz, 1H), 4.68 (br s, 1H), 4.52 – 4.28 (m, 2H), 3.88 (s, 3H), 3.82 (s, 3H), 3.14 – 2.94 (m, 3H), 2.68 – 2.60 (m, 1H), 2.43 – 2.29 (m, 2H), 1.95 – 1.69 (m, 5H), 1.66 – 1.34 (m, 4H), 1.33 – 1.20 (m, 1H), 0.95 (s, 1H), 0.54 (s, 1H); LC-MS (ESI⁺) *m/z*: 643.7 [M + H]⁺.

(3Z)-7-chloro-10,21-dimethoxy-2,2-dioxo-18-[(1S,5R)-8-propyl-8-azabicyclo[3.2.1]octan-3-yl]-2λ⁶,5-dithia-3,12,18-triazatetracyclo[18.3.1.0^{4,12}.0^{6,11}]tetracos-1(24),3,6,8,10,20,22-heptaen-19-one (**49n**). To a solution of **49k** (100 mg, 0.17 mmol, 1.0 equiv) in acetonitrile (3 mL) was added 1-iodopropane (24 μL, 0.25 mmol, 1.5 equiv) and triethylamine (58 μL, 0.41 mmol, 2.5 equiv) and the reaction heated to 80 °C for 7 h. The cooled reaction mixture was concentrated under reduced pressure and the residue diluted with a mixture of methanol and DCM and acidified with 4N HCl in 1,4-dioxane (1 drop). The mixture was loaded onto an ion-exchange cartridge (5g). The cartridge was sequentially washed with methanol and 2N ammonia in methanol. Analysis showed product was eluted during the initial methanol wash, which was concentrated under reduced pressure to afford the title product (87 mg, 0.13 mmol, 81% yield). LC-MS (ESI⁺) *m/z*: 647.4 [M + H]⁺.

(3Z)-7-chloro-18-[(1S,5R)-8-isobutyl-8-azabicyclo[3.2.1]octan-3-yl]-10,21-dimethoxy-2,2-dioxo-2λ⁶,5-dithia-3,12,18-triazatetracyclo[18.3.1.0^{4,12}.0^{6,11}]tetracos-1(24),3,6(11),7,9,20,22-heptaen-19-one (**49o**). To a suspension of **49k** (100 mg, 0.17 mmol, 1.0 equiv) in acetonitrile (3 mL) was added sodium iodide (2.50 mg, 0.02 mmol, 0.1 equiv), triethylamine (58 μL, 0.41 mmol, 2.5 equiv) and 1-bromo-2-methylpropane (27 μL, 0.25 mmol, 1.5 equiv) and the reaction heated to 80 °C overnight. A further portion of 1-bromo-2-methylpropane (27 μL, 0.25 mmol, 1.5 equiv) was added and the reaction heated to 80 °C for a further 24 h. The cooled reaction mixture was concentrated under reduced pressure and the residue was diluted with a mixture of methanol and DCM and acidified with 4 N HCl in 1,4-dioxane (1 drop). The mixture was loaded onto an ion-exchange cartridge (5g). The cartridge was sequentially washed with methanol and 2 N ammonia in methanol. Analysis showed product was eluted during the initial methanol wash, which was concentrated under reduced pressure to afford the title product (102 mg, 0.15 mmol, 93% yield). LC-MS (ESI⁺) *m/z*: 661.4 [M + H]⁺.

(3Z)-18-(1-acetyl-4-piperidyl)-7-chloro-10,21-dihydroxy-2,2-dioxo-2λ⁶,5-dithia-3,12,18-triazatetracyclo[18.3.1.0^{4,12}.0^{6,11}]tetracos-1(23),3,6,8,10,20(24),21-heptaen-19-one (**24**). The title compound was synthesized from **49i** according to general procedures GP1 and GP2. The desired compound was isolated as a white solid (27 mg, 0.046 mmol, 30% yield). ¹H NMR (400 MHz, DMSO-*d*₆) δ 7.66 (dd, *J* = 8.6, 2.3 Hz, 1H), 7.46 (s, 1H), 7.15 (d, *J* = 8.7 Hz, 1H), 6.85 – 6.77 (m, 2H), 4.55 – 4.45 (m, 3H), 4.15 (tt, *J* = 11.2, 4.9 Hz, 1H), 3.93 – 3.85 (m, 1H), 3.07 (t, *J* = 11.4 Hz, 1H), 2.81 (br s, 2H), 2.58 – 2.50 (m, 1H), 2.01 (s, 3H), 1.92 – 1.49 (m, 4H), 1.33 (br s, 2H), 1.11 (br s, 2H), 0.59 (br s, 2H); the two ArOH protons are observed as a very broad peak between δ = 3.0 – 6.0; ¹³C NMR (151 MHz, DMSO-*d*₆) (signals for the piperidine are a mixture of rotamers) δ 167.93, 167.69, 163.58, 156.33, 144.13, 131.25, 127.96, 126.94, 126.52, 125.21, 124.67, 124.42, 116.08, 115.60, 114.33, 53.31, 47.14, 45.71, 45.48, 40.60, 29.97 (major rotamer), 29.53 (minor rotamer) 29.27 (major rotamer), 28.87 (minor rotamer), 23.81, 21.28; HRMS (ESI⁺) *m/z*: calcd for [C₂₆H₂₉ClN₄O₆S₂+H]⁺ 593.1290; found 593.1291.

(3Z)-7-chloro-10,21-dihydroxy-2,2-dioxo-18-[(1R,5S)-8-propyl-8-azabicyclo[3.2.1]octan-3-yl]-2λ⁶,5-dithia-3,12,18-triazatetracyclo[18.3.1.0^{4,12}.0^{6,11}]tetracos-1(23),3,6(11),7,9,20(24),21-heptaen-19-

one;hydrochloride (**23**). The title compound was synthesized from **49n** according to general procedures GP1 and GP2. The desired compound was isolated as a white solid (31 mg, 0.047 mmol, 29% yield). ¹H NMR (400 MHz, DMSO-*d*₆) δ 10.92 (s, 1H), 10.83 (d, *J* = 3.9 Hz, 1H), 9.44 (br s, 1H), 7.72 (dd, *J* = 8.5, 2.3 Hz, 1H), 7.55 (d, *J* = 2.3 Hz, 1H), 7.23 (d, *J* = 8.7 Hz, 1H), 6.95 (d, *J* = 8.8 Hz, 1H), 6.93 (d, *J* = 8.5 Hz, 1H), 4.57 – 4.46 (m, 2H), 4.05 – 3.87 (m, 3H), 2.99 – 2.75 (m, 4H), 2.31 – 2.14 (m, 4H), 2.14 – 2.03 (m, 2H), 1.70 (q, *J* = 7.7 Hz, 2H), 1.42 (br s, 2H), 1.29 (br s, 2H), 0.89 (t, *J* = 7.3 Hz, 3H), 0.78 (v br s, 2H); two protons overlap with the residual solvent peak (confirmed by HSQC experiment); ¹³C NMR (151 MHz, DMSO-*d*₆) δ 167.39, 163.65, 156.39, 144.17, 131.41, 128.35, 127.13, 126.23, 125.20, 124.63, 124.40, 116.09, 115.57, 114.31, 58.41, 52.43, 49.77, 47.42, 44.34, 32.15 (br), 29.37, 28.50, 26.71, 23.96, 17.61, 10.89; HRMS (ESI⁺) *m/z*: calcd for [C₂₉H₃₅ClN₄O₅S₂+H]⁺ 619.1811; found 619.1811.

(3*Z*)-7-chloro-10,21-dihydroxy-18-[(1*R*,5*S*)-8-isobutyl-8-azabicyclo[3.2.1]octan-3-yl]-2,2-dioxo-2λ⁶,5-dithia-3,12,18-triazatetracyclo[18.3.1.0^{4,12}.0^{6,11}]tetracos-1(23),3,6(11),7,9,20(24),21-heptaen-19-one; hydrochloride (**27**). The title compound was synthesized from **49o** according to general procedures GP1 and GP2. The desired compound was isolated as a white solid (36 mg, 0.054 mmol, 43% yield). ¹H NMR (400 MHz, DMSO-*d*₆) δ 10.93 (s, 1H), 10.84 (s, 1H), 9.15 (br s, 1H), 7.72 (dd, *J* = 8.4, 2.4 Hz, 1H), 7.55 (s, 1H), 7.23 (d, *J* = 8.8 Hz, 1H), 6.99 – 6.90 (m, 2H), 4.57 – 4.46 (m, 2H), 3.94 (s, 2H), 3.75 – 3.63 (m, 1H), 3.53 – 3.43 (m, 1H), 2.90 (br s, 2H), 2.75 (s, 1H), 2.15 (s, 6H), 1.42 (br s, 2H), 1.30 (s, 3H), 0.98 (d, *J* = 6.6 Hz, 6H), 0.76 (br s, 2H), 2.65 – 2.55 (m, 2H). Complex spectra due to nitrogen inversion at the tertiary amine; HRMS (ESI⁺) *m/z*: calcd for [C₃₀H₃₇ClN₄O₅S₂+H]⁺ 633.1967; found 633.1970.

(3*Z*)-7-chloro-18-[1-(2,2-difluoroethyl)-4-piperidyl]-10,21-dihydroxy-2,2-dioxo-2λ⁶,5-dithia-3,12,18-triazatetracyclo[18.3.1.0^{4,12}.0^{6,11}]tetracos-1(24),3,6,8,10,20,22-heptaen-19-one (**25**). The title compound was synthesized from **49m** according to general procedures GP1 and GP2. The desired compound was isolated as a white solid (20 mg, 0.033 mmol, 19% yield). ¹H NMR (400 MHz, DMSO-*d*₆) δ 7.70 (dd, *J* = 8.5, 2.4 Hz, 1H), 7.50 (d, *J* = 2.4 Hz, 1H), 7.20 (d, *J* = 8.7 Hz, 1H), 6.89 (d, *J* = 8.5 Hz, 1H), 6.88 (d, *J* = 8.7 Hz, 1H), 6.11 (tt, ²*J*_{F,H} = 55.8, ³*J*_{H,H} = 4.3 Hz, 1H), 4.49 (t, *J* = 5.7 Hz, 2H), 3.97 (tt, *J* = 12.1, 3.9 Hz, 1H), 3.00 – 2.93 (m, 2H), 2.87 (br s, 2H), 2.72 (td, ³*J*_{F,H} = 15.7, ³*J*_{H,H} = 4.3 Hz, 2H), 2.23 (t, *J* = 13.0 Hz, 2H), 1.85 (qd, *J* = 12.0, 3.6 Hz, 2H), 1.65 (d, *J* = 11.7 Hz, 2H), 1.45 (br s, *J* = 6.9 Hz, 2H), 1.29 (br s, *J* = 7.7 Hz, 2H), 0.67 (br s, 2H); Very broad peak (δ_H 12.0 – 8.5 ppm) corresponds to the protons of the two ArOH protons; ¹³C NMR (151 MHz, DMSO-*d*₆) δ 167.61, 163.57, 156.29, 144.10, 131.24, 127.96, 126.90, 126.59, 125.21, 124.68, 124.43, 116.07, 115.93 (t, ¹*J*_{C,F} = 474 Hz), 115.61, 114.33, 59.00 (t, ²*J*_{C,F} = 96 Hz), 53.52, 52.73, 47.12, 45.34, 30.18, 29.26, 29.05, 23.76; ¹⁹F NMR (564 MHz, DMSO) δ -118.65; HRMS (ESI⁺) *m/z*: calcd for [C₂₆H₂₉ClF₂N₄O₅S₂+H]⁺ 615.1309; found 615.1304.

ethyl 5-(*N*-(3-(5-bromopentyl)-7-chloro-4-methoxybenzo[*d*]thiazol-2(3*H*)-ylidene)sulfamoyl)-2-((4-methoxybenzyl)amino)nicotinate (**59**). The title compound was synthesized from **58** according to the procedure for **48a** but using 1,5-dibromopentane. The desired product was isolated as a white powdery solid (5.70 g, 7.95 mmol, 72%

yield). ¹H NMR (400 MHz, CDCl₃) δ 8.84 (d, *J* = 2.5 Hz, 1H), 8.71 (t, *J* = 5.5 Hz, 1H), 8.67 (d, *J* = 2.5 Hz, 1H), 7.30 – 7.25 (m, 2H), 7.16 (d, *J* = 8.9 Hz, 1H), 6.89 – 6.82 (m, 3H), 4.70 (d, *J* = 5.5 Hz, 2H), 4.52 – 4.44 (m, 2H), 4.32 (q, *J* = 7.1 Hz, 2H), 3.93 (s, 3H), 3.78 (s, 3H), 3.34 (t, *J* = 6.7 Hz, 2H), 1.90 – 1.79 (m, 2H), 1.76 – 1.64 (m, 2H), 1.50 – 1.42 (m, 2H), 1.37 (t, *J* = 7.1 Hz, 3H); LC-MS (ESI⁺) *m/z*: 713.3 [M + H]⁺.

tert-Butyl (5*S*,8*r*)-8-((5-(7-chloro-2-(((5-(ethoxycarbonyl)-6-((4-methoxybenzyl)amino)pyridin-3-yl)sulfonyl)imino)-4-methoxybenzo[*d*]thiazol-3(2*H*)-yl)pentyl)amino)-1-azaspiro[4.5]decane-1-carboxylate (**60**). To a solution of **59**, (1.15 g, 1.62 mmol, 1.0 equiv) in acetonitrile (6 mL) was added potassium carbonate anhyd (536 mg, 3.88 mmol, 2.4 equiv) followed by *tert*-butyl-*cis*-8-amino-1-azaspiro[4.5]decane-1-carboxylate **83** (see Supporting Information) (493 mg, 1.94 mmol, 1.2 equiv) and the reaction mixture was heated at 80 °C for 60 h. The cooled mixture was concentrated under reduced pressure then partitioned between ethyl acetate (20 mL) and water (20 mL). The phases were separated and the aqueous extracted with ethyl acetate (2 × 20 mL). Combined organic extracts were dried (MgSO₄), concentrated under reduced pressure to afford the crude. Purified by flash column chromatography (SiO₂, gradient elution DCM/(MeOH + 0.1% NEt₃) = 95/5 to 85/15) to afford the title compound (770 mg, 0.87 mmol, 54% yield) as a glassy colourless solid. LC-MS (ESI⁺) *m/z*: 885.7 [M + H]⁺.

5-(*N*-(3-(5-(((5*S*,8*r*)-1-(*tert*-butoxycarbonyl)-1-azaspiro[4.5]decan-8-yl)amino)pentyl)-7-chloro-4-methoxybenzo[*d*]thiazol-2(3*H*)-ylidene)sulfamoyl)-2-((4-methoxybenzyl)amino)nicotinic acid (**61**). The title compound was synthesized from **60** according to the procedure for **57a**. The desired product was isolated as a white solid (711 mg, 0.83 mmol, 95% yield). LC-MS (ESI⁺) *m/z*: 857.6 [M + H]⁺.

tert-Butyl (5*S*,8*r*) (Z)-8-(1⁷-chloro-1⁴-methoxy-4⁶-((4-methoxybenzyl)amino)-3,3-dioxido-5-oxo-1²,1³-dihydro-3-thia-2,6-diaza-1(2,3)-benzo[*d*]thiazola-4(3,5)-pyridinacycloundecaphane-6-yl)-1-azaspiro[4.5]decane-1-carboxylate (**62**). The title compound was synthesized from **61** according to the procedure for **49j**. The desired compound was isolated as a white solid (298 mg, 0.36 mmol, 43% yield). ¹H NMR (400 MHz, CDCl₃) δ 8.70 (d, *J* = 2.2 Hz, 1H), 7.99 (d, *J* = 2.2 Hz, 1H), 7.25 – 7.20 (m, 2H), 7.16 (d, *J* = 8.7 Hz, 1H), 6.84 (d, *J* = 8.4 Hz, 3H), 6.02 (t, *J* = 5.5 Hz, 1H), 4.65 – 4.55 (m, 4H), 4.35 (s, 1H), 3.91 (s, 3H), 3.78 (d, *J* = 1.4 Hz, 3H), 3.41 (t, *J* = 6.8 Hz, 2H), 3.14 – 3.02 (m, 2H), 2.41 (dt, *J* = 13.6, 6.3 Hz, 2H), 2.16 (h, *J* = 7.5 Hz, 2H), 1.86 – 1.62 (m, 10H), 1.51 – 1.37 (m, 11H), 0.96 (br s, 2H); LC-MS (ESI⁺) *m/z*: 839.6 [M + H]⁺.

(Z)-1⁷-chloro-1⁴-hydroxy-4⁶-((4-hydroxybenzyl)amino)-6-((5*S*,8*r*)-1-azaspiro[4.5]decan-8-yl)-1²,1³-dihydro-3-thia-2,6-diaza-1(2,3)-benzo[*d*]thiazola-4(3,5)-pyridinacycloundecaphan-5-one 3,3-dioxide;hydrochloride (**29**). The title compound was synthesized from **62** according to general procedures GP1 and GP2. The desired compound was isolated as an off-white solid (26 mg, 0.03 mmol, 28% yield). ¹H NMR (600 MHz, DMSO-*d*₆) δ 10.97 (s, 1H), 9.04 (t, *J* = 5.6 Hz, 2H), 8.42 (d, *J* = 2.4 Hz, 1H), 7.73 (d, *J* = 2.4 Hz, 1H), 7.26 – 7.18 (m, 2H), 7.11 – 7.04 (m, 2H), 6.99 (d, *J* = 8.7 Hz, 1H), 6.70 – 6.64 (m, 2H), 4.51 (t, *J* = 5.8 Hz, 2H), 4.48 (d, *J* = 5.4 Hz, 2H), 4.29 – 4.13 (m, 1H), 3.26 (p, *J* = 6.3 Hz, 2H), 2.88 (br s, 2H), 2.07 – 2.00 (m, 2H), 1.97 – 1.90 (m, 2H), 1.90 – 1.81

(m, 4H), 1.80 – 1.76 (m, 2H), 1.72 – 1.63 (m, 2H), 1.59 (p, $J = 6.5$ Hz, 2H), 1.56 – 1.48 (m, 2H), 0.78 (p, $J = 7.1$ Hz, 2H); One proton is missing due to broadening; ^{13}C NMR (151 MHz, DMSO- d_6) δ 167.10, 163.25, 156.16, 155.30, 144.60, 144.19, 133.63, 129.75, 128.32, 125.24, 124.73, 124.40, 123.98, 117.68, 116.12, 115.61, 114.95, 65.14, 52.46, 46.65, 45.00, 43.90, 43.36, 37.56, 32.78, 30.12, 29.04, 25.49, 23.06, 21.66; HRMS (ESI $^+$) m/z : calcd for $[\text{C}_{34}\text{H}_{39}\text{ClN}_6\text{O}_5\text{S}_2+\text{H}]^+$ 711.2185; found 711.2191.

Ethyl 5-[(Z)-[3-[5-(5-bromopentyl)-7-chloro-4-methoxy-1,3-benzothiazol-2-ylidene]amino]sulfonyl-2-methylsulfanyl-pyridine-3-carboxylate (**64a**). A mixture of **63a** (see Supporting Information) (78.4 g, 165.4 mmol, 1.0 equiv), 1,5-dibromopentane (68 mL, 496.2 mmol, 3 equiv) and potassium carbonate anhyd (115.5 g, 827.1 mmol, 5 equiv) in DMF (1 L) was stirred for 16 h at rt. The mixture was filtered, and the filtrate concentrated under reduced pressure. The residue was extracted with ethyl acetate (2 x 500 mL) and combined organic extracts washed with water (500 mL), brine (500 mL), dried (Na_2SO_4), filtered, and evaporated under reduced pressure to afford the crude as a mixture of *N*-alkylated regioisomers. Purified by flash column chromatography (SiO_2 , gradient elution petroleum ether/EtOAc = 90/10 to 25/75). Evaporation of later eluting main fraction afforded the title compound as the major isomer (57.7 g, 92.6 mmol, 56% yield) as a white solid. ^1H NMR (400 MHz, CDCl_3) δ 9.09 (d, $J = 2.4$ Hz, 1H), 8.72 (d, $J = 2.3$ Hz, 1H), 7.19 (d, $J = 8.8$ Hz, 1H), 6.87 (d, $J = 8.8$ Hz, 1H), 4.53 – 4.46 (m, 2H), 4.41 (q, $J = 7.1$ Hz, 2H), 3.94 (s, 3H), 3.35 (t, $J = 6.6$ Hz, 2H), 2.55 (s, 3H), 1.84 (p, $J = 6.8$ Hz, 2H), 1.75 – 1.64 (m, 2H), 1.44 – 1.41 (m, 2H), 1.41 (t, $J = 7.1$ Hz, 3H); LC-MS (ESI $^+$) m/z : 624.1 $[\text{M} + \text{H}]^+$.

2D HMBC Data:

$^1\text{H}/^{13}\text{C}$ Label	δ H	δ C	HMBC
36,37	4.53 – 4.46 (m, 2H),	48.0	126.6(4),165.1(2)
2	-	165.1	4.47(36), 4.47(37)
4	-	126.6	4.47(36), 4.47(37)

Ethyl 5-[(Z)-[3-[5-[[4-(*cis-tert*-butoxycarbonylamino)cyclohexyl]amino]pentyl]-7-chloro-4-methoxy-1,3-benzothiazol-2-ylidene]amino]sulfonyl-2-methylsulfanyl-pyridine-3-carboxylate (**65a**).

A stirred mixture of **64a** (10.0 g, 16.1 mmol, 1.0 equiv), *tert*-butyl *N*-(*cis*-4-aminocyclohexyl)carbamate (4.13 g, 19.3 mmol, 1.2 equiv) and potassium carbonate anhyd (5.32 g, 38.5 mmol, 2.4 equiv) in acetonitrile (100 mL) was heated at 60 °C for 3 d. The cooled mixture was filtered to remove solids and the filtrate diluted with brine (50 mL) and extracted with ethyl acetate (2 x 50 mL). Organic extracts were washed with brine, dried (MgSO_4), further dried over a phase separator, then concentrated under reduced pressure to afford a residue which was recrystallised from ethanol to afford the title product (4.40 g, 5.24 mmol, 33% yield) as a white solid. ^1H NMR (400 MHz, CDCl_3) δ 9.07 (d, $J = 2.4$ Hz, 1H), 8.70 (d, $J = 2.4$ Hz, 1H), 7.18 (d, $J = 8.8$ Hz, 1H), 6.86 (d, $J = 8.8$ Hz, 1H), 4.78 (s, 1H), 4.51 – 4.43 (m, 2H), 4.40 (q, $J = 7.1$ Hz, 2H), 3.91 (s, 3H), 2.53 (s, 3H), 2.52 – 2.47 (m, 2H), 1.75 – 1.51 (m, 17H), 1.44 – 1.37 (m, 12H); LC-MS (ESI $^+$) m/z : 756.5 $[\text{M} + \text{H}]^+$.

5-[(Z)-[3-[5-[[4-(*cis-tert*-butoxycarbonylamino)cyclohexyl]amino]pentyl]-7-chloro-4-methoxy-1,3-benzothiazol-2-ylidene]amino]sulfonyl-2-methylsulfanyl-pyridine-3-carboxylic acid (**66a**).

To a solution of **65a**, (4.40 g, 5.82 mmol, 1.0 equiv) in ethanol (25 mL) was added 4 N LiOH (aq.) (7.27 mL, 29.1 mmol, 5.0 equiv) and the reaction stirred for 16 h at rt. The majority of the ethanol was removed under reduced pressure and the residue diluted with water and carefully acidified to pH 4 with HCl (aq.). The resulting gummy precipitate was collected by filtration, resolubilised in a mixture of DCM and methanol, dried (MgSO_4), filtered and evaporated under reduced pressure to afford a residue which was further dried under vacuum (50 °C, 16 h) to afford the title compound (4.17 g, 5.73 mmol, 99% yield) as a yellow solid. ^1H NMR (400 MHz, DMSO- d_6) δ 8.75 (d, $J = 2.5$ Hz, 1H), 8.38 (d, $J = 2.5$ Hz, 1H), 7.39 (d, $J = 8.9$ Hz, 1H), 7.18 (d, $J = 8.9$ Hz, 1H), 6.65 – 6.55 (m, 1H), 4.45 – 4.35 (m, 2H), 3.91 (s, 3H), 3.34 (s, 3H), 2.37 – 2.29 (m, 5H), 1.70 – 0.96 (m, 24H); LC-MS (ESI $^+$) m/z : 728.5 $[\text{M} + \text{H}]^+$.

tert-Butyl *N*-(*cis*-4-[(3Z)-7-chloro-10-methoxy-21-methylsulfanyl-2,2,19-trioxo-2 λ 6,5-dithia-3,12,18,22-tetrazatetracyclo[18.3.1.0 4,12 .0 6,11]]tetracosan-1(23),3,6(11),7,9,20(24),21-heptaen-18-yl]cyclohexyl]carbamate (**67a**). The title compound was synthesized from **66a** according to the procedure for **49j**. After a final trituration step using ethyl acetate, the desired product was isolated as a white solid (1.25 g, 1.76 mmol, 31% yield). ^1H NMR (400 MHz, DMSO- d_6) δ 8.84 (d, $J = 2.3$ Hz, 1H), 8.06 (d, $J = 2.3$ Hz, 1H), 7.43 (d, $J = 8.8$ Hz, 1H), 7.20 (d, $J = 8.9$ Hz, 1H), 6.97 (d, $J = 7.6$ Hz, 1H), 4.51 (br s, 2H), 4.13 (t, $J = 12.5$ Hz, 1H), 3.91 (br s, 3H), 3.67 (s, 1H), 2.55 (s, 3H), 1.95 – 1.79 (m, 2H), 1.79 – 1.66 (m, 2H), 1.65 – 1.45 (m, 6H), 1.45 – 1.26 (m, 11H), 0.74 (s, 2H); two protons are missing due to broadening or overlapping with the residual solvent signal; LC-MS (ESI $^+$) m/z : 710.4 $[\text{M} + \text{H}]^+$.

tert-Butyl *N*-(*cis*-4-[(3Z)-7-chloro-10-methoxy-21-methylsulfanyl-2,2,19-trioxo-2 λ 6,5-dithia-3,12,18,22-tetrazatetracyclo[18.3.1.0 4,12 .0 6,11]]tetracosan-1(23),3,6(11),7,9,20(24),21-heptaen-18-yl]cyclohexyl]carbamate (**68a**). To a solution of **67a** (1.25 g, 1.76 mmol, 1.0 equiv) in DCM (10 mL) cooled to 0 °C was added 3-chloroperbenzoic acid (1.18 g, 5.28 mmol, 3.0 equiv) in portions over 5 mins. The mixture was stirred for 6 h allowing to warm to rt *via* melting of the ice bath. The reaction was quenched with a saturated aqueous sodium hydrogen carbonate solution (25 mL) and extracted with DCM (25 mL). Organic extracts were washed with brine, dried (MgSO_4), filtered and dry loaded under reduced pressure. The residue was purified by flash column chromatography (SiO_2 , gradient elution with *i*-hexane/EtOAc = 50/50 to 0/100) to afford the title compound (1.08 g, 1.45 mmol, 82% yield) as an off-white solid. ^1H NMR (400 MHz, CDCl_3) δ 9.20 (d, $J = 2.1$ Hz, 1H), 8.38 (d, $J = 2.1$ Hz, 1H), 7.23 (d, $J = 8.8$ Hz, 1H), 6.89 (d, $J = 8.8$ Hz, 1H), 4.91 (br s, 1H), 4.77 – 4.65 (m, 1H), 4.60 – 4.44 (m, 1H), 3.92 (s, 3H), 3.86 (br s, 1H), 3.69 (br s, $J = 34.6$ Hz, 1H), 3.27 (s, 3H), 3.21 – 3.07 (m, 1H), 2.80 – 2.65 (m, 1H), 2.10 (br s, 2H), 1.99 – 1.88 (m, 2H), 1.84 – 1.71 (m, 2H), 1.71 – 1.55 (m, 4H), 1.45 (s, 9H), 1.42 – 1.31 (m, 2H), 1.17 (br s, 1H), 0.65 (br s, 1H); LC-MS (ESI $^+$) m/z : 763.2 $[\text{M} + \text{Na}]^+$.

tert-Butyl *N*-[4-[(3*Z*)-7-chloro-10-methoxy-21-[(4-methoxyphenyl)methylamino]-2,2,19-trioxo-2λ⁶,5-dithia-3,12,18,22-tetrazatetracyclo[18.3.1.0^{4,12}.0^{6,11}]tetracos-1(23),3,6(11),7,9,20(24),21-heptaen-18-yl]cyclohexyl]carbamate (**69a**). A mixture of **68a** (70 mg, 0.09 mmol, 1.0 equiv), (4-methoxyphenyl)methanamine (12.3 μL, 0.09 mmol, 1.0 equiv) and triethylamine (0.03 mL) in acetonitrile was heated at 65 °C for 19 h. The cooled reaction mixture was dry loaded under reduced pressure and purified by flash column chromatography (SiO₂, gradient elution with *i*-hexane/EtOAc = 50/50 to 0/100) to afford the title compound (75.0 mg, 0.094 mmol, 99% yield as a colorless solid. ¹H NMR (400 MHz, Chloroform-*d*) δ 8.71 (d, *J* = 2.3 Hz, 1H), 7.98 (d, *J* = 2.4 Hz, 1H), 7.25 – 7.20 (m, 2H), 7.17 (d, *J* = 8.8 Hz, 1H), 6.89 – 6.81 (m, 3H), 6.15 (br s, 1H), 4.83 (br s, 1H), 4.65 – 4.57 (m, 4H), 3.92 (s, 3H), 3.78 (s, 3H), 3.60 (br s, 1H), 3.00 – 2.90 (m, 2H), 1.98 – 1.89 (m, 2H), 1.83 – 1.73 (m, 2H), 1.71 – 1.57 (m, 8H), 1.46 (s, 9H), 1.05 (br s, 2H); one proton is missing due to broadening or overlapping with the residual solvent signal; LC-MS (ESI⁺) *m/z*: 799.8 [M + H]⁺.

tert-Butyl (3*S*)-3-[[[(3*Z*)-18-[*cis*-4-(*tert*-butoxycarbonylamino)cyclohexyl]-7-chloro-10-methoxy-2,2,19-trioxo-2λ⁶,5-dithia-3,12,18,22-tetrazatetracyclo[18.3.1.0^{4,12}.0^{6,11}]tetracos-1(23),3,6(11),7,9,20(24),21-heptaen-21-yl]amino]pyrrolidine-1-carboxylate (**69b**). To a solution of **68a** (150 mg, 0.20 mmol, 1.0 equiv) in NMP (1.5 mL) was added *tert*-butyl (3*S*)-3-aminopyrrolidine-1-carboxylate (186 mg, 0.40 mmol, 2.0 equiv) and the mixture was stirred at 110 °C for 16 h. The reaction was cooled to rt and quenched with water (10 mL). The precipitated solid was collected by filtration, washed with water (10 mL), and dried under vacuum at 50 °C to afford the title compound (140 mg, 0.15 mmol, 73% yield) as an off-white solid. ¹H NMR (400 MHz, DMSO-*d*₆) δ 8.49 (s, 1H), 7.73 (d, *J* = 2.4 Hz, 1H), 7.41 (d, *J* = 8.9 Hz, 1H), 7.19 (d, *J* = 9.1 Hz, 1H), 7.06 – 6.93 (m, 1H), 6.81 – 6.67 (m, 1H), 4.63 – 4.41 (m, 3H), 4.16 (t, 1H), 3.90 (s, 3H), 3.66 (br s, 1H), 3.55 – 3.43 (m, 1H), 3.25 – 3.06 (m, 1H), 2.85 (br s, 2H), 2.12 – 1.99 (m, 1H), 1.97 – 1.85 (m, 1H), 1.83 – 1.67 (m, 4H), 1.65 – 1.47 (m, 6H), 1.43 – 1.27 (m, 21H), 0.83 – 0.55 (m, 2H); one proton is missing due to broadening or overlapping with the residual solvent signal; LC-MS (ESI⁺) *m/z*: 848.4 [M + H]⁺.

tert-Butyl 4-[(3*Z*)-18-5-[(*Z*)-[3-[4-[[*cis*-4-(*tert*-butoxycarbonylamino)cyclohexyl]amino]-3-hydroxy-butyl]-7-chloro-4-methoxy-1,3-benzothiazol-2-ylidene]amino]sulfonyl-2-methoxy-benzoic acid-butoxycarbonylamino)cyclohexyl]-7-chloro-10-(methoxymethoxy)-2,2,19-trioxo-2λ⁶,5-dithia-3,12,18,22-tetrazatetracyclo[18.3.1.0^{4,12}.0^{6,11}]tetracos-1(23),3,6(11),7,9,20(24),21-heptaen-21-yl]piperazine-1-carboxylate (**69c**). To a solution of **68b** (see Supporting Information) (150 mg, 0.20 mmol, 1.0 equiv) in DMF (1 mL) was added *tert*-butyl piperazine-1-carboxylate (662 mg, 1.94 mmol, 10.0 equiv). The mixture was irradiated at 100 °C for 3 h. DIPEA (0.14 mL, 0.777 mmol, 4.0 equiv) was added and the mixture irradiated for a further 4 h. The cooled reaction was diluted with ice water and the resulting precipitate collected by filtration, washed with water (2 x 5 mL) and dried under vacuum to afford the title product as an impure (~33% UV purity) off-white solid (110 mg) which was engaged in the next step without further purification. LC-MS (ESI⁺) *m/z*: 777.8 [M-Boc + H]⁺.

tert-Butyl *N*-[4-[(3*Z*)-21-[5-[(*Z*)-[3-[4-[[*cis*-4-(*tert*-butoxycarbonylamino)cyclohexyl]amino]-3-hydroxy-butyl]-7-chloro-4-methoxy-1,3-benzothiazol-2-ylidene]amino]sulfonyl-2-methoxy-benzoic acid-butoxycarbonylamino)cyclohexyl]amino]-7-chloro-10-methoxy-2,2,19-trioxo-2λ⁶,5-dithia-3,12,18,22-tetrazatetracyclo[18.3.1.0^{4,12}.0^{6,11}]tetracos-1(23),3,6(11),7,9,20(24),21-heptaen-18-yl]cyclohexyl]carbamate (**69d**). The title compound was synthesized according to the procedure for **69c** using **68a** and *tert*-butyl *N*-(*cis*-4-aminocyclohexyl)carbamate. The desired product was isolated as an impure solid (125 mg, ~75% UV purity) that was engaged in the next step without further purification. LC-MS (ESI⁺) *m/z*: 878.2 [M + H]⁺.

tert-Butyl *N*-[1-[(3*Z*)-18-[*cis*-4-(*tert*-butoxycarbonylamino)cyclohexyl]-7-chloro-10-methoxy-2,2,19-trioxo-2λ⁶,5-dithia-3,12,18,22-tetrazatetracyclo[18.3.1.0^{4,12}.0^{6,11}]tetracos-1(23),3,6(11),7,9,20(24),21-heptaen-21-yl]-4-piperidyl]-*N*-[2-(*tert*-butoxycarbonylamino)ethyl]carbamate (**69e**). The title compound was synthesized according to the procedure for **69g** using *tert*-butyl *N*-[2-[(*cis*-4-aminocyclohexyl)amino]ethyl]carbamate and omitting the chromatographic step. The desired product was isolated as an impure solid (150 mg, ~45% UV purity) that was engaged in the next step without further purification LC-MS (ESI⁺) *m/z*: 919.5 [M + H]⁺.

tert-Butyl *N*-[2-[[4-[[[(3*Z*)-18-[*cis*-4-(*tert*-butoxycarbonylamino)cyclohexyl]-7-chloro-10-methoxy-2,2,19-trioxo-2λ⁶,5-dithia-3,12,18,22-tetrazatetracyclo[18.3.1.0^{4,12}.0^{6,11}]tetracos-1(23),3,6(11),7,9,20(24),21-heptaen-21-yl]amino]cyclohexyl]amino]ethyl]carbamate (**69f**). The title compound was synthesized according to the procedure for **69g** using *tert*-butyl *N*-[2-(*tert*-butoxycarbonyl(methyl)amino)ethyl]-*N*-(4-piperidyl)carbamate **87**. The desired product was isolated omitting the chromatographic step as an impure solid (~80% UV purity) (180 mg) that was engaged in the next step without further purification LC-MS (ESI⁺) *m/z*: 919.3 [M + H]⁺.

tert-Butyl *N*-[1-[1-[(3*Z*)-18-[*cis*-4-(*tert*-butoxycarbonylamino)cyclohexyl]-7-chloro-10-methoxy-2,2,19-trioxo-2λ⁶,5-dithia-3,12,18,22-tetrazatetracyclo[18.3.1.0^{4,12}.0^{6,11}]tetracos-1(24),3,6(11),7,9,20,22-heptaen-21-yl]-4-piperidyl]-4-piperidyl]carbamate (**69g**). To a solution of **68a** (300 mg, 0.40 mmol, 1.0 equiv) in DMSO (3.0 mL) was added *tert*-butyl *N*-[1-(4-piperidyl)-4-piperidyl]carbamate (229 mg, 0.81 mmol, 2.0 equiv) and DIPEA (0.28 mL, 4.0 equiv) and the mixture stirred at 100 °C for 22 h. The reaction was cooled to rt and quenched with water (10 mL). The precipitated solid was collected by filtration, washed with water (10 mL), and dried on the filter. The solid product was solubilised in DCM (10 mL), dried (MgSO₄) and filtered through a hydrophobic frit. Organics were dry loaded under reduced pressure and purified by flash column chromatography (SiO₂, gradient elution with MTBE/(EtOAc:EtOH 3:1) = 100/0 to 0/100) to afford the title compound (73.0 mg, 0.077 mmol, 19% yield) as a light-brown solid. ¹H NMR (400 MHz, CDCl₃) δ 8.66 (d, *J* = 2.5 Hz, 1H), 7.88 (d, *J* = 2.5 Hz, 1H), 7.14 (d, *J* = 8.8 Hz, 1H), 6.82 (d, *J* = 8.8 Hz, 1H), 4.99 (br s, 1H), 4.76 – 4.60 (m, 1H), 4.55 – 4.37 (m, 2H), 4.25 (d, *J* = 13.2 Hz, 2H), 3.98 – 3.81 (m, 4H), 3.38 (br s, 2H), 3.15 – 2.98 (m, 1H), 2.96 – 2.77 (m, 5H), 2.49 (s, 1H), 2.42 – 2.13 (m, 4H), 1.99 – 1.78 (m, 6H), 1.72 – 1.32

(m, 29H), 1.15 (br s, 2H), 0.43 – 0.26 (m, 1H); LC-MS (ESI⁺) *m/z*: 945.7 [M + H]⁺.

(3Z)-21-amino-18-(4-aminocyclohexyl)-7-chloro-10-hydroxy-2,2-dioxo-2λ⁶,5-dithia-3,12,18,22-tetrazatetracyclo[18.3.1.0^{4,12}.0^{6,11}]tetracos-1(23),3,6,8,10,20(24),21-heptaen-19-one;hydrochloride (**30**). The title compound was synthesized from **69a** according to general procedures GP1 and GP2. The desired compound was isolated as a white solid (3 mg, 0.005 mmol, 5% yield). ¹H NMR (400 MHz, DMSO-*d*₆) δ 10.87 (s, 1H), 8.39 (d, *J* = 2.4 Hz, 1H), 7.96 – 7.77 (m, 3H), 7.73 (d, *J* = 2.4 Hz, 1H), 7.25 (d, *J* = 8.7 Hz, 1H), 6.93 (d, *J* = 8.7 Hz, 1H), 6.75 (br s, 2H), 4.51 (t, *J* = 6.0 Hz, 2H), 4.19 (br s, 1H), 2.89 (br s, 2H), 1.97 – 1.83 (m, 2H), 1.81 – 1.68 (m, 6H), 1.65 – 1.55 (m, 2H), 1.55 – 1.43 (m, 2H), 0.82 – 0.65 (m, 2H); One proton is missing due to overlap with the residual water peak LC-MS (ESI⁺) *m/z*: calcd for [C₂₄H₂₉ClN₆O₄S₂+H]⁺ 565.1; found 565.51.

(3Z)-18-(4-aminocyclohexyl)-7-chloro-10-hydroxy-2,2-dioxo-21-[[3S]-pyrrolidin-3-yl]amino]-2λ⁶,5-dithia-3,12,18,22-tetrazatetracyclo[18.3.1.0^{4,12}.0^{6,11}]tetracos-1(23),3,6,8,10,20(24),21-heptaen-19-one;dihydrochloride (**31**). The title compound was synthesized from **69b** according to general procedures GP1 and GP2. The desired compound was isolated as a light-brown solid (40 mg, 0.06 mmol, 21% yield). ¹H NMR (600 MHz, DMSO-*d*₆) δ 11.07 (s, 1H), 9.34 – 9.26 (m, 1H), 9.26 – 9.17 (m, 1H), 8.51 (d, *J* = 2.3 Hz, 1H), 8.28 – 8.17 (m, 3H), 7.78 (d, *J* = 2.4 Hz, 1H), 7.25 (d, *J* = 8.7 Hz, 1H), 7.03 (d, *J* = 8.7 Hz, 1H), 6.94 (d, *J* = 6.9 Hz, 1H), 4.75 – 4.67 (m, 1H), 4.50 (t, *J* = 5.8 Hz, 2H), 4.30 – 4.23 (m, 1H), 3.44 – 3.34 (m, 2H), 3.34 – 3.26 (m, 1H), 3.19 – 3.11 (m, 1H), 3.11 – 3.04 (m, 1H), 2.90 (br s, 2H), 2.25 – 2.14 (m, 1H), 1.99 – 1.77 (m, 5H), 1.77 – 1.67 (m, 4H), 1.59 (quint, *J* = 6.5 Hz, 2H), 1.56 – 1.47 (m, 2H), 0.77 – 0.66 (m, 2H); ¹³C NMR (151 MHz, DMSO) δ 166.65, 163.43, 154.66, 144.34, 144.32, 134.15, 125.21, 125.03, 124.67, 124.49, 118.46, 116.20, 115.52, 52.55, 49.87, 48.69, 46.69, 44.91, 44.37, 43.76, 30.41, 29.86, 29.14, 27.74, 23.44, 23.08; HRMS (ESI⁺) calcd for [C₂₈H₃₆ClN₇O₄S₂ + H]⁺ 634.2032; found 634.2037.

(3Z)-18-(4-aminocyclohexyl)-7-chloro-10-hydroxy-2,2-dioxo-21-piperazin-1-yl-2λ⁶,5-dithia-3,12,18,22-tetrazatetracyclo[18.3.1.0^{4,12}.0^{6,11}]tetracos-1(23),3,6,8,10,20(24),21-heptaen-19-one;dihydrochloride (**32**). To a solution of **69c** (110 mg, 0.13 mmol, 1.0 equiv) in DCM cooled to 0 °C was added 4.0 M HCl in 1,4-dioxane (0.14 mL, 4.0 equiv). The mixture was stirred for 21 h allowing to warm to rt. A further 4.0 equiv of 4.0 M HCl in 1,4-dioxane was added and the mixture stirred for a further 21 h. Methanol was added, and the mixture loaded onto an ion-exchange cartridge pre-equilibrated with 10% acetic acid in methanol. The cartridge was flushed with methanol (approximately 1 CV) then the product eluted with 2 N ammonia in MeOH. Solvent from the basic eluent was removed under reduced pressure and the residue purified by reverse phase preparative HPLC. The title compound was then obtained according to general procedure GP2. The desired compound was isolated as a white solid (18 mg, 0.026 mmol, 13% yield over 3 steps). ¹H NMR (600 MHz, DMSO-*d*₆) δ 11.12 (s, 1H), 9.51 – 9.41 (m, 2H), 8.61 (d, *J* = 2.4 Hz, 1H), 8.28 – 8.16 (m, 3H), 7.84 (d, *J* = 2.4 Hz, 1H), 7.25 (d, *J* = 8.6 Hz, 1H), 7.05 (d, *J* = 8.7 Hz, 1H), 4.58 – 4.51 (m, 1H), 4.50 – 4.44 (m, 1H), 4.19 – 4.12 (m, 1H), 3.46 – 3.32 (m, 2H), 3.16 – 3.07 (m, 4H), 2.78 – 2.69 (m, 1H), 2.02 – 1.88 (m, 4H), 1.80 – 1.67 (m, 3H), 1.66 – 1.56 (m, 2H), 1.55 – 1.45 (m, 2H), 1.29

– 1.21 (m, 1H), 0.97 – 0.87 (m, 1H), 0.39 – 0.29 (m, 1H); four protons are missing due to overlap with the residual water peak and/or broadening; ¹³C NMR (151 MHz, DMSO-*d*₆) δ 168.31, 163.91, 155.63, 144.44, 143.83, 137.39, 127.17, 125.23, 124.67, 124.60, 120.59, 116.26, 115.47, 53.50, 47.10, 44.86, 44.82, 43.74, 42.27, 30.13, 29.41, 27.77, 27.52, 23.86, 23.64, 22.20; HRMS (ESI⁺) *m/z*: calcd for [C₂₈H₃₆ClN₇O₄S₂+H]⁺ 634.2032; found 634.2032.

(3Z)-18-(4-aminocyclohexyl)-21-[[4-aminocyclohexyl]amino]-7-chloro-10-hydroxy-2,2-dioxo-2λ⁶,5-dithia-3,12,18,22-tetrazatetracyclo[18.3.1.0^{4,12}.0^{6,11}]tetracos-1(23),3,6,8,10,20(24),21-heptaen-19-one;dihydrochloride (**33**). The title compound was synthesized from **69d** according to general procedures GP1 and GP2. The desired compound was isolated as a white solid (13 mg, 0.018 mmol, 13% yield over 3 steps). ¹H NMR (600 MHz, DMSO-*d*₆) δ 10.99 (s, 1H), 8.48 (d, *J* = 2.3 Hz, 1H), 8.17 (d, *J* = 5.9 Hz, 3H), 8.01 (d, *J* = 5.6 Hz, 3H), 7.82 (d, *J* = 2.4 Hz, 1H), 7.25 (d, *J* = 8.7 Hz, 1H), 6.99 (d, *J* = 8.7 Hz, 1H), 5.80 (d, *J* = 6.9 Hz, 1H), 4.51 (t, *J* = 5.9 Hz, 2H), 4.27 – 4.20 (m, 1H), 4.14 – 4.07 (m, 1H), 3.16 (br s, 1H), 3.04 (br s, 2H), 1.99 – 1.87 (m, 4H), 1.84 – 1.50 (m, 16H), 0.80 – 0.72 (m, 2H); one proton overlaps with the residual water peak (confirmed by HSQC experiment); HRMS (ESI⁺) *m/z*: calcd for [C₃₀H₄₀ClN₇O₄S₂+H]⁺ 662.2345; found 662.2341.

(3Z)-18-(4-aminocyclohexyl)-21-[[4-(2-aminoethylamino)cyclohexyl]amino]-7-chloro-10-hydroxy-2,2-dioxo-2λ⁶,5-dithia-3,12,18,22-tetrazatetracyclo[18.3.1.0^{4,12}.0^{6,11}]tetracos-1(23),3,6,8,10,20(24),21-heptaen-19-one;trihydrochloride (**34**). The title compound was synthesized from **69e** according to general procedures GP1 and GP2. The desired compound was isolated as a white solid (26 mg, 0.032 mmol, 16% yield over 3 steps). ¹H NMR (600 MHz, DMSO-*d*₆) δ 11.04 (s, 1H), 9.58 – 9.46 (m, 2H), 8.48 (d, *J* = 2.4 Hz, 1H), 8.46 – 8.37 (m, 3H), 8.27 – 8.17 (m, 3H), 7.80 (d, *J* = 2.4 Hz, 1H), 7.25 (d, *J* = 8.7 Hz, 1H), 7.02 (d, *J* = 8.7 Hz, 1H), 5.75 (d, *J* = 6.4 Hz, 1H), 4.51 (t, *J* = 5.7 Hz, 2H), 4.26 – 4.19 (m, 1H), 4.17 – 4.11 (m, 1H), 3.37 (s, 1H), 3.29 – 3.16 (m, 5H), 2.05 – 1.44 (m, 22H), 0.80 – 0.71 (m, 2H); ¹³C NMR (151 MHz, DMSO-*d*₆) δ 167.32, 163.35, 154.91, 144.63, 144.30, 133.97, 125.23, 124.90, 124.72, 124.45, 117.75, 116.16, 115.54, 54.67, 53.14, 46.79, 45.51, 45.04, 44.83, 41.46, 35.39, 30.63, 29.06, 27.57, 26.58, 23.99, 23.40, 23.21; HRMS (ESI⁺) calcd for [C₃₂H₄₅ClN₈O₄S₂+H]⁺ 705.2767; found 705.2771.

(3Z)-18-(4-aminocyclohexyl)-7-chloro-10-hydroxy-21-[4-[2-(methylamino)ethylamino]-1-piperidyl]-2,2-dioxo-2λ⁶,5-dithia-3,12,18,22-tetrazatetracyclo[18.3.1.0^{4,12}.0^{6,11}]tetracos-1(23),3,6,8,10,20(24),21-heptaen-19-one;trihydrochloride (**35**). The title compound was synthesized from **69f** according to general procedures GP1 and GP2. The desired compound was isolated as a light-brown solid (21 mg, 0.026 mmol, 13% yield over 3 steps). ¹H NMR (600 MHz, DMSO-*d*₆) δ 11.08 (s, 1H), 9.73 (ddd, *J* = 16.7, 12.0, 6.4 Hz, 2H), 9.46 – 9.35 (m, 2H), 8.56 (d, *J* = 2.4 Hz, 1H), 8.27 – 8.16 (m, 3H), 7.77 (d, *J* = 2.4 Hz, 1H), 7.25 (d, *J* = 8.7 Hz, 1H), 7.04 (d, *J* = 8.7 Hz, 1H), 4.58 – 4.44 (m, 2H), 4.22 – 4.15 (m, 1H), 4.15 – 4.05 (m, 2H), 3.50 – 3.41 (m, 1H), 3.41 – 3.33 (m, 2H), 3.33 – 3.23 (m, 4H), 3.03 – 2.92 (m, 2H), 2.74 – 2.64 (m, 1H), 2.58 (t, *J* = 5.3 Hz, 3H), 2.15 – 2.05 (m, 2H), 2.04 – 1.86 (m, 4H), 1.84 – 1.46 (m, 9H), 1.29 – 1.16 (m, 1H), 0.97 – 0.87 (m, 1H), 0.37 – 0.27 (m, 1H); ¹³C NMR (151 MHz, DMSO-*d*₆) δ 169.14, 164.30, 156.16, 144.88, 144.41,

137.93, 126.62, 125.73, 125.17, 125.02, 120.63, 116.72, 115.97, 54.36, 54.21, 47.60, 45.78, 45.61, 45.33, 45.14, 44.70, 39.04, 32.77, 30.51, 29.96, 28.27, 28.19, 28.05, 27.95, 24.44, 24.30, 22.79; carbon at 39.04 ppm overlaps with the DMSO solvent peak (observed in HSQC experiment); HRMS (ESI⁺) *m/z*: calcd for [C₃₂H₄₅ClN₈O₄S₂+H]⁺ 705.2767; found 705.2772.

(3Z)-18-(4-aminocyclohexyl)-21-[4-(4-amino-1-piperidyl)-1-piperidyl]-7-chloro-10-hydroxy-2,2-dioxo-2λ⁶,5-dithia-3,12,18,22-tetrazatetracyclo[18.3.1.0^{4,12}.0^{6,11}]tetracos-1(23),3,6,8,10,20(24),21-heptaen-19-one; trihydrochloride (**36**). The title compound was synthesized from **69g** according to general procedures GP1 and GP2. The desired compound was isolated as a white solid, (101 mg, 0.12 mmol, 75% yield). ¹H NMR (600 MHz, DMSO-*d*₆) δ 11.16 – 11.04 (m, 1H), 10.92 (t, *J* = 11.0 Hz, 1H), 8.60 – 8.57 (m, 0.44H), 8.55 (d, *J* = 2.4 Hz, 1H), 8.41 (d, *J* = 5.4 Hz, 2.57H), 8.32 – 8.18 (m, 3H), 7.76 (d, *J* = 2.4 Hz, 1H), 7.25 (d, *J* = 8.7 Hz, 1H), 7.07 – 7.02 (m, 1H), 4.58 – 4.43 (m, 2H), 4.29 – 4.07 (m, 3H), 3.55 – 3.42 (m, 4H), 3.42 – 3.34 (m, 2H), 3.34 – 3.24 (m, 1H), 3.11 – 2.89 (m, 4H), 2.75 – 2.66 (m, 1H), 2.16 – 2.07 (m, 3H), 2.07 – 1.90 (m, 6H), 1.81 – 1.48 (m, 9H), 1.29 – 1.19 (m, 1H), 0.98 – 0.85 (m, 1H), 0.39 – 0.29 (m, 1H); ¹³C NMR (151 MHz, DMSO-*d*₆) δ 169.19, 164.27, 155.85, 144.90, 144.39, 137.84, 126.40, 125.73, 125.15, 125.02, 120.29, 116.72, 115.95, 62.67, 54.09, 47.55, 47.13, 45.84, 45.66, 45.52, 45.43, 45.35, 43.75, 30.67, 29.97, 28.27, 28.00, 27.42, 26.32, 26.13, 24.30, 24.22, 22.62; one carbon is missing due to overlapping or broadening; HRMS (ESI⁺) *m/z*: calcd for [C₃₄H₄₇ClN₈O₄S₂+H]⁺ 731.2923; found 731.2932.

¹H NMR determined solubilities. All spectra to measure compound solubilities were acquired using a Varian 400 MHz NMR spectrometer with a 5 mm OneNMR probe and Vnmrj 4.2 software. Samples were made up at 0.5 mM with 5% DMSO-*d*₆ in D₂O and 20 mM Tris-*d*₁₁. Spectra were recorded with a recycle delay of 60 s and 64 scans (400 MHz). The spectrometer was calibrated using DMSO-*d*₆ stocks made from three weighings of caffeine and averaged from three solutions made from each of these weighings. Data was analysed in ACD version 12 NMR processing software to determine the compound concentration.

¹H-¹⁵N HSQC NMR Experiments. ¹H-¹⁵N HSQC NMR experiments were acquired using 40–130 μM uniformly ¹⁵N-labeled KRas^{G12D}-GDP or KRas-^{G12D}-GMPPNP in 20 mM Tris, 50 mM NaCl, 5 mM MgCl₂, pH 7.5. *K*_D determination was carried out by collecting ¹H-¹⁵N HSQC spectra at 5 ligand concentrations. The stock solution of the ligand (50 or 100 mM in DMSO-*d*₆) was previously checked and passed all the internal quality control checkpoints with regard to purity, buffer solubility and structure confirmation. Prior to any ligand titration a reference ¹H-¹⁵N HSQC spectrum was acquired. For this study a 600 MHz Varian VNMRS instrument equipped with a HCN cold probe was used. All spectra were acquired using 256 t1 increments at 298 K and processed with Vnmrj 4.2 and analysed using CCPN 1.3 and 2.5⁴⁴.

NMR CSP Measurements and *K*_D. Regions of interest in the spectra individuated as strong changes in both ¹⁵N and ¹H dimensions were annotated, and the chemical shift of both nuclei was recorded for each point during titration starting from the reference with no ligand present. Changes in the spectra were consistent with the fast exchange

regime. This allows the calculation of the *K*_D for the ligands in a straightforward way.

Briefly the differences obtained for those peaks that change position in a straight line where there is no suspicion of a possible conformational analysis were calculated using the following equation using Graphpad or within the CCPNMR software.

$$\text{CSP(H/N)} = [(0.15 \delta_N)^2 + \delta_H^2]^{1/2}$$

The data obtained were fitted using the following equation:

$$\Delta\delta_{\text{obs}} = \Delta\delta_{\infty} [b + a + K_D - ((b + a + K_D)^2 - 4ab)]^{1/2} / 2a$$

$$a = [P] + [PL], b = [L] + [PL]$$

$$\Delta\delta_{\text{obs}} = \delta_{\text{obs}} - \delta_{\text{free}}, \Delta\delta_{\infty} = \delta_{\text{bound}} - \delta_{\text{free}}$$

The *K*_D was shared between the datasets for different residues that were mapped previously as regions of interest obtaining the *K*_D by optimising it globally or by averaging the *K*_D determined for multiple residues. The standard deviations quoted are calculated from the variability for multiple residues or from the global fit.

Mapping CSP on the Protein Structure. The CSP values obtained from the last titration point (0.8 or 1 mM) were collected in order to map them onto the protein. For this an iterative threshold was used by calculating the SD of all the chemical shifts iteratively⁴⁴ and keeping only the ones that were higher than the SD at each iteration. The process was repeated three times and the bands were assigned a gradient colour. PyMOL⁴⁵ was used to colour the respective perturbation categories and to visualise the binding site of the ligands.

SPR Binding Assay. SPR experiments for all elaborated compounds were conducted on a Biacore 8K+ instrument (Cytiva). Purified KRas proteins were captured via the biotinylated Avi-tag on Biacore Series S streptavidin sensor chips in running buffer containing 50 mM HEPES, pH 7.5, 150 mM NaCl, 0.5 mM MgCl₂, 0.1% Tween20, 10 μM nucleotide, and either 2% (compounds **15–17**, **20–23**, **26–29**, **31**, **32**) or 5% (compounds **18**, **19**, **24**, **25**, **33–36**) DMSO to obtain capture levels of approximately 2000 RU. Protein was captured on flow cell 2 across all 8 channels using 200 nM stock solutions, with flow cell 1 used as the reference surface (biotin blocked streptavidin). Remaining streptavidin binding sites were then blocked with 3 x 60 s injections of biotin. Analysis and sample compartment temperatures were set to 25 °C.

Compounds were screened in an 8-point titration, 3-fold concentration series from either 50 μM or 5 μM top concentration, depending on compound affinity, with blanks samples (0 μM) run before and after each compound. Control compounds were run at the start and end of every assay to confirm protein activity over time. Flow rate was set to 30 μL/min. Association was measured for 60 s and dissociation for 60–120 s. A solvent correction curve was run from either 1.5%–2.5% DMSO, or 4%–6% DMSO for 2% DMSO and 5% DMSO running buffers respectively, at the start and end of each run, as well as every 48 cycles.

The sensorgrams were reference and blank subtracted, and solvent corrected prior to fitting to a Langmuir 1:1 binding model, using Biacore Insight Evaluation software (Cytiva). *K*_D measurements were performed in duplicate, with affinities measured at steady state for compounds that

did not show significant curvature in the association and dissociation phases. Kinetic 1:1 fits were performed for compounds where sufficient curvature in the sensorgrams was present.

KRas-Raf Homogenous Time-Resolved Fluorescence (HTRF) Assay. Purified recombinant KRas^{G12D}(1-169)-His₁₀-Avi-GMPPNP and RafRBD(51-131)-3xFLAG proteins were diluted in 1x assay buffer containing 30 mM HEPES, pH 7.0, 2 mM MgCl₂, 25 mM NaCl, 1% v/v glycerol, 0.01% v/v bovine serum albumin (BSA) and 2.5 mM dithiothreitol (DTT) for a final assay concentration of 100 nM and 50 nM respectively. The KRas^{G12D}(1-169)-His₁₀-Avi and RafRBD(51-131)-3xFLAG proteins were subsequently combined with the corresponding donor fluorophore Streptavidin-d2 (PerkinElmer-Cisbio; 610SADLF) and acceptor fluorophore MAb (IgG1) Anti-FLAG M2-Tb cryptate (PerkinElmer-Cisbio; 61FG2TLF) to attain a final assay fluorophore concentration of 50 ng-well⁻¹ and 1.3 ng-well⁻¹ respectively. In addition, a control protein 3xFLAG-RafRBD-Avi incubated with both donor and acceptor fluorophores was included in all compound screening assays. The recombinant proteins and their associated donor/acceptor fluorophores were incubated on ice for 60 min. For compound screening, 10-point (3-fold) serial dilution of compounds were prepared in DMSO with a final top concentration of 100 μM. The diluted compounds were subsequently transferred to the relevant wells of a 384-well microplate, followed by the addition of both protein-fluorophore combinations. Streptavidin-d2 only and Streptavidin-d2 plus anti-FLAG M2-Tb cryptate were included as negative controls. The assay plates were incubated at ambient temperature for 60 min prior to an end-point fluorescent read using a Tecan Infinite M1000 PRO microplate reader. Excitation wavelength for the donor fluorophore was 340 nm and emission wavelengths for the acceptor fluorophore were 620/655 nm.

HTRF selectivity assay were set up using the above methodology and the following panel of Ras single point mutants and isoforms; KRas(2-169)-His₁₀-Avi, KRas^{G12D}(2-169)-His₁₀-Avi, KRas^{G13D}(1-169)-His₁₀-Avi, KRas^{G12C}(1-169)-His₁₀-Avi, KRas^{G12V}(1-169)-His₁₀-Avi, KRas^{Q61K}(2-169)-His₁₀-Avi, NRas(2-167)-His₁₀-Avi and HRas(2-166)-His₁₀-Avi.

Nucleotide Exchange Assay (NEA): Nucleotide loading. Purified recombinant KRas^{G12D}(1-169) protein was loaded with a fluorescently labelled nucleotide (MANT-GDP) by incubating the protein with a 20-fold molar excess of labelled nucleotide in a buffer composed of 20 mM Tris-HCl, pH 7.5, 50 mM NaCl, 4 mM EDTA and 1 mM DTT for 1.5 h at 4 °C. Nucleotide loading reactions were supplemented with 10 mM MgCl₂ and incubated for a further 1 h at 4 °C. Unbound fluorescently labelled nucleotide was removed via buffer exchange using a NAP-5 DNA purification column (Cytiva) pre-equilibrated with the NEA reaction buffer (40 mM HEPES-KOH, pH 7.5, 10 mM MgCl₂ and 1 mM DTT).

NEA. MANT-GDP-loaded KRas^{G12D}(1-169) and the GEF SOS1(546-1049) recombinant proteins were diluted in 1x NEA buffer (55.5 mM HEPES, pH 7.5, 13.8 mM MgCl₂ and 1.38 mM DTT) to attain a final assay concentration of 1 μM and 100 nM respectively. For compound screening, 10-point (3-fold) serial dilution of compounds were prepared in DMSO with a final top concentration of 100 μM. The diluted compounds were subsequently transferred to the

relevant wells of a 96-well microplate, followed by the addition of KRas^{G12D}(1-169) and SOS1(546-1049) proteins.

Initial fluorescence (F₁) was measured using a Tecan Infinite M1000 PRO microplate reader (excitation at 360 nm, emission at 430 nm, bandwidth 20 nm). Nucleotide exchange was initiated via the addition of the non-hydrolysable nucleotide analog GTPγS at a final assay concentration of 200 μM. Assay plates were incubated on a microplate shaker for 1.5 h at ambient temperature prior to a second fluorescence read (F₂) using the aforementioned emission/excitation wavelengths. The percentage effect was calculated by dividing F₂ by F₁ and multiplying by 100.

Nucleotide Exchange Assay with Ras-Raf HTRF Readout (NEA w HTRF). Purified recombinant KRas^{G12D}(1-169)-His₁₀-Avi-GDP, RafRBD(51-131)-3xFLAG and SOS1(546-1049) proteins were diluted in 1x assay buffer (30 mM HEPES, pH 7.0, 2 mM MgCl₂, 25 mM NaCl, 1% v/v glycerol, 0.01% v/v BSA and 2.5 mM DTT) for a final assay concentration of 200 nM, 50 nM and 1 nM respectively. The KRas^{G12D}(1-169)-His₁₀-Avi and RafRBD(51-131)-3xFLAG proteins were combined with the corresponding donor fluorophore Streptavidin-d2 (PerkinElmer-Cisbio; 610SADLF) and acceptor fluorophore MAb (IgG1) Anti-FLAG M2-Tb cryptate (PerkinElmer-Cisbio; 61FG2TLF) to attain a final assay fluorophore concentration of 50 ng-well⁻¹ and 1.3 ng-well⁻¹ respectively. The recombinant proteins and their associated donor/acceptor fluorophores were pre-incubated on ice for 60 min. For compound screening, 10-point (3-fold) serial dilution of compounds were prepared in DMSO with a final top concentration of 100 μM. The diluted compounds were transferred to the relevant wells of a 384-well microplate, followed by the addition of both Ras and Raf protein-fluorophore combinations. Nucleotide exchange was initiated via the addition of SOS1 and the non-hydrolysable nucleotide analogue GMPPNP at a final assay concentration of 100 μM. The assay plates were incubated at ambient temperature for 60 min prior to an end-point fluorescent read using a Tecan Infinite M1000 PRO microplate reader. Excitation wavelength for the donor fluorophore was 340 nm and emission wavelengths for the acceptor fluorophore were 620/655 nm.

Protein Production. (Proteins used in NMR, SPR, NEA and crystallography) Genes for production of recombinant KRas4B^{G12D}(1-169), Avi-KRas4B^{G12D}(1-169), KRas4A^{C118S}(1-169), Avi-NRas(1-169) and Avi-HRas(1-166) were synthesised by Genewiz (Suzhou, China) as *E. coli* optimised DNA sequences and cloned to the NcoI and XhoI sites of pBDDP-SPR3 to contain an N-terminal double-His₈ affinity tag followed by a TEV protease cleavage site (ENLYFQG).⁴⁶ The “Avi” constructs contained an additional Avi-tag (GLNDIFEAQKIEWHE) downstream of the TEV cleavage site.

The constructs without Avi-tag were expressed in *E. coli* Rosetta2 (DE3) pLysS cells (Merck) cultured overnight at 37 °C in autoinduction media (AIM) LB broth (Formedium). For *in vivo* biotinylation, the constructs containing an Avi-tag were expressed in *E. coli* CVB101 cells (Avidity, Inc.) previously lysogenized with the λ phage DE3 by using the λDE3 Lysogenization Kit (Merck) and cultured in Terrific Broth (Formedium) supplemented with 50 μM biotin. Once the culture reached an O.D. 600 of 0.6, the incubator

temperature was reduced to 18 °C, and the expression was induced by the addition of isopropyl- β -D-1-thiogalactopyranoside (IPTG) to a final concentration of 0.5 mM. The cells were pelleted after 18 h and stored at -80 °C.

To produce ^{15}N -labelled KRas4B^{G12D}(1–169), transformed Rosetta2 (DE3) pLysS cells were cultured at 37 °C in 3 L Terrific Broth to O.D. 600 of 0.6, then centrifuged, washed and resuspended in 1 L minimal medium containing 1 g of $^{15}\text{NH}_4\text{Cl}$ and 4 g of glucose. Before induction, cells were shaken for 1 h at 23 °C and then protein expression was initiated by the addition of IPTG to a final concentration of 0.5 mM. Cells were harvested by centrifugation after 18 h and stored at -80 °C.

Cell pellets were resuspended in lysis buffer (50 mM Tris-HCl, pH 7.5, 300 mM NaCl, 5% glycerol, 10 mM imidazole, 1 mM phenylmethylsulphonyl fluoride (PMSF) and DNase I (Sigma)) and lysed by mechanical homogenization. The lysate was centrifuged at 20,000 rpm for 90 min, 4 °C. The clarified lysate was applied to a 5 mL HisTrap FF column (Cytiva) pre-equilibrated with 50 mM Tris-HCl, pH 7.5, 500 mM NaCl, 5% glycerol, 10 mM imidazole. After washing the column, the protein of interest was eluted on a linear gradient of same buffer containing 1 M imidazole and treated with TEV protease for removal of the double-His₆ tag. The sample was applied to a HiLoad 26/60 Superdex 75 pg size exclusion chromatography column (Cytiva) pre-equilibrated with 10 mM Tris-HCl, pH 7.5, 50 mM NaCl, 2 mM MgCl₂. At this point, the final purified Ras proteins were mainly GDP bound, as confirmed by HPLC analysis (previously described in Gray *et al*, 2017)⁴⁷.

(Proteins used in the HTRF assays) Genes for production of recombinant HRas(1–166), NRas(1–169) and KRas4B(1–169), both wild-type and single-point mutants (G12D, G12C, G12V, G13D and Q61K), were synthesised by ATUM, Inc. as *E. coli* optimised DNA sequences with flanking Gateway attB1 and attB2 sites. Sequences containing C-terminal His₁₀-Avi tags had the sequence ASGSHHHHHHHHSGENLYFQSGGGGLNDIFEAKIEWH E appended to the C-terminus, while the N-terminus of all constructs contained an optimized *E. coli* ribosome-binding site. Synthetic templates were recombined using Gateway BP cloning into pDonr-255 to generate Entry clones and were subsequently recombined using Gateway LR cloning into pDest-521 (Addgene #159688) to generate bacterial T7 promoter-based expression clones.

3xFLAG-tagged Raf Ras-binding domain (RafRBD, amino acids 51–131) was synthesized by ATUM, Inc. as noted above, with an N-terminal TEV protease cleavage site followed by a 3xFLAG tag (DYKDHDGDYKDHDIDYKDDDDK) and a C-terminal Avi-tag. Entry clones of this construct were recombined using LR recombination into pDest-566 (Addgene #11517) to generate *E. coli* expression constructs with an N-terminal His₆-MBP (maltose-binding protein) fusion tag.

Proteins were expressed in *E. coli* BL21 StarTM (Thermo Fisher Scientific) harbouring the pRARE plasmid (expressing rare tRNAs) and pBirA (expressing biotin ligase; Avidity, Inc.) using the Dynamite protocol as outlined in Taylor *et al* (2017)⁴⁸ with overnight induction at 16 °C. 0.2 mM D-biotin was added 1 h prior to induction to support biotinylation *in vivo*. All proteins were purified as outlined in Kopra *et al*

(2020)⁴⁹ for KRas(1–169), with modifications for the C-terminal tagged Ras constructs. Specifically, steps pertaining to TEV protease digestion were omitted for these constructs, the SEC load sample was adjusted to 10 mM EDTA (to prevent dimer formation), and the SEC running buffer was at 2 mM MgCl₂. Ras proteins were exchanged into GMPPNP as described in Bonsor *et al* (2022).⁵⁰

Protein crystallization and diffraction data collection. All crystallisation experiments were carried out by sitting-drop vapour diffusion at 19 °C using drops of a 1:1 mixture of a liganded protein sample and the reservoir solution. Liganded protein was obtained by supplementing protein stock at \approx 25 mg/mL with 10% compound stock in DMSO (50 mM stock concentration for **8**, **9**, **11**, **14** and **15**; 10 mM stock concentration otherwise) and incubation on ice for one hour.

KRas4A^{C118S}(1–169)-GDP ligand complexes were crystallised in 1.7 μL drops over a reservoir containing 25–28% polyethylene glycol 8000, 300–500 mM LiCl and either no buffer or 100 mM *bis-tris* propane, pH 6.2–8.7. In general, microseeding was used to improve reproducibility. Clusters of needles or plates would generally appear within 24 hours and continue to grow for several days. Crystals were harvested by rapid addition of 0.4 μL ethylene glycol directly to a crystallisation drop, followed immediately by flash-cooling in liquid nitrogen.

KRas4A^{C118S}(1–169)-GMPPNP ligand complexes were crystallized in 1.0 μL drops over a reservoir of 16–28% polyethylene glycol 3350, 100–150 mM MgCl₂, 10 mM CoCl₂ and 100 mM HEPES, pH 7.5. Small but single crystals would appear within three days. Crystals were harvested by brief transfer to a droplet consisting of 0.28 μL ethylene glycol and 0.9 μL of the relevant mother liquor followed by flash-cooling in liquid nitrogen.

All data were collected at 100 K and automatically processed/scaled at Diamond Light Source (Didcot, UK), using XDS⁵¹, DIALS⁵² and AIMLESS⁵³ under control of xia2⁵⁴, fast_dp⁵⁵ or autoPROC⁵⁶; see Table S10 for data collection details.

Structure determination and refinement. Data truncation and general handling were carried out using CCP4.⁵⁷ Initially, structures were solved by molecular replacement with MOLREP⁵⁸ using search models derived from PDB entries 4DSU²⁶ (for KRas-GDP) or 3GFT (for KRas-GMPPNP). Additional structures in the same crystal form were phased by rigid body refinement of the protein component of an earlier structure using REFMAC5.⁵⁹ Cycles of model building and refinement were carried out using Coot⁶⁰ and REFMAC5, ligand topologies were generated using PRODRG.⁶¹ The quality of final models was assessed using PROCHECK⁶² and MolProbity.⁶³ Figures depicting structures were produced using PyMOL 2.3.0.⁴⁵ Data and model statistics are summarised in Table S10.

PERK HTRF assay. MIA PaCa-2 cells (ATCC, LGC Standards, Teddington, UK) were cultured in DMEM medium (Thermo Fisher Scientific) supplemented with 10% FBS and 2 mM L-glutamine. NCI-H1437 cells were maintained in RPMI medium (Thermo Fisher Scientific) supplemented with 10% FBS, 2 mM L-glutamine, 1 mM sodium pyruvate and 10 mM HEPES.

Cellular HTRF technology for phosphorylated ERK1/2 (Thr202/Tyr204) (Cisbio, Oxford Biosystems, Abingdon, UK) was used accordingly to manufacturer instructions. Briefly, MIA PaCa-2 cells were seeded in clear 96-well plates at a density of 1.2×10^4 cells per well and were incubated overnight at 37 °C. The day after, indicated drug dilutions were added with a final DMSO concentration of 0.5%. Cells were then incubated at 37 °C for 3 h. Media was removed, cells were washed twice with PBS, then lysed with supplemented lysis buffer and incubated for 30 min at room temperature on a plate shaker at 400 rpm. Premixed antibody was added and incubated at room temperature in the dark for 16 h. The plate was read on a Tecan Infinite M1000 PRO at two different wavelengths (665 nm and 620 nm). The ratio of the acceptor and donor emission signals for each well was calculated according to the following formula: $\text{signal}(665 \text{ nm}) / \text{signal}(620 \text{ nm}) \times 10^4$. The HTRF ratio was normalised to the DMSO-treated control cells.

Ras-Raf NanoBiT assay. HEK293A containing SmBiT-Raf and LgBiT-Ras clones (generated in house) were plated in phenol-free RPMI medium supplemented with 5% FBS, 2 mM L-glutamine, 1 mM sodium pyruvate and 10 mM HEPES. HEK293t SmBiT-NRF2, LgBiT-KEAP1 negative control cell line was cultured in phenol-free DMEM medium supplemented with 5% FBS, 2 mM L-glutamine, 1 mM sodium pyruvate and 10 mM HEPES. All clones were seeded in Collagen I coated 96-well white plates (Corning, Arizon, USA) at a density of 15,800 cells per well. The following day dilutions were carried out to give a final DMSO concentration of 0.1%. Cells were then stimulated with 100 ng/ml EGF diluted in OptiMEM (Thermo Fisher Scientific). For the NanoBiT assay the manufacturer instructions were followed (Nano-Glo Live cell assay system, Promega). Plates were further incubated for 23 min at room temperature and luminescence was measured using the Tecan Infinite M1000P RO plate reader with an integration time of 300 ms.

Generation of KRas mutant NanoBiT cells. pFN28A CMV_Neo flexi vector containing LgBiT-KRas^{WT} (gift from Novartis) was used as a template to generate the mutant-expressing plasmids (Genewiz, Essex, UK). HEK293A SmBiT-Raf cells (gift from Novartis) cells were transfected with 100 ng per well of the appropriated mutant plasmid using Fugene HD (Promega, Southampton, UK) according to the manufacturer's protocol. Following 5–7 d of culture in selection antibiotic monoclonal populations of cells were isolated by performing standard limiting dilution procedure. LgBiT-KRas^{WT} mutant levels were determined by western blot using an anti-LgBiT antibody (Promega).

ASSOCIATED CONTENT

Supporting Information

The Supporting Information is available free of charge at <https://pubs.acs.org/>

Supplementary figures, charts, tables, biophysical, biological and biochemical data; Pull-down assay, 3D spheroid generation and Cell Titer Glo, *in vitro* and *in vivo* assay information; X-ray data collection and refinement statistics; analytical data for compounds **1**, **5**; Experimental procedures for compounds **50**, **58**, **63a**, **63b**, **83**, **87**; ¹H, ¹³C NMR spectra and HPLC traces for compounds 1–36 (PDF)

Molecular formula strings (CSV) with some associated biochemical and biophysical data.

Accession codes

KRas ligand complex crystal structures have been deposited in the wwPDB with the following identifiers: 9GGT (**8**), 9GGU (**9**), 9G0Y (**11**), 9GGV (**14**), 9G4B (**15**), 9GGW (**16**), 9GGX (**19**), 9GGY (**29**), 9GGZ (**31**), 9GH0 (**32**), 9GH1 (**34**), 9GH2 (**36**). Authors will release the atomic coordinates and experimental data upon article publication.

AUTHOR INFORMATION

Corresponding Authors

Charles W. Parry - Cancer Research Horizons, CRUK Scotland Institute, Garscube Estate, Switchback Road, Glasgow, G61 1BD, UK; Email: Charles.Parry@cancer.org.uk

John B. Taylor - Cancer Research Horizons, CRUK Scotland Institute, Garscube Estate, Switchback Road, Glasgow, G61 1BD, UK; Email: John.Taylor@cancer.org.uk

Present Addresses

#J.B.: Kesmalea Therapeutics, Arc West London, Manbre Wharf, Manbre Rd, London, W6 9RH, UK.

§A.B.: CRUK Scotland Institute, Garscube Estate, Switchback Road, Glasgow, G61 1BD, UK.

†M.J.D.: 3rd Floor, 1 Ashley Road, Altrincham, Cheshire, WA14 2DT, UK.

‡D.M., A.P.: BioAscent Discovery Ltd, Bo'Ness Road, Newhouse, Lanarkshire, ML1 5UH, UK.

§H.M.: Nine, Edinburgh BioQuarter, 9 Little France Road, Edinburgh, EH16 4UX, UK.

¶J.E.: Treeline Biosciences, 11180 Roselle St, San Diego, CA 92121, USA.

•N.M.C.: Antibody Analytics, Antibody Analytics Discovery Centre, Newhut Road, Motherwell, Scotland, ML1 3ST, UK.

△A.G.: The Discovery Centre (DISC), AstraZeneca PLC, Biomedical Campus, 1 Francis Crick Ave., Trumpington, Cambridge, CB2 0AA, UK.

♠M.M.: Edinburgh Innovations, 1st Floor, Murchison House, King's Buildings, 10 Max Born Crescent, Edinburgh, EH9 3BF, UK.

Author Contributions

M.J.D. initiated the project; J.B. and H.M. led the project; J.B., H.M., M.M., and J.E. managed the Novartis collaboration; K.B., D.A.G., N.D., F.Z., N.S. and C.V.-V. contributed to the Novartis collaboration; F.P. led the biology team; D.M. and J.B.T. were responsible for medicinal chemistry strategy; D.M., J.B.T., R.W. and C.W.P. designed compounds, synthetic routes and managed external chemistry resource; D.M., J.B.T., K.D., P.S., C.W., S.D., A.H., R.W. and C.W.P. synthesized the compounds; K.C. performed the NMR fragment screen and NMR assays; R.N. prepared NMR figures; K.P., A.G. and N.M.C. performed SPR and ITC assays; M.M. led the biochemistry strategy and developed and performed the NEA assay; J.P.C. developed and performed HTRF assays; L.D.H. performed biochemical assays; C.H.G. led the protein science strategy; M.H., J.K. and C.C.P. expressed and purified proteins for the assays; A.W.S. carried out crystallography, refined inhibitor complexes and prepared all final figures; F.P., A.B., N.R. and A.E.-B. performed cell and NanoBiT assays; A.P. performed computational chemistry. All authors have given approval to the final version of the manuscript. The manuscript was written by C.W.P., F.P., and A.W.S.

Funding Sources

The project was funded by Cancer Research UK (Core Grant Numbers C7932/A17096 and DRCDPRGMApr2020\100006). Funding was also obtained from Novartis and CRT Pioneer Fund (Sixth Element Capital).

Notes

The authors declare no competing financial interest.

ACKNOWLEDGMENT

The authors would like to thank the following teams and people for their valuable contributions to this work. Prof. Terence Rabbitts (University of Oxford) and team for their work on fragment screening strategies. Dominic Esposito and team (Frederick National Laboratory for Cancer Research) for the supply of proteins used in the HTRF assays. The Chemistry team at Syngene International Ltd. (Bangalore, India): John Kallikat, Ravikumar Velayutham and team. The Chemistry team at Medicilon Inc. (Shanghai, China): Yongmei Xu, Peng Wei and team. The authors would also like to thank Diamond Light Source for beamtime (proposals mx8659, mx11651, mx16258 and sw26339) and the staff of beamlines i03, i04, i04-1 and i24 for their assistance. We also would like to thank Kevin Doyle and Michael Waring for useful discussions during the preparation of this manuscript, Reach Separations for chiral separation and analyses, Jennifer Baker for high resolution mass spectrometric analyses, Michael Kilday for compound management and Richard Papworth and Hollie Wilson for informatics support.

ABBREVIATIONS

cat, catalytic domain; CCPN, Collaborative Computing Project for NMR; CRC, Colorectal cancer; CSP, Chemical Shift Perturbation CV, Column Volume; DMEM, Dulbecco's Modified Eagle Medium; FBS, Foetal bovine serum; GAP, GTPase-accelerating protein; GDP, guanosine diphosphate; GEF, Guanine Nucleotide Exchange Factor; GMPPNP, Guanosine 5'-O-(β,γ -imidotriphosphate); GTP, Guanosine Triphosphate; GTP γ S, Guanosine 5'-O-(γ -thio)triphosphate; HRas, Harvey rat sarcoma; HATU, *N*-[(dimethylamino)-1*H*-1,2,3-triazolo-[4,5-*b*]pyridin-1-ylmethylene]-*N*-methylmethanaminium hexafluorophosphate *N*-oxide; HEPES, 4-(2-hydroxyethyl)-1-piperazineethanesulfonic acid; LB, Luria-Bertani broth; KRas, Kirsten rat sarcoma; LgBiT, large BiT; *m*-CPBA, *meta*-Chloroperoxybenzoic acid; MEK, Mitogen-activated protein kinase; NanoBiT, NanoLuc Binary Technology; NRas, neuroblastoma RAS; NSCLC, non-small cell lung cancer; PHB, *para*-hydroxy benzyl; PK, Pharmacokinetic; Raf, Rapidly Accelerated Fibrosarcoma; RALGDS, Ral Guanine Nucleotide Dissociation Stimulator; RafRBD, Raf Ras-Binding Domain; SAR, Structure-activity relationships; SBDD, Structure-based Drug Design; SD, Standard deviation; SHP2, Src Homology-2 domain-containing Protein Tyrosine Phosphatase-2; SmBiT, Small BiT; SOS1, Son of Sevenless homolog 1; TCEP, *Tris* (2-carboxyethyl) phosphine; tPSA, Topological Polar Surface Area; μ wave, microwave.

REFERENCES

- (1) Bos, J. L. Ras Oncogenes in Human Cancer: a Review. *Cancer Res* **1989**, *49*, 4682-4689.
- (2) Prior, I. A.; Lewis, P. D.; Mattos, C. A Comprehensive Survey of Ras Mutations in Cancer. *Cancer Res* **2012**, *72*, 2457-2467.
- (3) Simanshu, D. K.; Nissley, D. V.; McCormick, F. RAS Proteins and Their Regulators in Human Disease. *Cell* **2017**, *170*, 17-33.
- (4) Puneekar, S. R.; Velcheti, V.; Neel, B. G.; Wong, K. K. The Current State of the Art and Future Trends in RAS-Targeted Cancer Therapies. *Nat Rev Clin Oncol* **2022**, *19*, 637-655.
- (5) Canon, J.; Rex, K.; Saiki, A. Y.; Mohr, C.; Cooke, K.; Bagal, D.; Gaida, K.; Holt, T.; Knutson, C. G.; Koppada, N.; Lanman, B. A.;

Werner, J.; Rapaport, A. S.; San Miguel, T.; Ortiz, R.; Osgood, T.; Sun, J.-R.; Zhu, X.; McCarter, J. D.; Volak, L. P.; Houk, B. E.; Fakhri, M. G.; O'Neil, B. H.; Price, T. J.; Falchook, G. S.; Desai, J.; Kuo, J.; Govindan, R.; Hong, D. S.; Ouyang, W.; Henary, H.; Arvedson, T.; Cee, V. J.; Lipford, J. R. The Clinical KRAS(G12C) Inhibitor AMG 510 Drives Anti-Tumour Immunity. *Nature* **2019**, *575*, 217-223.

(6) Fell, J. B.; Fischer, J. P.; Baer, B. R.; Blake, J. F.; Bouhana, K.; Briere, D. M.; Brown, K. D.; Burgess, L. E.; Burns, A. C.; Burkard, M. R.; Chiang, H.; Chicarelli, M. J.; Cook, A. W.; Gaudino, J. J.; Hallin, J.; Hanson, L.; Hartley, D. P.; Hicken, E. J.; Hingorani, G. P.; Hinklin, R. J.; Mejia, M. J.; Olson, P.; Otten, J. N.; Rhodes, S. P.; Rodriguez, M. E.; Savechenkov, P.; Smith, D. J.; Sudhakar, N.; Sullivan, F. X.; Tang, T. P.; Vigers, G. P.; Wollenberg, L.; Christensen, J. G.; Marx, M. A. Identification of the Clinical Development Candidate MRTX849, a Covalent KRASG12C Inhibitor for the Treatment of Cancer. *J Med Chem* **2020**, *63*, 6679-6693.

(7) Hong, D. S.; Fakhri, M. G.; Strickler, J. H.; Desai, J.; Durm, G. A.; Shapiro, G. I.; Falchook, G. S.; Price, T. J.; Sacher, A.; Denlinger, C. S.; Bang, Y.-J.; Dy, G. K.; Krauss, J. C.; Kuboki, Y.; Kuo, J. C.; Coveler, A. L.; Park, K.; Kim, T. W.; Barlesi, F.; Munster, P. N.; Ramalingam, S. S.; Burns, T. F.; Meric-Bernstam, F.; Henary, H.; Ngang, J.; Ngarmchamnarith, G.; Kim, J.; Houk, B. E.; Canon, J.; Lipford, J. R.; Friberg, G.; Lito, P.; Govindan, R.; Li, B. T. KRAS^{G12C} Inhibition with Sotorasib in Advanced Solid Tumors. *N Engl J Med* **2020**, *383*, 1207-1217.

(8) Awad, M. M.; Liu, S.; Rybkin, I.; Arbour, K. C.; Dilly, J.; Zhu, V. W.; Johnson, M. L.; Heist, R. S.; Patil, T.; Riely, G. J.; Jacobson, J. O.; Yang, X.; Persky, N. S.; Root, D. E.; Lowder, K. E.; Feng, H.; Zhang, S. S.; Haigis, K. M.; Hung, Y. P.; Sholl, L. M.; Wolpin, B. M.; Wiese, J.; Christiansen, J.; Lee, J.; Schrock, A. B.; Lim, L. P.; Garg, K.; Li, M.; Engstrom, L. D.; Waters, L.; Lawson, J. D.; Olson, P.; Lito, P.; Ou, S. I.; Christensen, J. G.; Janne, P. A.; Aguirre, A. J. Acquired Resistance to KRAS(G12C) Inhibition in Cancer. *N Engl J Med* **2021**, *384*, 2382-2393.

(9) Solanki, H. S.; Welsh, E. A.; Fang, B.; Izumi, V.; Darville, L.; Stone, B.; Franzese, R.; Chavan, S.; Kinose, F.; Imbody, D.; Koomen, J. M.; Rix, U.; Haura, E. B. Cell Type-Specific Adaptive Signaling Responses to KRAS(G12C) Inhibition. *Clin Cancer Res* **2021**, *27*, 2533-2548.

(10) Suzuki, S.; Yonesaka, K.; Teramura, T.; Takehara, T.; Kato, R.; Sakai, H.; Haratani, K.; Tanizaki, J.; Kawakami, H.; Hayashi, H.; Sakai, K.; Nishio, K.; Nakagawa, K. KRAS Inhibitor Resistance in MET-Amplified KRAS (G12C) Non-Small Cell Lung Cancer Induced by RAS- and Non-RAS-Mediated Cell Signaling Mechanisms. *Clin Cancer Res* **2021**, *27*, 5697-5707.

(11) Tanaka, N.; Lin, J. J.; Li, C.; Ryan, M. B.; Zhang, J.; Kiedrowski, L. A.; Michel, A. G.; Syed, M. U.; Fella, K. A.; Sakhi, M.; Baiev, I.; Juric, D.; Gainor, J. F.; Klempner, S. J.; Lennerz, J. K.; Siravegna, G.; Bar-Peled, L.; Hata, A. N.; Heist, R. S.; Corcoran, R. B. Clinical Acquired Resistance to KRAS(G12C) Inhibition through a Novel KRAS Switch-II Pocket Mutation and Polyclonal Alterations Converging on RAS-MAPK Reactivation. *Cancer Discov* **2021**, *11*, 1913-1922.

(12) Amodio, V.; Yaeger, R.; Arcella, P.; Cancelliere, C.; Lamba, S.; Lorenzato, A.; Arena, S.; Montone, M.; Mussolin, B.; Bian, Y.; Whaley, A.; Pinnelli, M.; Murciano-Goroff, Y. R.; Vakiani, E.; Valeri, N.; Liao, W. L.; Bhalkikar, A.; Thyparambil, S.; Zhao, H. Y.; de Stanchina, E.; Marsoni, S.; Siena, S.; Bertotti, A.; Trusolino, L.; Li, B. T.; Rosen, N.; Di Nicolantonio, F.; Bardelli, A.; Misale, S. EGFR Blockade Reverts Resistance to KRAS(G12C) Inhibition in Colorectal Cancer. *Cancer Discov* **2020**, *10*, 1129-1139.

(13) Xue, J. Y.; Zhao, Y.; Aronowitz, J.; Mai, T. T.; Vides, A.; Qeriqi, B.; Kim, D.; Li, C.; de Stanchina, E.; Mazutis, L.; Risso, D.; Lito, P. Rapid Non-Uniform Adaptation to Conformation-Specific KRAS(G12C) Inhibition. *Nature* **2020**, *577*, 421-425.

- (14) Salmon, M.; Alvarez-Diaz, R.; Fustero-Torre, C.; Brehey, O.; Lechuga, C. G.; Sanclemente, M.; Fernandez-Garcia, F.; Lopez-Garcia, A.; Martin-Guijarro, M. C.; Rodriguez-Perales, S.; Bousquet-Mur, E.; Morales-Cacho, L.; Mulero, F.; Al-Shahrour, F.; Martinez, L.; Dominguez, O.; Caleiras, E.; Ortega, S.; Guerra, C.; Musteanu, M.; Drosten, M.; Barbacid, M. KRAS Oncogene Ablation Prevents Resistance in Advanced Lung Adenocarcinoma. *J Clin Invest* **2023**, *133*, e164413.
- (15) Molina-Arcas, M.; Moore, C.; Rana, S.; van Maldegem, F.; Mugarza, E.; Romero-Clavijo, P.; Herbert, E.; Horswell, S.; Li, L. S.; Janes, M. R.; Hancock, D. C.; Downward, J. Development of Combination Therapies to Maximize the Impact of KRAS-G12C Inhibitors in Lung Cancer. *Sci Transl Med* **2019**, *11*.
- (16) Escher, T. E.; Satchell, K. J. F. RAS Degraders: The New Frontier for RAS-Driven Cancers. *Mol Ther* **2023**.
- (17) Zhang, X.; Zhao, T.; Sun, M.; Li, P.; Lai, M.; Xie, L.; Chen, J.; Ding, J.; Xie, H.; Zhou, J.; Zhang, H. Design, Synthesis and Biological Evaluation of KRAS(G12C)-PROTACs. *Bioorg Med Chem* **2023**, *78*, 117153.
- (18) Zhou, H.; Gan, Y.; Li, Y.; Chen, X.; Guo, Y.; Wang, R. Degradation of Rat Sarcoma Proteins Targeting the Post-Translational Prenyl Modifications via Cascade Azidation/Fluorination and Click Reaction. *J Med Chem* **2023**, *66*, 7243-7252.
- (19) Gross, P. H.; Sheets, K. J.; Warren, N. A.; Ghosh, S.; Varghese, R. E.; Wass, K. K. E.; Kadimisetty, K. Accelerating PROTAC Drug Discovery: Establishing a Relationship Between Ubiquitination and Target Protein Degradation. *Biochem Biophys Res Commun* **2022**, *628*, 68-75.
- (20) Kim, D.; Herdeis, L.; Rudolph, D.; Zhao, Y.; Böttcher, J.; Vides, A.; Ayala-Santos, C. I.; Pourfarjam, Y.; Cuevas-Navarro, A.; Xue, J. Y.; Mantoulidis, A.; Bröker, J.; Wunberg, T.; Schaaf, O.; Popow, J.; Wolkerstorfer, B.; Kropatsch, K. G.; Qu, R.; de Stanchina, E.; Sang, B.; Li, C.; McConnell, D. B.; Kraut, N.; Lito, P. Pan-KRAS Inhibitor Disables Oncogenic Signalling and Tumour Growth. *Nature* **2023**.
- (21) Holderfield, M.; Lee, B. J.; Jiang, J.; Tomlinson, A.; Seamon, K. J.; Mira, A.; Patrucco, E.; Goodhart, G.; Dilly, J.; Gindin, Y.; Dinglasan, N.; Wang, Y.; Lai, L. P.; Cai, S.; Jiang, L.; Nasholm, N.; Shifrin, N.; Blaj, C.; Shah, H.; Evans, J. W.; Montazer, N.; Lai, O.; Shi, J.; Ahler, E.; Quintana, E.; Chang, S.; Salvador, A.; Marquez, A.; Cregg, J.; Liu, Y.; Milin, A.; Chen, A.; Ziv, T. B.; Parsons, D.; Knox, J. E.; Klomp, J. E.; Roth, J.; Rees, M.; Ronan, M.; Cuevas-Navarro, A.; Hu, F.; Lito, P.; Santamaria, D.; Aguirre, A. J.; Waters, A. M.; Der, C. J.; Ambrogio, C.; Wang, Z.; Gill, A. L.; Koltun, E. S.; Smith, J. A. M.; Wildes, D.; Singh, M. Concurrent Inhibition of Oncogenic and Wild-Type RAS-GTP for Cancer Therapy. *Nature* **2024**, *629*, 919-926.
- (22) Janes, M. R.; Zhang, J.; Li, L. S.; Hansen, R.; Peters, U.; Guo, X.; Chen, Y.; Babbar, A.; Firdaus, S. J.; Darjania, L.; Feng, J.; Chen, J. H.; Li, S.; Li, S.; Long, Y. O.; Thach, C.; Liu, Y.; Zariw, A.; Ely, T.; Kucharski, J. M.; Kessler, L. V.; Wu, T.; Yu, K.; Wang, Y.; Yao, Y.; Deng, X.; Zarrinkar, P. P.; Brehmer, D.; Dhanak, D.; Lorenzi, M. V.; Hu-Lowe, D.; Patricelli, M. P.; Ren, P.; Liu, Y. Targeting KRAS Mutant Cancers with a Covalent G12C-Specific Inhibitor. *Cell* **2018**, *172*, 578-589.
- (23) Ostrem, J. M.; Peters, U.; Sos, M. L.; Wells, J. A.; Shokat, K. M. K-Ras(G12C) Inhibitors Allosterically Control GTP Affinity and Effector Interactions. *Nature* **2013**, *503*, 548-551.
- (24) Hunter, J. C.; Manandhar, A.; Carrasco, M. A.; Gurbani, D.; Gondi, S.; Westover, K. D. Biochemical and Structural Analysis of Common Cancer-Associated KRAS Mutations. *Mol Cancer Res* **2015**, *13*, 1325-1335.
- (25) Kessler, D.; Gmachl, M.; Mantoulidis, A.; Martin, L. J.; Zoepfel, A.; Mayer, M.; Gollner, A.; Covini, D.; Fischer, S.; Gerstberger, T.; Gmaschitz, T.; Goodwin, C.; Greb, P.; Haring, D.; Hela, W.; Hoffmann, J.; Karolyi-Oezguer, J.; Knesl, P.; Kornigg, S.; Koegl, M.; Kousek, R.; Lamarre, L.; Moser, F.; Munico-Martinez, S.; Peinsipp, C.; Phan, J.; Rinnenthal, J.; Sai, J.; Salamon, C.; Scherbantini, Y.; Schipany, K.; Schnitzer, R.; Schrenk, A.; Sharps, B.; Sisler, G.; Sun, Q.; Waterson, A.; Wolkerstorfer, B.; Zeeb, M.; Pearson, M.; Fesik, S. W.; McConnell, D. B. Drugging an Undruggable Pocket on KRAS. *Proc Natl Acad Sci U S A* **2019**, *116*, 15823-15829.
- (26) Maurer, T.; Garrenton, L. S.; Oh, A.; Pitts, K.; Anderson, D. J.; Skelton, N. J.; Fauber, B. P.; Pan, B.; Malek, S.; Stokoe, D.; Ludlam, M. J.; Bowman, K. K.; Wu, J.; Giannetti, A. M.; Starovasnik, M. A.; Mellman, I.; Jackson, P. K.; Rudolph, J.; Wang, W.; Fang, G. Small-Molecule Ligands Bind to a Distinct Pocket in Ras and Inhibit SOS-Mediated Nucleotide Exchange Activity. *Proc Natl Acad Sci U S A* **2012**, *109*, 5299-5304.
- (27) Sun, Q.; Burke, J. P.; Phan, J.; Burns, M. C.; Olejniczak, E. T.; Waterson, A. G.; Lee, T.; Rossanese, O. W.; Fesik, S. W. Discovery of Small Molecules that Bind to K-Ras and Inhibit Sos-Mediated Activation. *Angew Chem Int Ed Engl* **2012**, *51*, 6140-6143.
- (28) Williamson, M. P. Using Chemical Shift Perturbation to Characterise Ligand Binding. *Prog Nucl Magn Reson Spectrosc* **2013**, *73*, 1-16.
- (29) Quevedo, C. E.; Cruz-Migoni, A.; Bery, N.; Miller, A.; Tanaka, T.; Petch, D.; Bataille, C. J. R.; Lee, L. Y. W.; Fallon, P. S.; Tulmin, H.; Ehebauer, M. T.; Fernandez-Fuentes, N.; Russell, A. J.; Carr, S. B.; Phillips, S. E. V.; Rabbitts, T. H. Small Molecule Inhibitors of RAS-Effector Protein Interactions Derived Using an Intracellular Antibody Fragment. *Nat Commun* **2018**, *9*, 3169.
- (30) Baell, J. B.; Holloway, G. A. New Substructure Filters for Removal of Pan Assay Interference Compounds (PAINS) from Screening Libraries and for Their Exclusion in Bioassays. *J Med Chem* **2010**, *53*, 2719-2740.
- (31) Hopkins, A. L.; Groom, C. R.; Alex, A. Ligand Efficiency: a Useful Metric for Lead Selection. *Drug Discov Today* **2004**, *9*, 430-431.
- (32) Garcia Jimenez, D.; Poongavanam, V.; Kihlberg, J. Macrocycles in Drug Discovery—Learning from the Past for the Future. *J Med Chem* **2023**.
- (33) Sticke, D. F.; Presta, L. G.; Dill, K. A.; Rose, G. D. Hydrogen Bonding in Globular Proteins. *J Mol Biol* **1992**, *226*, 1143-1159.
- (34) Dixon, A. S.; Schwinn, M. K.; Hall, M. P.; Zimmerman, K.; Otto, P.; Lubben, T. H.; Butler, B. L.; Binkowski, B. F.; Machleidt, T.; Kirkland, T. A.; Wood, M. G.; Eggers, C. T.; Encell, L. P.; Wood, K. V. NanoLuc Complementation Reporter Optimized for Accurate Measurement of Protein Interactions in Cells. *ACS Chem Biol* **2016**, *11*, 400-408.
- (35) Fujita-Sato, S.; Galeas, J.; Truitt, M.; Pitt, C.; Urisman, A.; Bandyopadhyay, S.; Ruggero, D.; McCormick, F. Enhanced MET Translation and Signaling Sustains K-Ras-Driven Proliferation under Anchorage-Independent Growth Conditions. *Cancer Res* **2015**, *75*, 2851-2862.
- (36) Gannon, H. S.; Kaplan, N.; Tsherniak, A.; Vazquez, F.; Weir, B. A.; Hahn, W. C.; Meyerson, M. Identification of an "Exceptional Responder" Cell Line to MEK1 Inhibition: Clinical Implications for MEK-Targeted Therapy. *Mol Cancer Res* **2016**, *14*, 207-215.
- (37) Tran, T. H.; Chan, A. H.; Young, L. C.; Bindu, L.; Neale, C.; Messing, S.; Dharmiah, S.; Taylor, T.; Denson, J.-P.; Esposito, D.; Nissley, D. V.; Stephen, A. G.; McCormick, F.; Simanshu, D. K. KRAS Interaction with RAF1 RAS-Binding Domain and Cysteine-Rich Domain Provides Insights into RAS-Mediated RAF Activation. *Nat Commun* **2021**, *12*, 1176.
- (38) Kapoor, A.; Travesset, A. Differential Dynamics of RAS Isoforms in GDP- and GTP-Bound States. *Proteins* **2015**, *83*, 1091-1106.
- (39) Tanaka, T.; Thomas, J.; Van Montfort, R.; Miller, A.; Rabbitts, T. Pan RAS-Binding Compounds Selected from a Chemical Library by Inhibiting Interaction between RAS and a Reduced Affinity Intracellular Antibody. *Sci Rep* **2021**, *11*, 1712.

- (40) Ryan, M. B.; Fece de la Cruz, F.; Phat, S.; Myers, D. T.; Wong, E.; Shahzade, H. A.; Hong, C. B.; Corcoran, R. B. Vertical Pathway Inhibition Overcomes Adaptive Feedback Resistance to KRAS(G12C) Inhibition. *Clin Cancer Res* **2020**, *26*, 1633-1643.
- (41) Britten, C. D. Targeting ErbB Receptor Signaling: a Pan-ErbB Approach to Cancer. *Mol Cancer Ther* **2004**, *3*, 1335-1342.
- (42) Ather, F.; Hamidi, H.; Fejzo, M. S.; Letrent, S.; Finn, R. S.; Kabbinar, F.; Head, C.; Wong, S. G. Dacomitinib, an Irreversible Pan-ErbB Inhibitor Significantly Abrogates Growth in Head and Neck Cancer Models that Exhibit Low Response to Cetuximab. *PLoS One* **2013**, *8*, e56112.
- (43) Lakhan, R.; Rai, B. J. Synthesis of Some New 3-(2'-benzothiazolyl)-4(3H)-Quinazolinones as Antifungal Agents. *J. Chem. Eng. Data* **1986**, *31*, 501-502.
- (44) Vranken, W. F.; Boucher, W.; Stevens, T. J.; Fogh, R. H.; Pajon, A.; Llinas, M.; Ulrich, E. L.; Markley, J. L.; Ionides, J.; Laue, E. D. The CCPN Data Model for NMR Spectroscopy: Development of a Software Pipeline. *Proteins* **2005**, *59*, 687-696.
- (45) The PyMOL Molecular Graphics System, Version 2.3.0 Schrödinger, LLC.
- (46) Konczal, J.; Gray, C. H. Streamlining Workflow and Automation to Accelerate Laboratory Scale Protein Production. *Protein Expr Purif* **2017**, *133*, 160-169.
- (47) Gray, C. H.; Konczal, J.; Mezna, M.; Ismail, S.; Bower, J.; Drysdale, M. A Fully Automated Procedure for the Parallel, Multidimensional Purification and Nucleotide Loading of the Human GTPases KRas, Rac1 and RalB. *Protein Expr Purif* **2017**, *132*, 75-84.
- (48) Taylor, T.; Denson, J. P.; Esposito, D. Optimizing Expression and Solubility of Proteins in *E. coli* Using Modified Media and Induction Parameters. *Methods Mol Biol* **2017**, *1586*, 65-82.
- (49) Kopra, K.; Vuorinen, E.; Abreu-Blanco, M.; Wang, Q.; Eskonen, V.; Gillette, W.; Pulliainen, A. T.; Holderfield, M.; Härmä, H. Homogeneous Dual-Parametric-Coupled Assay for Simultaneous Nucleotide Exchange and KRAS/RAF-RBD Interaction Monitoring. *Anal Chem* **2020**, *92*, 4971-4979.
- (50) Bonsor, D. A.; Alexander, P.; Snead, K.; Hartig, N.; Drew, M.; Messing, S.; Finci, L. I.; Nissley, D. V.; McCormick, F.; Esposito, D.; Rodriguez-Viciana, P.; Stephen, A. G.; Simanshu, D. K. Structure of the SHOC2-MRAS-PP1C Complex Provides Insights Into RAF Activation and Noonan Syndrome. *Nat Struct Mol Biol* **2022**, *29*, 966-977.
- (51) Kabsch, W. XDS. *Acta Crystallogr D Biol Crystallogr* **2010**, *66*, 125-132.
- (52) Winter, G.; Waterman, D. G.; Parkhurst, J. M.; Brewster, A. S.; Gildea, R. J.; Gerstel, M.; Fuentes-Montero, L.; Vollmar, M.; Michels-Clark, T.; Young, I. D.; Sauter, N. K.; Evans, G. DIALS: Implementation and Evaluation of a New Integration Package. *Acta Crystallogr D Struct Biol* **2018**, *74*, 85-97.
- (53) Evans, P. R.; Murshudov, G. N. How Good Are My Data and What is the Resolution? *Acta Crystallogr D Biol Crystallogr* **2013**, *69*, 1204-1214.
- (54) Winter, G. XIA2: an Expert System for Macromolecular Crystallography Data Reduction. *J Appl Cryst* **2010**, *43*, 186-190.
- (55) Winter, G.; McAuley, K. E. Automated Data Collection for Macromolecular Crystallography. *Methods* **2011**, *55*, 81-93.
- (56) Vonrhein, C.; Flensburg, C.; Keller, P.; Sharff, A.; Smart, O.; Paciorek, W.; Womack, T.; Bricogne, G. Data Processing and Analysis with the autoPROC Toolbox. *Acta Crystallogr D Biol Crystallogr* **2011**, *67*, 293-302.
- (57) Winn, M. D.; Ballard, C. C.; Cowtan, K. D.; Dodson, E. J.; Emsley, P.; Evans, P. R.; Keegan, R. M.; Krissinel, E. B.; Leslie, A. G.; McCoy, A.; McNicholas, S. J.; Murshudov, G. N.; Pannu, N. S.; Potterton, E. A.; Powell, H. R.; Read, R. J.; Vagin, A.; Wilson, K. S. Overview of the CCP4 Suite and Current Developments. *Acta Crystallogr D Biol Crystallogr* **2011**, *67*, 235-242.
- (58) Vagin, A.; Teplyakov, A. MOLREP: an Automated Program for Molecular Replacement. *J Appl Cryst* **1997**, *30*, 1022-1025.
- (59) Murshudov, G. N.; Skubak, P.; Lebedev, A. A.; Pannu, N. S.; Steiner, R. A.; Nicholls, R. A.; Winn, M. D.; Long, F.; Vagin, A. A. REFMAC5 for the Refinement of Macromolecular Crystal Structures. *Acta Crystallogr D Biol Crystallogr* **2011**, *67*, 355-367.
- (60) Emsley, P.; Lohkamp, B.; Scott, W. G.; Cowtan, K. Features and Development of Coot. *Acta Crystallogr D Biol Crystallogr* **2010**, *66*, 486-501.
- (61) Schuttelkopf, A. W.; van Aalten, D. M. F. PRODRG: a Tool for High-Throughput Crystallography of Protein-Ligand Complexes. *Acta Crystallogr D Biol Crystallogr* **2004**, *60*, 1355-1363.
- (62) Laskowski, R. A.; MacArthur, M. W.; Moss, D. S.; Thornton, J. M. PROCHECK: a Program to Check the Stereochemical Quality of Protein Structures. *J Appl Cryst* **1993**, *26*, 283-291.
- (63) Williams, C. J.; Headd, J. J.; Moriarty, N. W.; Prisant, M. G.; Videau, L. L.; Deis, L. N.; Verma, V.; Keedy, D. A.; Hintze, B. J.; Chen, V. B.; Jain, S.; Lewis, S. M.; Arendall, W. B., 3rd; Snoeyink, J.; Adams, P. D.; Lovell, S. C.; Richardson, J. S.; Richardson, D. C. MolProbity: More and Better Reference Data for Improved All-Atom Structure Validation. *Protein Sci* **2018**, *27*, 293-315.

Insert Table of Contents artwork here

